Sacramento Mountains Hydrogeology Study

Final Technical Report
Prepared for Otero Soil and Water Conservation District

June 2012

Open-file Report 543

New Mexico Bureau
of Geology and
Mineral Resources

AQUIFER MAPPING PROGRAM

B. T. Newton, G. C. Rawling,
S. S. Timmons, L. Land, P. S. Johnson,
T. J. Kludt, and J. M. Timmons

The views and conclusions are those of the authors, and should not be interpreted as necessarily representing the official policies, either expressed or implied, of the State of New Mexico.

New Mexico Bureau of Geology and Mineral Resources

A division of New Mexico Institute of Mining and Technology

Socorro, NM 87801
(575) 835-5490
Fax (575) 835-6333
www.geoinfo.nmt.edu

Sacramento Mountains Hydrogeology Study

Final Technical Report
Prepared for Otero Soil and Water Conservation District

June 2012

Open-file Report 543

B. T. Newton, G. C. Rawling,
S. S. Timmons, L. Land, P. S. Johnson,
T. J. Kludt, and J. M. Timmons

Graphic Design: Brigitte Felix

New Mexico Bureau of Geology and Mineral Resources

PROJECT FUNDING

Funding for this work came from
the Otero Soil and Water Conservation District
through legislative appropriation administered
by the New Mexico State Department
of Agriculture at New Mexico State University,
Las Cruces, New Mexico.
Additional funding for geologic mapping in
the study area has been awarded through
the National Cooperative Geologic Mapping
Program (STATEMAP).

TABLE OF CONTENTS

TABLES

APPENDICES

EXECUTIVE SUMMARY

In 2005, the New Mexico Bureau of Geology and Mineral Resources initiated a hydrogeology study in the southern Sacramento Mountains with funding from legislative appropriations through the Otero Soil and Water Conservation district. The project was initiated and research funding was continued because of concerns about future water resources for local communities in the southern Sacramento Mountains. Over the past decade, water managers and residents have observed decreasing spring discharge and streamflow in the area, and significant declines of water-levels in wells. Land and resource managers have expressed interest in the potential to increase water availability by thinning woodlands in the mountain watersheds. The focus of this investigation has been to characterize the hydrogeologic framework of the southern Sacramento Mountains and surrounding areas. The results of this study also provide a foundation to assess the impact of tree thinning on groundwater-levels, spring discharge and streamflow in an ongoing study of a small mountain watershed.

Understanding the regional hydrologic system is important for sustainable water resource management in local communities. Much of the groundwater in the Sacramento Mountains ultimately recharges adjacent regional aquifer systems. Previous studies have indicated that significant quantities of groundwater in the Salt Basin to the south and the Roswell Artesian Basin aquifer to the east originate as precipitation in the Sacramento Mountains. However, the dominant mechanisms by which this water travels from the mountains to surrounding aquifers have not been well understood.

The goals of this regional hydrogeologic investigation were (1) to delineate areas of groundwater recharge; (2) determine directions and rates of groundwater movement; and (3) develop a conceptual model of interactions between different aquifers and the groundwater and surface water systems. Methods used for this study include geologic mapping, groundwater-level measurements, and geochemical and isotopic techniques. This report describes the results of this multi-scale study.

The study area is located on the eastern slope of the southern Sacramento Mountains, west of Roswell and Artesia. It extends from the crest of the mountains near Sunspot, east to the village of Hope, in western Eddy County; and from the southern boundary of the Mescalero Apache Reservation to just south of the villages of Timberon and Piñon, covering approximately 2,400 square miles. Elevations within the study area range from 9,400 feet along the crest of the mountain range, to 4,000 feet at the eastern study boundary on the Pecos Slope. This gradational change in elevation correlates with observed vegetation patterns and the distribution of precipitation. Dominant vegetation changes from mixed conifers in the high mountains to piñon, juniper and grasslands to the east at lower elevations. Average annual precipitation ranges from 26 inches in the high mountains to approximately 12 inches at the eastern study boundary. Up to 50% of the annual precipitation falls during the monsoon season (July through September). The winter months are generally the driest time of year. However, the high mountains often receive a significant amount of snow. Over the course of this investigation, the Sacramento Mountains received record amounts of rainfall during the summers of 2006 and 2008.

The surface water system is comprised of intermittent high mountain streams that drain into the Rio Peñasco and Sacramento River. The Rio Peñasco flows to the east toward the Roswell Artesian Basin, and the Sacramento River flows to the southeast toward the Salt Basin. Hundreds of springs in the high mountains feed these two rivers and their tributaries. Despite the large number of springs, there are few perennial streams in the study area. It is common for streams to flow down gradient for a few miles, infiltrate into the subsurface, and resurface again at a downstream location due to the nature of the bedrock.

The Yeso and San Andres Formations are the two primary geologic units in the study area. These sedimentary rocks were deposited during

the Permian Period, approximately 260 to 270 million years ago. The Yeso Formation is exposed in valley bottoms and on lower valley slopes in the high mountains west of Mayhill. East of Mayhill on the Pecos Slope, the Yeso Formation plunges beneath the surface and generally is not exposed. The Yeso is a heterogeneous formation composed of discontinuous limestone, siltstone, and sandstone, dipping gently to the east. The high degree of lithologic heterogeneity observed both vertically and laterally in the Yeso Formation has a profound effect on the regional hydrologic system. The overlying San Andres Formation is made up of light-to-dark-gray and bluish-gray carbonate rocks and comprises the upper portions of valley slopes. It caps mountain ridges west of Mayhill. East of Mayhill, the San Andres Formation is the primary geologic unit exposed at the surface.

Important geologic structures that influence groundwater and surface water flow include faults and joints (fractures). There are two regional fracture systems that appear to influence drainage orientations and spring locations. The Sacramento River drainage, which extends southeast of Sunspot, through Timberon, and out of the study area, is structurally controlled by a zone of normal faults and associated folds. The northeast-trending segment of the Rio Peñasco drainage near Mayhill follows the Mayhill Fault, which has minor west-side-down displacement.

The Yeso Formation is the primary aquifer in the study area. West of the Mayhill Fault, where the Yeso Formation is exposed, fractured limestone and dolomite beds are the main source of water for most springs and wells. Groundwater flows preferentially through these rocks primarily due to karst processes that result in solution enlarged fractures and conduits that easily transmit water. In addition to these karst processes, surficial exposure and heterogeneity of the Yeso formation along with the presence of regional fracture systems result in a complex multi-layered system of perched aquifers that discharge at hundreds of springs at several stratigraphic levels. These perched aquifers are interconnected by fracture systems and mountain streams. In the eastern portion of the study area, limestone in the San Andres Formation becomes more important as an aquifer, ultimately merging with the artesian aquifer system in the Roswell Basin.

During the summers of 2006 and 2008, groundwater-level increases were observed in most wells being monitored in the study area. Abundant monsoon rains during these two years resulted in two of the wettest months on record in the study area. In July 2008, a remnant of Hurricane Dolly dropped over four inches of rain in the high mountains. Both short-term and long-term water-level rises occurred in response to these events. Wells with a short-term response (STR wells) displayed rapid water-level rises and declines, and most of these wells are less than 300 feet deep. By contrast, water-levels rose slowly in long-term response wells (up to 18 months) and showed very little decline. Most of the long-term response wells (LTR wells) are greater than 300 feet deep. The different water-level responses to these recharge events demonstrate the complexities of the high mountain groundwater system discussed above. STR wells are likely those drilled in shallow perched aquifers that discharge at a down-gradient spring, while LTR wells are probably drilled in deeper, more regional aquifers.

We divided the study area into four regional aquifer systems: the high mountain aquifer system, the Pecos Slope aquifer, the Tularosa Basin mountain front aquifer, and the Salt Basin aquifer. The high mountain aquifer system and Pecos Slope aquifer are the focus of this study. A regional water table map based on well water-levels and spring elevations shows that groundwater generally flows from high elevations in the west to lower elevations in the east. Within the high mountain aquifer system, local and intermediate-scale flow paths can differ significantly from the this regional flow direction due to local relief, regional fracture systems and the heterogeneity of the Yeso Formation as discussed above. However, along the Pecos Slope, groundwater flow directions and depths to water indicated by the water table map are more representative of this regional aquifer system.

The water chemistry and stable isotopic composition of groundwater changes systematically along the regional groundwater flow path (from high elevations to low elevations) due to cumulative effects of ongoing natural processes. Water chemistry in springs and wells at high elevations is dominated by calcium and bicarbonate ions that are the product of carbonate dissolution. From west to east, going down gradient and into the Pecos Slope aquifer, the concentration of sulfate

and magnesium ions in groundwater increases due to continuous water-rock interactions in a process called dedolomitization. The stable isotopic composition of groundwater shows an evaporative signature due to evaporation in mountain streams. The evaporative effects on the isotopic composition of groundwater increase as it flows through the high mountain aquifer system. This trend is indicative of the connectivity between perched carbonate aquifers via the surface water system. Groundwater in high elevation perched aquifers discharges at springs. This discharge feeds mountains streams and then recharges another perched aquifer, which discharges at a lower elevation spring. This recycling process can happen several times before the water makes its way into the deeper regional aquifer system. These observed trends indicate that groundwater recharge occurs primarily at high elevations (above 8,200 feet) as snow and rain. Groundwater age-dating results support this finding with the youngest water occurring at high elevations.

Stable isotope data suggest that snowmelt usually contributes significantly more groundwater recharge than summer precipitation. However, extreme summer precipitation events, such as those observed in 2006 and 2008, can also recharge the groundwater system, resulting in significant increases in spring discharge, with corresponding rises in water-levels in wells and changes in the stable isotopic composition of groundwater. Stable isotope data indicate that extreme precipitation events in 2006 and 2008 flushed water from unsaturated pores, fractures, and epikarst features in the San Andres and Yeso Formations into saturated carbonate aquifers. There is an apparent volume threshold for this type of recharge to occur, as 2007 monsoons did not result in groundwater water-level increases.

East of Mayhill along the Pecos Slope, regional groundwater flow is dominantly to the east toward the Roswell Artesian Basin. Some groundwater also flows to the southeast toward the Salt Basin. Previous studies have suggested that groundwater ultimately originating as precipitation in the high mountains recharges the Roswell Artesian Basin east of the Pecos Slope aquifer. However, it has been unclear how much of that recharge occurs as subsurface groundwater flow and how much occurs by infiltration from streams that flow across the Pecos Slope. Previous investigators assumed that recharge occurred primarily as stream infiltration through solution-enlarged fractures and sinkholes in what has been referred to as the "principal intake area" along the eastern boundary of our current study area.

Chemistry, stable isotope and groundwater age data from this investigation indicate that a significant portion of groundwater recharge to the Pecos Slope, Roswell Artesian Basin, and Salt Basin is derived from subsurface groundwater flow from the high mountain aquifer system. In the high mountains, a mixture of snowmelt and high elevation rainfall infiltrates quickly through fractures and conduits and streambeds. Water flows through the series of perched aquifers that make up the high mountain aquifer system and into the Pecos Slope aquifer. There is little evidence of recharge from the surface along the Pecos Slope except for some seepage along the Rio Peñasco. There is some evidence of recharge at the eastern boundary of the study area due to seepage in ephemeral streams. Surface runoff captured by several sink holes scattered along the western region of the Pecos Slope also likely contributes to groundwater recharge. Our recharge estimates suggest that on average, 22% of precipitation that infiltrates into the subsurface in the high mountains region makes its way to the Roswell Artesian Basin and the Salt Basin.

This study provides valuable information about the hydrologic system in the southern Sacramento Mountains, an important water source for local communities, as well as surrounding regional aquifer systems. Our findings show the correlation of local climate conditions and the direct effect it has on the southern Sacramento Mountains aquifer system. Our data shows that in this area, recharge and groundwater availability is heavily dependent upon snowmelt but recharge also occurs with exceptional monsoon events. Results from this study also show how groundwater moves and is stored in the subsurface as the local geology is more clearly understood. As years of climate change lie ahead, and with increasing pressures of population growth, findings in this report will help land and water managers to develop strategies for sustainable water resource management.

I. INTRODUCTION

SIGNIFICANCE

This report presents the results of a hydrogeologic investigation of the southern Sacramento Mountains. The principal objective of this study is to develop a better understanding of the regional hydrogeologic framework that controls the occurrence and movement of groundwater in the region. Cloudcroft and numerous small, rural population centers, including Mayhill, Timberon, and Piñon, are located in the study area. These communities rely on high elevation watersheds in the Sacramento Mountains that serve as sources of recharge to local aquifers. These high elevation watersheds also feed the stream systems that connect to the Roswell Artesian Basin and the Salt Basin. Water managers and users across the region have observed declines in water-levels and spring discharge in the past few decades, with dramatic decreases in the early 2000s. The Sacramento Mountain watersheds have undergone significant land use and hydrologic changes during the 20th century, including changes in vegetation patterns, an increase in tree density, variable climatic conditions, localized and severe fire impacts, and new groundwater and surface water diversions.

In response to these stresses on the hydrologic system and uncertainties related to population growth and climate change, water resource managers are interested in developing innovative methods of land management that will help sustain their future water resources while maintaining a healthy environment. Thinning forests in the high mountain watersheds, for example, is currently being implemented to decrease fire hazard and increase forest health in general. There is great interest in the potential increase in groundwater recharge, spring discharge, and streamflow by thinning trees in recharge areas. Generally, the extent to which such treatments affect water yield is largely site-specific and depends on many factors, including the local geology, climate, vegetation, and hydrogeologic setting. This study characterizes the regional hydrogeology and provides the context for a watershed study that aims to evaluate the hydrologic response to specific land management practices, such as tree thinning.

Additionally, research on the Roswell Artesian Basin Aquifer since the 1930s has indicated that the Sacramento Mountains provide significant recharge to the Roswell Artesian Basin. This study adds to the understanding of the regional hydrogeology and provides evidence of the importance of high mountain precipitation in recharging adjacent regional aquifers.

DESCRIPTION OF STUDY AREA

The southern Sacramento Mountains study area, which occupies approximately 2400 square miles, encompasses the region between the western escarpment of the Sacramento Mountains near Alamogordo and the village of Hope to the east (Fig. 1). The area includes numerous mountain villages and rural developments, such as Cloudcroft, Mayhill, Timberon, Piñon, and Hope, within Otero, Chaves, Eddy, and Lincoln counties.

The Sacramento Mountains extend from Capitan in the north to Otero Mesa in the south (Fig. 2). This study focuses on the southern portion of this mountain range, south and southeast of Mescalero-Apache tribal lands. Several important physiographic and tectonic features surround the southern Sacramento Mountains and this study area. To the west is the Tularosa Basin, which is one of the major extensional sedimentary basins of the Rio Grande Rift. Otero Mesa, southwest of the study area, is a flat upland extending south from the Sacramento River valley across the state line into Texas. South of the study area are the northern Salt Basin, which is also an extensional tectonic basin, and the Guadalupe Mountains. The low-relief, eastern portion of the study area that slopes eastward to the Pecos Valley is known as the Pecos Slope. The Roswell Artesian Basin aquifer underlies the Pecos Valley and the easternmost Pecos Slope from northern Chaves County to Carlsbad (Fiedler and Nye, 1933; Havenor, 1968). North of the study area are the volcanic highlands of the Sierra Blanca and Capitan Mountains.

Extensional tectonics associated with the opening of the Rio Grande Rift formed the Tularosa Basin and uplifted the sedimentary rocks of the southern Sacramento Mountains over millions of years. Elevations in the study area include several peaks over 9,000 feet above sea level, and range down to approximately 4,000 feet above sea level on the Pecos Slope near

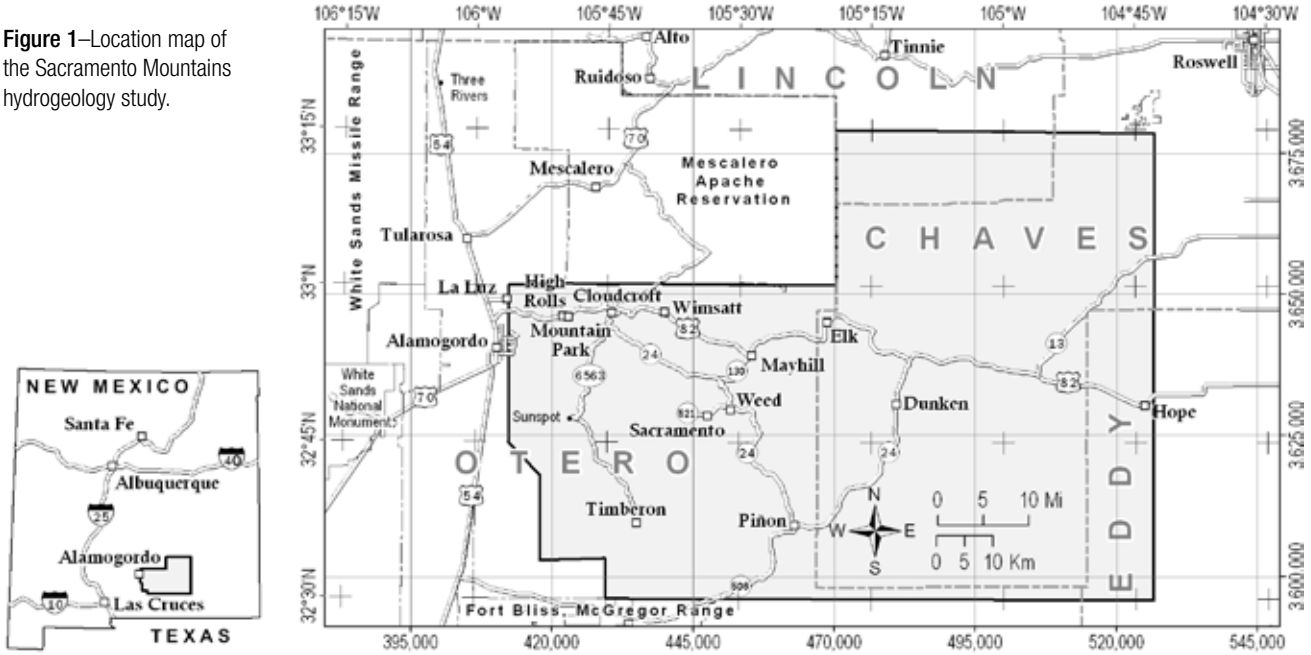

Figure 1–Location map of the Sacramento Mountains hydrogeology study.

Hope. Average annual precipitation in the study area correlates with elevation and varies from 26 inches at the crest to less than 12 inches on the eastern margin of the Pecos Slope. Most precipitation falls as summer monsoon rains and winter snow. Vegetation in the region reflects the elevation and precipitation variability with a mixed conifer forest at higher elevations, and piñon juniper vegetation at lower elevations.

PREVIOUS WORK

Geology

Meinzer and Hare (1915) performed the first geologic and hydrologic investigations in the vicinity of the study area. Although the geologic and hydrologic work in this seminal study only addressed the western escarpment of the Sacramento Mountains (in addition to the entire Tularosa Basin), the study notably contained the first topographic map of the Sacramento Mountain range.

Fiedler and Nye (1933) conducted a geologic and hydrologic study of the Roswell Artesian Basin. The westernmost portions of their study area (the Pecos Slope) coincide with the eastern portions of the present one. Nye's sections on the geology include detailed descriptions of the San Andres Formation (which he named the Picacho limestone) and the Yeso Formation (which he named the Nogal Formation).

Pray (1961) presented many stratigraphic sections of Paleozoic rocks and a detailed geologic map of the western escarpment of the Sacramento Mountains at 1:31,680-scale. This map has been incorporated into the geologic map in this study, with some modifications along the range crest south of Cloudcroft.

Moore et al (1988a, 1988b) mapped portions of the Mescalero Apache Reservation, which borders the study area to the north. The Hydrologic Atlas of Sloan and Garber (1971) includes a reconnaissance geologic map of the Mescalero Apache Reservation.

Kelley (1971) prepared the only previous geologic map covering the entire study area. His regional overview encompasses a very large area, from the Capitan Mountains in Lincoln County to the Guadalupe Mountains along the Texas border, most of western Chaves and Eddy Counties, and an area east of the Pecos River. Kelley's subdivision of the San Andres Formation is the same one used for the geologic mapping in this study. His geologic map covers the entire area of this investigation, but is at a very coarse scale (1:12,5000) and there are no cross sections. Our mapping at 1:24,000 has in general verified the mapping of Kelley, but in much more detail, and we incorporated the surface mapping with subsurface data to present three regional cross sections. Black (1973) extended the mapping of Kelley (1971) south across the eastern portion of Otero Mesa, covering southeastern Otero county to the west flank of the Guadalupe Mountains. Portions of the northern reaches of Black's (1973) map were incorporated into the geologic map in this study.

Harbour (1970) presented a regional study of the Hondo Sandstone member of the San Andres Formation in the northern Sacramento Mountains, north of the present study area. Kelley (1971) argued that the Hondo Sandstone is identical to the Glorieta Sandstone

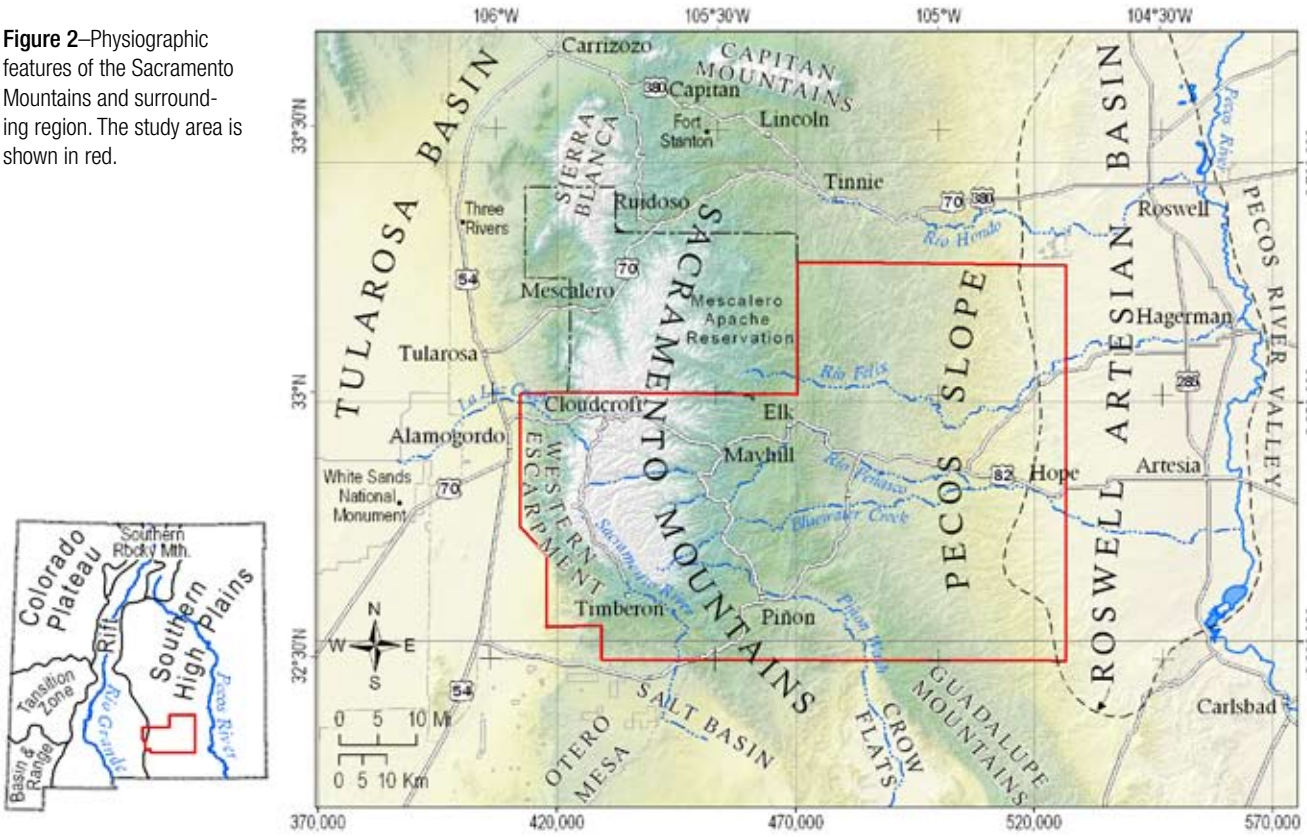

Figure 2–Physiographic features of the Sacramento Mountains and surrounding region. The study area is shown in red.

member, which thickens northward and becomes the Glorieta Sandstone of northern New Mexico, and that the term Hondo should be dropped. It is used in this report only in the context of its occurrence in older hydrologic literature. The Hondo Sandstone member of the San Andres Formation is the equivalent of the Glorieta Sandstone.

There are many water wells throughout the study area. Wasiolek and Gross (1983) presented logs of numerous water wells completed in the Yeso Formation in James and Cox Canyons and attempted to correlate stratigraphy within these wells down the canyons. Most of these wells are less than 400 feet deep. Wasiolek (1991) presented lithologic logs of several deep (up to 1200 feet) water wells completed in the Yeso Formation on the Mescalero Apache Reservation. Childers and Gross (1985) examined geophysical and lithologic logs of oil test wells penetrating the Yeso Formation on the western Pecos Slope between Mayhill and Hope to characterize the Yeso Formation aquifer. Black (1973, 1975), Childers and Gross (1985), King and Harder (1985), and Broadhead (2002) provide inventories of oil test wells and available geophysical logs in the eastern and southern portions of the present study area and adjacent parts of the region to the south and west. These are available in the petroleum records department of the NMBGMR.

Several of the yearly New Mexico Geological Society (NMGS) Guidebooks (Barker et al., 1991; Love et al., 1993; Lueth et al., 2002; Land et al., 2006) cover regions in and adjacent to the study area. The field trip logs, articles, and references in these books are excellent resources on the geology and hydrology of the southern Sacramento Mountains.

Hydrology

The Sacramento Mountains region is rather sparsely populated, with limited agricultural resources. For this reason, much of the previous work relevant to hydrology of the Sacramento Mountains has focused on more populated and more agricultural areas in adjacent groundwater basins. The Tularosa Basin to the west has been studied (e.g., McLean, 1970; 1975; Jennings, 1986, and many others), and to a much greater extent the Roswell Artesian Basin to the east, where more abundant water resources support a higher level of agricultural activity. The Roswell Artesian Basin underlies the west side of the lower Pecos Valley from central Eddy County to about 15 miles north of Roswell (Fiedler and Nye, 1933; Land and Newton, 2008) (Fig. 2). Hydrologic investigations of the Roswell Basin have generated a substantial body of work, some of it directly relevant to the Sacramento Mountains watershed

Renick (1926) wrote what may have been the first report that specifically addresses aspects of the hydrogeology of the southern Sacramento Mountains. Hood (1960) reported the first chemical analyses of water samples collected from springs and wells in the southern Sacramento Mountains. Mourant (1963) conducted a comprehensive hydrologic investigation of the Rio Hondo drainage basin in the northern Sacramento Mountains.

Fiedler and Nye (1933) conducted the first comprehensive investigation of geology and groundwater resources in the Roswell Artesian Basin. The Sacramento Mountains were viewed as of secondary importance in their study, except as a source of surface water that could recharge the artesian aquifer where it was exposed on the Pecos Slope. According to the conceptual model developed by Fiedler and Nye (1933), most recharge to the artesian aquifer occurs within a narrow belt on the Pecos Slope a few miles west of Roswell (Fig. 3). Along this narrow belt, losing streams such as the Rio Hondo, Rio Felix, and Rio Peñasco lose their water through solution enlarged fractures and sinkholes in the San Andres Formation. Fiedler and Nye (1933) referred to this belt as the Principal Intake Area, or PIA, establishing a paradigm for groundwater recharge in the Roswell Artesian Basin that has persisted for decades. Fiedler and Nye (1933) discounted the possibility of significant recharge from deeper aquifers such as the Glorieta Sandstone (Hondo Sandstone of Harbour (1970)) and Yeso Formation because of their low hydraulic conductivity, and the poor water quality associated with those units.

Later workers (e.g., Bean, 1949) suggested that substantial recharge to the artesian aquifer system may originate in areas west and northwest of the Roswell Artesian Basin, in the foothills of the Sacramento Mountains (Fig. 3). Motts and Cushman (1964) conducted a thorough appraisal of the potential for artificial recharge to the artesian aquifer system through sinkholes and karst fissures on the Pecos Slope. Their study extended into the eastern fringes of the Sacramento Mountains.

Beginning in the early 1970s, a number of graduate students at New Mexico Tech under the supervision of Dr. Gerardo Gross began a series of investigations of the hydrology and groundwater residence time in the San Andres artesian aquifer system of the Roswell Artesian Basin, and in the adjacent Sacramento Mountains (Rabinowitz and Gross, 1972; Gross et al., 1976; Rabinowitz et al., 1977; Duffy et al., 1978; Davis et al., 1979; Gross et al., 1979; Gross and Hoy, 1980; Rehfeldt and Gross, 1981; Hoy and Gross, 1982; Gross et al., 1982; Gross, 1982; Wasiolek and Gross, 1983; Gross, 1985; Childers and Gross, 1985; Simcox and Gross, 1985). Most of these studies have been documented in a series of reports published by the New Mexico Tech Geophysical Research Center and the New Mexico Water Resources Research Institute, and involved extensive use of groundwater tracers, including tritium and stable isotopes of oxygen and deuterium.

The first report in this series was published as a set of three papers in the Journal of Hydrology (Rabinowitz et al., 1977). The authors measured the tritium content of water samples from wells completed in the Roswell Artesian Basin, and correlated tritium activity peaks in well samples with bomb tritium peaks in meteoric water associated with atmospheric nuclear testing in the mid-20th century. Based on this analysis, Rabinowitz et al. (1977) conclude that groundwater in the northern Roswell Artesian Basin has a residence time of just four years, and a particle flow velocity of 65 feet/day (Gross et al., 1982). This hydrologic model implicitly assumes piston flow through the artesian aquifer, originating from a line source of nearly instantaneous recharge in the Principal Intake Area on the Pecos Slope, based

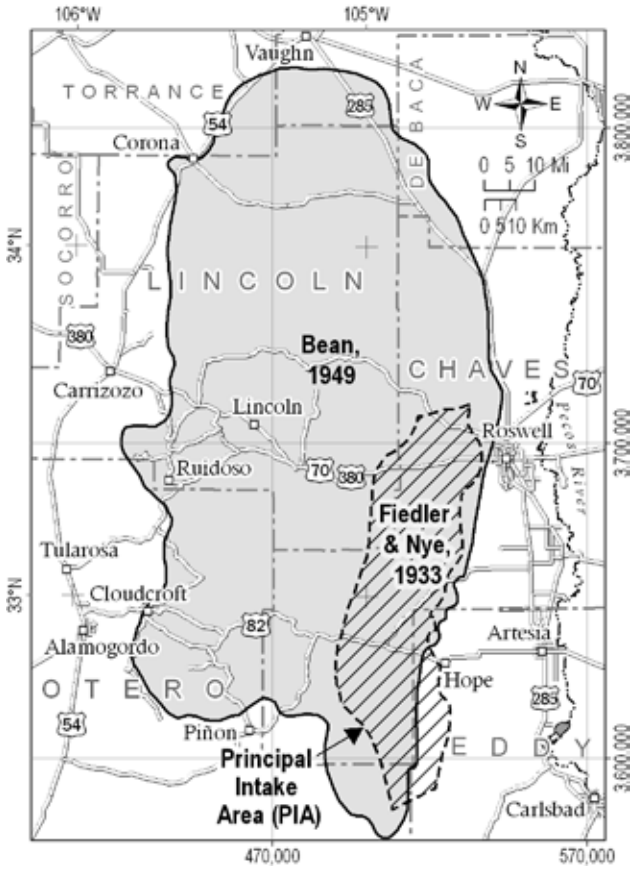

Figure 3–Recharge areas from previous studies for the Roswell Artesian Basin. Areas highlighted were identified by Fielder and Nye (1933) and Bean (1949).

on the original hydrologic paradigm developed by Fiedler and Nye (1933).

Fiedler and Nye (1933) estimated total annual recharge in the Roswell Artesian Basin to be 250,000 acre-feet/year. This estimate is based on calculation of total discharges from artesian wells, natural springs, and baseflow into the Pecos River. Gross and his students used water-level and stream runoff data to estimate total recharge due to channel losses in the Rio Hondo, Rio Felix, and Rio Peñasco to be ~38,000 acre-feet/year. Because surface recharge from these losing streams cannot account for total basin recharge, Gross and his students use this discrepancy to argue in support of a deep recharge component being more important than previous workers had assumed.

Gross and his students generally took a broader view of the greater Roswell Artesian Basin, wherein the catchment area for recharge extends to the crest of the Sacramento Mountains. They also focused more attention on deep sources of recharge from the Yeso Formation and the Glorieta (or Hondo) sandstone member of the San Andres Formation, the primary and secondary aquifers in the Sacramento Mountains (cf. Mourant, 1963; Wasiolek and Gross, 1983). This perspective contrasts with that of earlier workers such as Fiedler and Nye (1933), who regarded the Yeso Formation and Glorieta Sandstone as aquitards. Other recent workers also present contrasting views to Fiedler and Nye (1933). Reiter and Jordan's (1996) hydrogeothermal study of the lower Pecos Valley also extended into the Sacramento Mountains, and provided support for a deep source of recharge to the Roswell Artesian Basin.

There is a dearth of information about the hydrology of Mescalero Apache tribal lands in the middle of the Sacramento Mountains. Two unpublished contractors' reports (Woodward-Clyde Consultants, 1978, and Hydro-Geochem, 1982) provide information on the installation and testing of deep wells drilled into the Yeso Formation and on water-levels and chemical analyses of well samples collected on the Reservation. However, these documents are not readily available in the public domain. Published hydrologic information for the Reservation is limited to a paper by Wasiolek (1991), Sloan and Garber's (1971) map of the water table within the Yeso Formation, and Welder's (1975) preliminary report on drill sites on the Reservation.

Since the wave of investigations conducted by Dr. Gross and his students in the 1970s and 1980s, a number of papers of more limited scope have been published that address the hydrology of the Sacramento Mountains (e.g., Abercrombie, 2003; Riesterer et al., 2006; Land and Huff, 2010; Sigstedt, 2010; Ritchie, 2011). However, the present study constitutes the first comprehensive investigation of the regional hydrology of the southern Sacramento Mountains in the past 20 years.

Documents related to this study include lineament analyses by Walsh (2008) and analyses of carbon-14 age dates of groundwater along the Pecos Slope between Cloudcroft and Hope, New Mexico (Morse, 2010). An additional publication related to this study describes the impact of sulfuric acid weathering on the dissolution of carbonate bedrock in the Sacramento Mountains (Szynkiewicz et al., 2012).

PURPOSE AND SCOPE

Most scientists working in the region have recognized the importance of the Sacramento Mountains as a recharge area that feeds groundwater systems in adjacent basins and aquifers, but how groundwater moves through the subsurface and on what time scales has been poorly constrained. Understanding the regional hydrogeologic system in the Sacramento Mountains is important for managing water resources as the local population increases, and provides information relevant to adjacent hydrologic systems. A number of workers have published reports or maps on some aspects of the geology and hydrology in the Sacramento Mountains, but there has been no comprehensive investigation of the groundwater and surface water hydrology of the area in the last twenty years. Beginning in 2005, the New Mexico Bureau of Geology and Mineral Resources (NMBGMR), a division of New Mexico Tech, commenced a hydrogeologic study of the southern Sacramento Mountains with the following primary goals:

- Delineate areas of groundwater recharge
- Determine the direction and rates of groundwater movement
- Develop a conceptual model of the interconnectedness, if any, among the various aquifers in the region and the groundwater and surface water systems

This report is a comprehensive summary of data collection and interpretation to improve understanding of the hydrogeologic system in the southern Sacramento Mountains. Data and details pertaining to certain methods of data interpretation are presented in the Appendices. This Open-file Report serves as the final deliverable for the contract with the Otero Soil and Water Conservation District. Data and interpretations from this study should provide a framework for future research and water-planning in the region.

II. METHODS

DATA DESCRIPTION AND PURPOSE

Existing and previously reported data used in this study include published geologic maps, subsurface geologic data from well records and lithologic logs, hydrologic consultants' reports, weather station data, and historical depth-to-water and water quality data from published and unpublished sources.

New data collected by the NMBGMR, contractors and students from 2005 to 2009 include:

- Geologic mapping at 1:24,000-scale, with detailed cross sections
- Fracture and geologic lineament measurements and analyses
- Soil surveying
- Subsurface geologic unit descriptions from well cuttings
- GPS measurements of field site locations (UTM) and detailed characterization of spring and well sites
- One-time and repeated depth-to-water measurements in wells
- Streamflow measurements
- One-time and repeated geochemical, isotopic, and environmental tracer sampling from wells, springs, streams, and precipitation

Details about the new data collected and techniques used for this study are described below. In this report, we use the terms "regional" and "local" to describe large and small scale observations, respectively. When the terms regional or large-scale are used, we are referring to an area covering tens of square miles. Local or small-scale terminology refers to an area that is less than a few square miles, such as a canyon or small watershed.

GEOLOGIC DATA

Surface and subsurface geologic data can assist in the identification of aquifers and protection of groundwater supplies, and aid in locating water-supply wells. These data are fundamental for all environmental studies and land-use plans. The primary objective of geologic mapping is to characterize the geology in sufficient detail to allow the information to be used in matters of practical economic and environmental concern to governments, communities, and planners, as well as to satisfy the goals of basic science.

Geologic consultants were commissioned to perform more detailed surveys related to this study. A careful review and assessment of soils in a drainage along James Canyon was conducted by Frechette (2008). Several new water wells that were drilled along James Canyon had cuttings described and reviewed in detail by Zeigler et al. (2010). Walsh (2008) interpreted fracture and lineament measurements as part of this study. A total of 170 joints at 70 sites were measured in the high mountains west of the Pecos Slope (Fig. 2). Using field observations, along with aerial photo interpretation and GIS analyses, the geomorphic influence of regional fracture trends and lineaments on stream valley orientations and spring locations was addressed.

Geologic maps and cross sections

For this study, a total of 21 geologic maps were completed on 7.5 minute quadrangles at a scale of 1:24,000 (Fig. 4). Geologic mapping in the southern Sacramento Mountains began in the fall of 2005 and was completed in the spring of 2009. In addition to

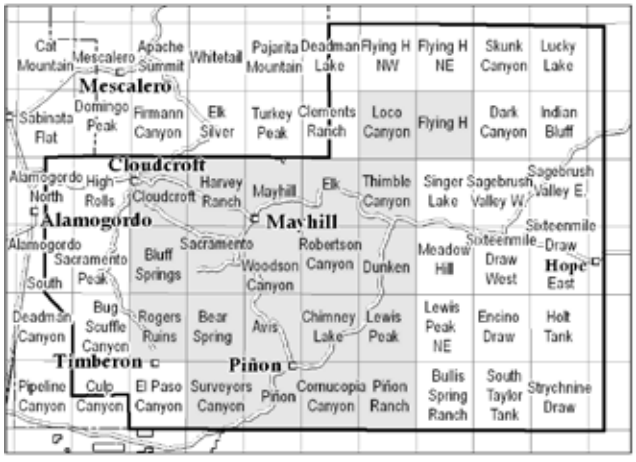

Figure 4–Published 1:24,000-scale geologic maps completed for this study.

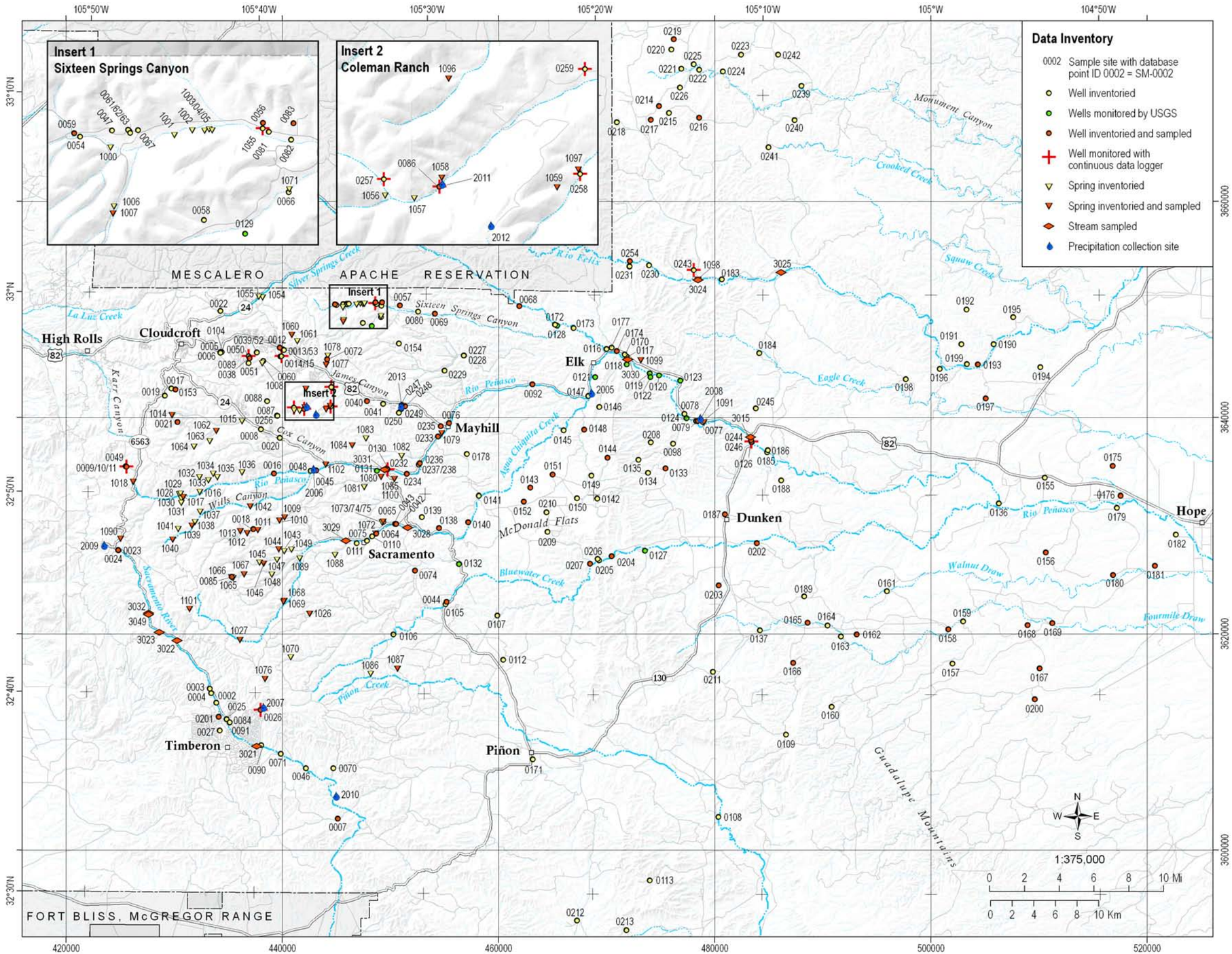

Figure 5–Site inventory map. Points on map indicate locations of wells, springs, streams and precipitation stations used in this study. Sites with UTM coordinates are listed in Appendix 1.

standard geologic field mapping procedures, much of the geology, especially in the sparsely wooded eastern portion of the study area, was interpreted from aerial photographs. Subdivision of the members of the San Andres Formation into its constituent members was performed in this way. These interpretations were locally field checked and compared to the existing map of Kelley (1971). In most places, the interpretations are similar. The new mapping was compiled with Pray's (1961) map of the western escarpment, and the northern region of Black's (1973) map of Otero Mesa. The regional cross sections were drawn using subsurface data such as lithologic and geophysical logs from water, oil, and gas wells. Numerous well cuttings in storage at the NMBGMR in Socorro were examined to aid in determining unit boundaries and to confirm unit boundaries picked on scout cards and geophysical logs. The geologic compilations map and cross sections for this study have been released separately as NMBGMR Open-file Report 537.

LOCATION OF SITES

All sample and measurement sites (wells, springs, streams, precipitation collectors) were located using a hand-held Garmin 76 or 76S global positioning system (GPS) device and were assigned a study identification number (SM-####) (Fig. 5; Appendix 1). The elevations of the sites were derived in ArcGIS from a 10-meter horizontal resolution digital elevation model. All spring sites were characterized in the field in terms of the physical characteristics of the discharge point and site conditions. Wells used in this study were inventoried in detail to describe the type of well, its construction, and a description of the measuring point used for water-level measurement.

WATER-LEVEL DATA

Water-level measurements can provide insight about the occurrence and direction of groundwater flow. Repeated water-level

measurements and/or continuous measurements provide information about daily, monthly and seasonal fluctuations that occur in an aquifer system. For this study, water-level measurements were obtained from numerous private and municipal wells (Fig. 5). All attempts were made to identify the well record associated with each well from the New Mexico Office of the State Engineer. The well records provide details about the drilling and construction of the well, in addition to the geologic units encountered while drilling. Well records for wells used in this study are found in Appendix 2.

Water-level measurements in most wells were made on a monthly to bimonthly basis between fall 2005 and summer 2009 (Appendix 3). From a specific measuring point on each well, depth to water measurements were made by staff of NMBGMR using one of several different techniques. To insure accuracy, water-levels measured with a steel tape were repeated until the measurement was within 0.02 feet of an earlier measurement. In wells with no dedicated pump equipment, water-levels were measured with a Solinst™ electronic sounder. A Ravensgate Corporation sonic water-level meter was also used to determine approximate depths to water.

During the course of the study, 12 wells were monitored with continuous water-level recorders for various time intervals ranging from a few months to several years (Fig. 5, Appendix 4). These were programmed to record water-level and temperature at 15 minute intervals for the first few months, then hourly intervals for the duration of the study. All but one of the wells was unequipped, thus giving continuous water-levels unaffected by well pumping. Water-level recorders were checked and downloaded every three to four months, and water-levels were measured manually at those times.

STREAMFLOW MEASUREMENTS

Streamflow measurements were made in locations where the stream was relatively uniform, u-shaped, and had only one stream channel (no split channels). Streamflow in various locations was measured using a propeller-style flow meter (Global Water Flow Probe). Following USGS guidelines (Rantz et al., 1982), the average velocity was calculated by measuring the cross sectional area of the stream. The area was then divided into subsections in which each section encompassed no more than 5% of the total discharge. Locations of streamflow measurements are shown on Figure 6, and all average streamflow measurements for these sites are found in Appendix 5.

GEOCHEMICAL METHODS

Chemical and isotopic analyses of precipitation, stream, spring, and well waters provide insight into the flow path of groundwater, where it is recharged, and its residence time in the subsurface. For this study, water was sampled for a number of analyses including major ion chemistry, trace metal chemistry, stable isotopes of oxygen, hydrogen and sulfur, and several naturally occurring environmental tracers which provide estimates of groundwater age.

Precipitation

We collected precipitation in the southern Sacramento Mountains on a regular basis beginning in 2006 using a simple collection device made of a funnel, a tube, and a one-gallon glass bottle. In the winter, a 1-foot section of 4 inch PVC pipe was attached to the funnel to allow snow to accumulate. The total volume of water that accumulated in the glass sample vessel between sampling events was measured, and a subsample was collected to be analyzed for stable isotopes of oxygen and hydrogen. Several large volume samples were analyzed for tritium. Figure 5 shows locations of the precipitation sampling stations. The locations of the precipitation collectors were chosen to represent the full range of elevations within the study area (Table 1). In general, samples were collected every 3 months (March, June, September, and December) in order to assess the seasonal variability of the average isotopic composition of precipitation. However, this time interval between sampling events sometimes varied due to over-filling of the sample vessels during extreme precipitation events.

Table 1–Site elevations and periods of precipitation collection.

Point ID	Elevation (ft asl)	Date Installed	Date Removed
SM-2005	5,935	15-Mar-06	02-Jun-09
SM-2006	7,204	16-Mar-06	02-Jun-09
SM-2007	7,360	15-Dec-06	22-May-07
SM-2008	5,461	15-Dec-06	17-Jun-09
SM-2009	9,203	16-Mar-06	02-Jun-09
SM-2010	6,132	23-May-07	02-Jun-09
SM-2011	7,770	26-Oct-07	05-Dec-07
SM-2012	8,468	05-Dec-07	Continues

Field parameters

When sampling water at stream, spring or well sites, field parameters were recorded. As wells were purged, sampling was initiated once field parameters had stabilized. Temperature, specific conductance,

pH, and dissolved oxygen (DO) were determined in the field with portable meters (Thermo Orion™ 290A+pH meter, YSI™ Model 85, Orion™ DO meter Model 810, and YSI™ Model 556 Multiprobe). Where possible, the oxidation reduction potential (ORP) was also recorded. The DO probe was calibrated onsite before sampling. The pH electrode was calibrated weekly against pH 7 and 10 buffers.

Major ions and trace metals

For general ion and trace metal chemistry, well and spring samples were collected using new, certified clean polypropylene containers after three repeated rinses. Samples for general ion chemistry analyses were collected using 250-ml polypropylene bottles. Water samples for trace metal chemistry were immediately filtered (where possible) through an inline 0.45 µm filter into 125-ml polypropylene bottles and acidified to pH <2 using ultra-pure nitric acid. If a trace metal chemistry sample could not be field filtered and acidified, it was immediately filtered and acidified in the laboratory. All chemistry samples were stored in an ice chest, transferred to the NMBGMR chemistry laboratory, and stored in a refrigerator until analyzed (within 1 week). Alkalinity (as mg/L HCO_3) was determined in the NMBGMR chemistry laboratory by titration. Laboratory measurements of pH were performed with an Orion 420A meter, and conductivity using a YSI 3200 meter. A chemical analysis for anions (Cl, SO_4 and NO_3) was performed

A

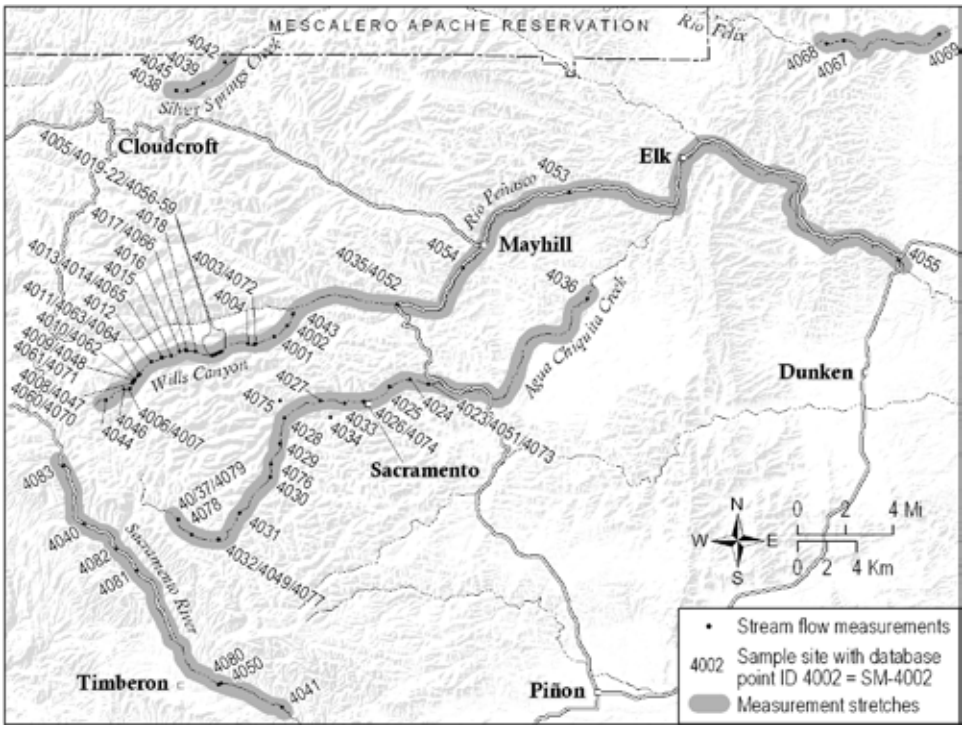

Figure 6–Streamflow measurements in the Sacramento Mountains.
A–Locations of measurements collected in 2007 and 2008. Data can be found in Appendix 5.
B–Measurement site in Wills Canyon.
C–The Rio Peñasco at site SM-4055.

B

C

using a Dionex DX-600 ion chromatograph. Cations (Na, K, Ca, and Mg) were analyzed using a Perkin Elmer OPTIMA 5300 DV Inductively Coupled Plasma Optical Emission Spectrometer (ICP-OES). Trace metals were analyzed by Inductively Coupled Plasma Mass Spectroscopy (ICPMS) using an Agilent 7500 IS. The quality of the chemical analyses was carefully inspected by analyzing blanks, standards, duplicate samples, and checking ion balances. The ion balance errors for the analyses were generally within ±5%.

Stable isotopes of hydrogen and oxygen

Stable isotopes of oxygen-18 (^{18}O) and hydrogen-2 (deuterium, ^{2}H) were analyzed in samples from precipitation, wells, streams, and springs. Samples were collected in 25 mL amber glass bottles after three repeated rinses. No air bubbles were present in the samples, and bottles were kept from direct sunlight. Samples were stored at room temperature in sealed bottles until analysis at the New Mexico Institute of Mining and Technology, Department of Earth and Environmental Sciences stable isotope laboratory on a Thermo Finnigan Delta Plus XP™ isotope ratio mass spectrometer. Analytical uncertainties for $\delta^{2}H$ and $\delta^{18}O$ are typically less than 1 per mil (‰) and 0.1‰, respectively.

Systematics of stable isotopes

Stable isotopes of hydrogen and oxygen are useful tools for tracking precipitation through a hydrologic system. The nucleus of most oxygen atoms contains 16 subatomic particles: 8 protons and 8 neutrons. A small fraction of all oxygen atoms (approximately 0.2%) contains 10 neutrons, for a total of 18 subatomic particles in the nucleus. This isotope of oxygen is referred to as oxygen-18, or ^{18}O. Most hydrogen atoms consist of a single proton in the nucleus orbited by a single electron. A very small fraction of hydrogen atoms (approximately 0.016%) also contains one neutron in the nucleus, for a total of two subatomic particles. This isotope of hydrogen is referred to as deuterium and abbreviated as D.

The isotopic composition of a water sample refers to the ratio of the heavier isotopes to the lighter isotopes (R) for the hydrogen and oxygen that make up the water molecules. Because these stable isotopes are actually part of the water molecule, small variations in these ratios act as labels that allow tracking of waters with different stable isotopic signatures. All isotopic compositions in this report are presented as relative concentrations, or the per mil deviation of R of a sample from R of a standard shown in equation below:

$$\delta = \left(\frac{R_{sample} - R_{standard}}{R_{standard}} \right) * 1000‰$$

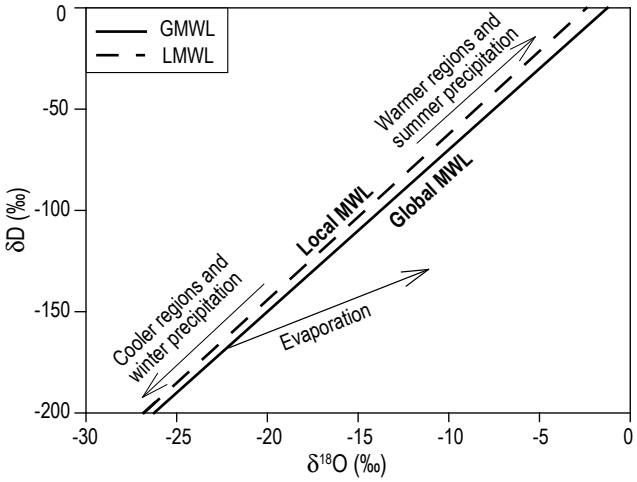

Figure 7–Schematic of stable isotope systematics. The relative position of the global meteoric water line (Global MWL or GMWL) is shown based on worldwide samples. A local meteoric water line (Local MWL or LMWL) was developed by this study for the southern Sacramento Mountains.

A negative value of $\delta^{18}O$ or δD indicates that the water sample is depleted in the heavier isotopes with respect to the standard. Standard Mean Ocean Water (SMOW) is the reference standard for stable isotopes of hydrogen and oxygen.

Because a water molecule is made up of both hydrogen and oxygen, it is advantageous to evaluate δD and $\delta^{18}O$ data simultaneously. Figure 7 shows a graph with δD on the y-axis and $\delta^{18}O$ on the x-axis. On such a plot, the isotopic compositions of precipitation samples collected worldwide plot close to a line called the global meteoric water line (GMWL) due to the predictable effects of evaporation and condensation (Craig, 1961). In general, precipitation in warmer regions will plot toward the heavier end of the GMWL (less negative values), and precipitation from cooler regions will plot towards the lighter end (more negative values). At any given location, a seasonal trend may be evident with winter precipitation plotting on the GMWL toward the lighter end and summer precipitation toward the heavier end. The GMWL represents a global average variation in the isotopic composition of precipitation. In a study such as this, it is necessary to collect local precipitation and define a local meteoric water line (LMWL), whose slope and y-intercept (deuterium excess) may vary slightly from the GMWL due to local climatic conditions.

The effects of evaporation are illustrated in Figure 7. As precipitation evaporates, the isotopic composition of the residual water evolves away from the meteoric water line (global or local) along an evaporation line, whose slope depends on the conditions under which evaporation has taken place.

Tritium

Tritium concentrations were analyzed in water samples from wells, streams, springs and precipitation. Samples were collected in two 500 mL polypropylene bottles, or one 1 L polypropylene bottle, after rinsing three times. Most samples were shipped to the University of Miami Tritium Laboratory where they were analyzed by internal gas proportional counting with electrolytic enrichment. For these samples, a sampling protocol described at www.rsmas.miami.edu/groups/tritium/advice-sampling-tritium.html was followed. The enrichment step increases tritium concentrations in the sample about 60-fold through volume reduction, yielding lower detection limits. Accuracy of this low-level measurement is 0.10 tritium unit (TU) (0.3 pCi/L of water), or 3.0%, whichever is greater. The stated errors, typically 0.09 TU, are one standard deviation.

Some samples were also analyzed by helium ingrowth at the University of Utah Dissolved and Noble Gas Laboratory. These samples were collected according to procedures described at http://www.earth.utah.edu/noblegaslab/how-to.html. Within the lab, after samples have had sufficient time to decay, the levels of helium-3 were measured on a mass spectrometer producing results with measurement error of ±3% of the value. The detection limit with this method is typically 0.1 TU.

Systematics of tritium

Tritium (^{3}H) is a short-lived radioactive isotope of hydrogen with a half-life of 12.32 years, and is a commonly-used tracer for determining the relative age of groundwater less than fifty years old. The vast majority of hydrogen atoms consist of a single, positively-charged proton in the nucleus of the atom and a single, negatively-charged electron orbiting the nucleus. The nucleus of the tritium isotope of hydrogen also includes two neutrons. Tritium concentrations are expressed in Tritium Units (TU), wherein one TU indicates a tritium-hydrogen atomic abundance ratio of 10^{-18} (Clark and Fritz, 1997).

Tritium is produced naturally in the stratosphere by cosmic radiation, and enters the hydrologic cycle via precipitation. Large volumes of anthropogenic tritium were produced between 1951 and 1962 by atmospheric testing of thermonuclear weapons, creating a "bomb" tritium spike in groundwater that has been used as a tracer in many hydrologic investigations (e.g., Rabinowitz et al., 1977). By 1990, bomb-levels of tritium had decreased in the atmosphere and tritium concentrations have mostly returned to naturally occurring levels. Use of the tritium isotope for dating modern groundwater now relies upon the largely natural ^{3}H signal (Clark and Fritz, 1997).

Unlike most environmental tracers, tritium atoms are directly incorporated into the water molecule and thus are not subject to alteration when exposed to atmospheric gases. Without knowing the background tritium concentration during recharge, a rather complicated input function must be assumed, and in most cases the absolute age of groundwater cannot be precisely determined using ^{3}H alone. Tritium is nevertheless a very useful tracer for making qualitative assessments of groundwater residence time. Waters with a concentration of 5 to 15 TU are considered to be modern groundwater, less than 5–10 years old. Tritium concentrations of 0.8 to 4 TU probably represent a mixture of recent and sub-modern recharge. Water samples less than 0.8 TU are assumed to be sub-modern, recharged prior to 1952 (Clark and Fritz, 1997).

Atmospheric concentrations of tritium display significant spatial and seasonal variations. The greatest increase in tritium concentrations in the atmosphere occurs during the spring in mid-latitude zones due to displacement of the jet stream (Clark and Fritz, 1997).

Tritium-helium and noble gases

Tritium/Helium-3 and dissolved noble gas samples were collected at several wells and two springs in the study area. These samples were collected using the copper tube method for wells, and at two springs using advanced diffusion samplers provided by the University of Utah Dissolved and Noble Gas Laboratory. Methods of sample collection described at www.earth.utah.edu/noblegaslab/how-to.html were followed. Analyses of gases included N_2, Ar, Ne, Kr, Xe, ^{3}He and ^{4}He, with errors of ± ½ to 1% of value for vium, and ± 1 to 4% of value for all other gases. Samples were stored at room temperature, then shipped to and analyzed at the University of Utah Dissolved and Noble Gas Laboratory.

Systematics of tritium-helium and noble gases

Tritium is subject to radioactive decay by beta emission to yield its daughter product, helium-3 (^{3}He). By measuring ^{3}H together with its daughter, ^{3}He, a true radiometric groundwater age can be determined that does not rely on a tritium input function (Solomon and Sudicky, 1991). Under ideal circumstances, the tritium-helium method of dating groundwater is remarkably accurate for water samples less than 40 years old (Clark and Fritz, 1997; Kazemi et al., 2006).

In addition to tritiogenic helium produced by tritium decay, other sources of ^{3}He include mantle-derived helium; nucleogenic helium produced by radioactive decay of uranium and thorium nuclides in the earth's crust; and atmospheric helium, which includes an excess air component. Numerous observations have

shown that groundwater frequently contains more atmospheric gas than can be accounted for by equilibrium solubility with the atmosphere. This excess air is probably a result of transient rise in the water table that does not fully displace the gas phase, but it can also be artificially introduced during well construction or development (Cook et al., 2006). Additionally, excess air can be a problem if air bubbles remain in the sampling equipment when the sample is collected, or if air bubbles are produced by a submersible pump in the well (Solomon and Cook, 2000).

In relatively young groundwater the contribution of nucleogenic and mantle helium is insignificant, and the most important correction that must be made is for excess air. This correction can be made by analysis of the concentrations of some noble gases such as neon, or from the nitrogen-argon ratio in the sample (Kazemi et al., 2006).

The ratio of helium-3 to helium-4 is a common parameter that is measured during noble gas analysis (Solomon, 2000). Because primordial helium derived from mantle sources consists of the ^{3}He isotope – the same isotope of helium produced by radioactive decay of tritium in groundwater – it must be accounted for when conducting studies of groundwater residence time using tritium-helium methodology. Elevated $^{3}He/^{4}He$ ratios in groundwater samples indicate that those waters may contain a significant percentage of mantle-derived helium-3 (Newell et al., 2005; Crossey et al., 2006). Analyses that we have obtained provide ratios of $^{3}He/^{4}He$ ratios in the sample compared to ratios of $^{3}He/^{4}He$ in the atmosphere (R/Ra). The $^{3}He/^{4}He$ ratio of the atmosphere is considered a constant, so any variation in the R/Ra number is a result of the $^{3}He/^{4}He$ ratio from the sample.

Carbon isotopes

Select spring and well samples were analyzed for carbon-14 (^{14}C) activity and $^{13}C/^{12}C$ ratios ($\delta^{13}C$) to determine groundwater age. Water samples were collected in two 500 mL polypropylene bottles, or one 1 L polypropylene bottle, after rinsing three times. Sampling procedures described at www.radiocarbon.com/groundwater.htm were used, with the exception of the addition of NaOH. Samples were kept chilled until shipment for analysis at Beta Analytic (www.radiocarbon.com). The ^{14}C activity and $^{13}C/^{12}C$ ratios of the water sample were derived from the dissolved inorganic carbon (DIC) by accelerator mass spectrometry. Measured $\delta^{13}C$ values were calculated relative to the PDB-1 standard. Results are reported as ^{14}C activity (in percent modern carbon (pMC)) and as the apparent radiocarbon age (in radiocarbon years before present (RCYBP), where "present" = 1950 CE), with an uncertainty of one standard deviation. No corrections for geochemical effects have been completed, and the reported apparent ^{14}C ages do not precisely represent the residence time of the water within the aquifer. The ^{14}C activity and apparent ^{14}C age are used as a relational tool to interpret hydrologic differences between wells.

Systematics of carbon isotopes

Carbon-14 is a naturally-occurring radioactive isotope of carbon that is produced naturally in the atmosphere by cosmic radiation. Carbon-14 was produced by atmospheric thermonuclear testing during the mid-20th century, similar to tritium. ^{14}C radioactivity of inorganic carbon in water is expressed in units of percent modern carbon (pMC) relative to the abundance of ^{14}C in atmospheric CO_2. Once isolated from atmospheric and soil gases, the abundance of ^{14}C decreases at a rate governed by its half-life of 5,730 years. The pMC of a water sample can be used to estimate its residence time up to ~50,000 radiocarbon years before present (rcbyp). An accurate estimate of residence time in closed systems requires correction of measured pMC values for the effects of carbon mass transfer during geochemical reactions with carbonate host rock along groundwater flow paths. In open systems, where carbon mass transfer can take place between water and atmospheric gases, pMC values can also be corrected if the system is well-characterized (Phillips and Castro, 2003).

Carbon-13 (^{13}C) is a naturally-occurring stable isotope of carbon. $^{13}C/^{12}C$ ratios of inorganic carbon in water are expressed in the per mil (‰) difference ($\delta^{13}C$) between a sample and the PeeDee Belemnite standard (PDB). The PDB is defined to have a $\delta^{13}C$ value of 0‰. Typical $\delta^{13}C$ values are near 0‰ for marine carbonates and -7 to -8‰ for atmospheric CO_2. A combination of equilibrium and kinetic fractionation that takes place during the uptake of CO_2 by plants via photosynthesis and the release of CO_2 in the soil by plant and microbial respiration results in soil CO_2 being isotopically depleted with respect to atmospheric CO_2. $\delta^{13}C$ values for CO_2 respired from soils range from -27 to -14‰ (Amundson et al., 1998). The $\delta^{13}C$ of inorganic carbon in water can serve as an indicator of water/rock/gas interactions along groundwater flow paths (Kalin, 2000) and is often used to correct measured groundwater pMC values for the effects of carbon mass-transfer geochemical reactions with carbonate host rock.

Chlorofluorocarbons

CFC samples were collected from well and spring discharge, with no atmospheric exposure, into three 125-mL glass bottles with foil-lined caps. The bottles and caps were thoroughly rinsed with sample water, and were filled and capped underwater in a

plastic bucket. Sampling followed stringent protocols described at www.rsmas.miami.edu/groups/tritium/advice-sampling-cfc.html. Samples were shipped to the University of Miami Tritium Laboratory where they were analyzed using a purge-and-trap gas chromatograph with an electron capture detector. The limit of detection for the method is 0.001×10^{-12} moles/kg of water (pmol/kg). Precision of CFC11, CFC12 and CFC113 analyses is 2% or less and the accuracy of CFC12 derived recharge ages is 2 years or less.

Systematics of CFCs

Chlorofluorocarbons are a class of volatile, synthetic compounds of carbon, chlorine and fluorine that have been used in refrigeration and other industrial applications since the 1930s (Plummer and Busenberg, 2000). The CFC compounds most commonly used in hydrologic studies are CFC11, CFC12, and CFC113 (Plummer et al., 2006). Atmospheric concentrations of CFC compounds increased in a quasi-exponential fashion from the 1950s through 1980s (Fig. 8), and the history of their concentrations is well-known or has been reconstructed from production/release data. Because CFCs contribute to destruction of the ozone layer, their production has been limited by international agreements, and in response atmospheric concentrations of CFCs have leveled off and begun to decrease since the 1990s.

Chlorofluorocarbons enter the hydrologic cycle through precipitation as a dissolved gas. The amount of gas dissolved in groundwater is dependent upon recharge temperature and recharge elevation (lower temperatures and higher elevations result in lower atmospheric and groundwater CFC concentrations). Therefore, recharge elevation and temperature need to be estimated to calculate the age. Incorrect estimation of these parameters will result in erroneous dates. Used as a groundwater tracer, CFC compounds can provide virtual year-to-year dating sensitivity for water recharged before 1990. Estimates of residence time for groundwater recharged since the 1990s are somewhat ambiguous because of declining CFC levels beginning in the late 20th century (Plummer and Busenberg, 2000; Phillips and Castro, 2003; International Atomic Energy Agency, 2006). However, CFC concentration ratios (e.g., CFC113/CFC12) may also be used to determine groundwater age. Using CFC concentration ratios has extended the application of these tracers for groundwater dating into the 21st century. The use of CFC ratios has particular application to quantifying binary mixtures of young groundwater (containing CFCs) and pre-modern groundwater (zero CFC concentration), since the CFC ratio can be used to define the age and volumetric fraction of the young component (Han et al., 2001; Plummer et al., 2006).

When using CFCs to date groundwater samples, the CFC12 date is usually considered the most reliable. CFC12 has the highest atmospheric concentrations (Fig. 8) and thus has the highest absolute concentrations in natural water samples. CFC113 has the lowest atmospheric concentrations and was introduced into the atmosphere later than the other two CFC species. CFC11 has a greater potential for contamination and microbial degradation (Plummer and Busenberg, 2000).

The simplest model for estimating groundwater age based on CFC concentrations is the piston flow model, which assumes that after recharge occurs, the tracer becomes incorporated into a parcel of water and moves through the aquifer to points of discharge at the mean velocity of groundwater. Hydrodynamic dispersion and molecular diffusion are considered negligible, and the age based on the piston flow model is referred to as the apparent age of the groundwater sample (Bethke and Johnson, 2002a; 2002b). Other models of groundwater age distribution include exponential models and binary mixing models, which assume mixing of two groundwater sources of different ages (Plummer et al., 2006; Solomon et al., 2006).

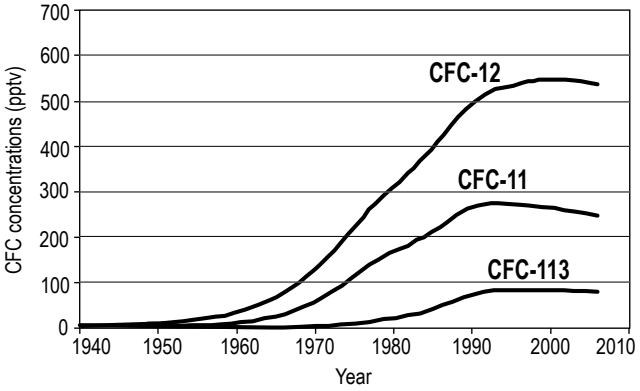

Figure 8–Atmospheric concentrations of chlorofluorocarbons in parts per trillion by volume (pptv).

III. RESULTS

GEOLOGY

Regional Geology

Sacramento Mountains, Pecos Slope, and Roswell Artesian Basin

East of the crest of the Sacramento Mountains to the Pecos Slope, the exposed rocks are the Permian Yeso (Py) and San Andres (Psa) Formations, which dip gently (2-3°) to the east (Figs. 9 and 10). These are the most important geologic units in the study area and are described in detail in the following stratigraphy section. Between the eastern boundary of the study area and the Pecos River, Quaternary alluvium and upland deposits cover redbeds and gypsum of the Permian Artesia Group, which overlies the San Andres Formation and forms the relatively impermeable upper aquitard of the Roswell Artesian Basin aquifer (Land and Newton, 2008).

Along the steep western escarpment of the Sacramento Mountains, the geology is more complex. This area is dominated by steep cliffs composed of Paleozoic sedimentary rocks, dominantly carbonates, with significant faults and folds. The range itself is uplifted along the Alamogordo fault, which forms the eastern boundary of the Tularosa Basin (Figs. 9 and 10).

Northern Sacramento Mountains

The high-elevation, canyon-dissected plateau of the southern Sacramento Mountains continues north of the study area for many miles to the granite intrusion that forms the Capitan Mountains. The Sierra Blanca igneous complex is a deeply eroded stratovolcano with layered lava flows and extrusive breccias intruded by several syenitic plutons. It is situated northwest of the study area and west of Ruidoso. This complex was emplaced in the core of the Sierra Blanca Basin, a Laramide–age (late Cretaceous – Paleogene) sedimentary basin which is partially filled with Eocene-age sediments (Moore et al., 1991; Cather, 1991; Rawling, 2009). The Sierra Blanca Basin can be seen on Figure 9 as the northeast-trending roughly oval-shaped outcrop pattern of Cretaceous sedimentary rocks (dark green on map) surrounding the Sierra Blanca igneous complex.

Tularosa Basin

The Tularosa Basin is located west of the steep western escarpment of the Sacramento Mountains. It is one of the major extensional sedimentary basins of the Rio Grande Rift and is one of the few to have internal drainage. The basin is filled with thousands of feet of late Tertiary and Quaternary sediments (Seager et al., 1987, Adams and Keller, 1994). The Alamogordo fault, a west-side down normal fault with thousands of feet of vertical displacement, separates the basin from the mountains.

Otero Mesa and Salt Basin

Otero Mesa and the Salt Basin are southwest and south of the study area, respectively. Otero Mesa is underlain by Permian sedimentary rocks correlative to those in the study area. The rocks are generally flat-lying, but faulting and folding is locally evident, particularly in the northeast sector (Black, 1976). The hydrologic system in fractured carbonate rocks underlying Otero Mesa has been the focus of detailed study (Mayer and Sharp, 1998). The Salt Basin is another extensional sedimentary basin related to the Rio Grande Rift and, like the Tularosa Basin, is filled with late Tertiary and Quaternary sediments. It is separated from the Guadalupe Mountains to the east by a zone of west-side down normal faulting that extends north to the latitude of Piñon (Kelley, 1971, Muehlberger et al., 1978).

Stratigraphy

Yeso Formation

Good natural exposures of the Yeso Formation are rare, as it is usually covered with colluvium from the overlying, more resistant San Andres Formation or by valley bottom alluvium. A complete section is not exposed east of the range crest. Pray (1961) measured a complete section 1239 feet thick on the west flank of Orendorf Peak three miles west of Timberon at the southwest corner of the present study area. Kelley (1971) measured a complete section 1220 feet thick in Tularosa Canyon 11 miles to the north of the present study area. Two deep wells that penetrated the Yeso Formation are the Apache Replacement well (Figs. 10 and 11A), drilled in 2006 and located less than 2 miles east of Cloudcroft, and the

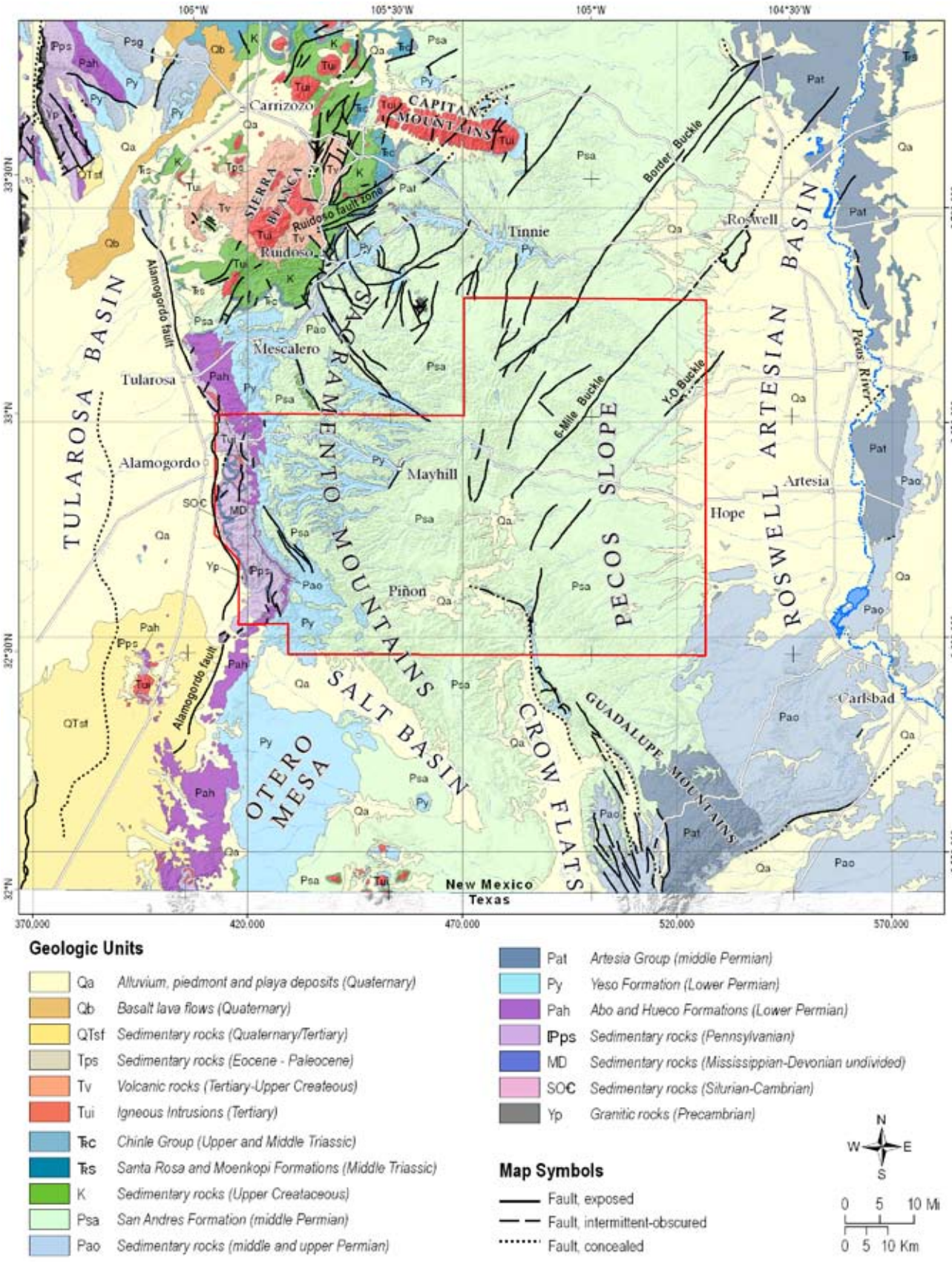

Figure 9–Regional geologic setting with study area shown in red.

Southern Production Company #1 oil test well, located between Cloudcroft and the Rio Peñasco. Based on his section and the Southern Production Company # 1 oil test well, Pray (1961) estimated the Yeso Formation at 1,200 to 1,800 feet in the western Sacramento Mountains. The differences are probably due to initial stratigraphic variation and dissolution of evaporites.

The Yeso Formation in the Orendorf Peak section of Pray (1961) is composed of gray limestone with minor gray to tan dolomite (47%), gray, buff, and reddish shale (30%), and yellow to tan siltstone and fine sandstone (9%), with 95 feet of gypsum and mixed gypsum and shale (9%) at the base of the formation. The upper 320 feet of Southern Production Company #1 oil test well was composed largely of limestone and dolomite. Similarly, the Village of Cloudcroft Apache replacement well, which penetrated1650 feet of the Yeso Formation, showed predominantly limestone and dolomite, with significant intervals of claystone and mudstone, and minor sandstone (Street and Perry, 2007). Anhydrite and/or gypsum were first observed 1240 feet below the top of the Yeso Formation in this well. Anhydrite and minor halite were observed below 940 feet below the top of the Yeso Formation in the Southern Production Company #1 oil test well but at 260 feet depth in the surface section of Pray (1961). No evaporites have been observed in surface exposures in the study area. In the area encompassing this study, Kelley (1971) and Pray (1961) both noted that the gypsum content of the Yeso Formation increases to the north and the carbonate content increases to the south.

Soluble carbonate rocks, such as limestone, dolomite, and calcareous sediments, are abundant in the stratigraphy of the upper Yeso Formation. Intraformational dissolution-collapse features and chaotic bedding dips are common in road-cut exposures of the upper Yeso Formation (Fig. 11B, C) and solution-enlarged fractures are abundant in bedrock pavements exposed in stream channels (Walsh, 2008). Due to initial stratigraphic heterogeneity and that caused by subsequent dissolution, individual beds are not traceable laterally for more than a few tens of meters in outcrops, and beds in general cannot be unambigously correlated between outcrops or wells. Zeigler et al. (2010) examined cuttings from four water wells less than 4 miles apart in canyons tributary to James Canyon and showed that individual beds in the Yeso Formation could not be correlated at depth (in contrast to work by Wasiolek and Gross (1983)). However, reasonable correlations of transgressive and regressive intervals in the stratigraphy can be made based on the vertical groupings of gross lithologic characteristics rather than individual beds (Zeigler et al., 2010).

San Andres Formation

The San Andres Formation is composed of light to dark gray and bluish-gray carbonate rocks (limestone and dolomite). Freshly broken surfaces are darker gray than weathered surfaces and often fetid. The formation contains karst features including large cavernous fractures and sinkholes. Subdivision of the San Andres into the lower dominantly thick-bedded Rio Bonito Member and middle dominantly medium- to thin-bedded Bonney Canyon member (Kelley, 1971) was based largely on interpretation of aerial photographs. In most areas, the differences in the nature of the bedding are not reliably distinguishable on the ground. Kelley (1971) estimated thicknesses for the Rio Bonito Member at 250-350 feet and the Bonney Canyon Member at up to 300 feet. Based on our mapping, cross sections, and well-log interpretations, the thicknesses are ~580 and 400 feet, respectively, in the vicinity of regional cross section A (Fig. 10B). These differences are significant, but Kelley mapped at a much smaller scale (1:125,000) using a mix of air photo and topographic bases, and presented no cross sections or well control to constrain his thickness estimates. Thickness variations on the order of ± 100 feet are likely in both members across the study area.

In the southern stratigraphic section of Pray (1961) on Orendorf Peak, the basal portion of the San Andres Formation consists of the Hondo Member, a 113-foot interval of limestone and dolomite topped by an 8-foot bed of medium grained, quartz sandstone, known as the Hondo Sandstone (equivalent to the Glorieta Sandstone). While the Hondo Sandstone is a significant mappable unit further north in the Hondo River drainage, it is insignificant in the southern Sacramento Mountains.

A small exposure of the uppermost member of the San Andres Formation, the Four-Mile Draw member, is present in the northeast corner of the study area. On aerial photographs it looks even-textured, less-prominently bedded, and slightly darker, grayish-brown appearance than the underlying Bonney Canyon member. Although this member contains abundant gypsum elsewhere (Kelley, 1971), in the study area it is composed of thin bedded, locally brecciated dolomite (Zeigler, personal communication, 2007). The total thickness is not exposed, but is at least 100 feet.

Surficial deposits and soils

Geologic units younger than the San Andres Formation are generalized in this report into Quaternary undivided alluvium and Quaternary and Tertiary terraces and gravels. The undivided alluvium includes unconsolidated alluvium in modern drainages, areas of colluvium, aeolian sand sheets, travertine and tufa deposits around springs, and broad flat terraces

and valley bottoms underlain by fine-grained sediment. The terrace and gravel unit includes coarse grained sediments and gravels that have been incised by modern drainages. Some of these gravels are well lithified and may be as old as Miocene.

Frechette (2008) conducted a soil survey for this study within a tributary to James Canyon. He examined soils developed above the San Andres Formation and Yeso Formation and in a small ridgetop basin filled with alluvium. Topographic position and slope, together with parent material, are the dominant factors controlling soil development in the study area, with lesser effects due to local vegetation type and slope aspect. We expect the soils described below to be typical of those throughout the high mountains west of Mayhill.

Soils developed on the San Andres Formation and the upper 30 to 60 feet of the Yeso Formation are largely formed from San Andres Formation parent material, due to the down-slope movement of colluvium. These soils are thin (generally less than 3 feet) and weakly developed, with A horizons and R/A horizons of silty loam with 30-50% angular pebbles and cobbles of limestone, grading into fractured bedrock. Soils are thickest at the base of slopes and thinnest near ridge crests, again indicating down-slope movement of material. Soils are also thicker on densely vegetated, north facing slopes than on sparsely vegetated, south facing slopes. Most of the bedrock weathering is mechanical, as there is little carbonate accumulation. Much of the fine mineral fraction probably originates as windblown dust. These soils are likely to have high infiltration rates and, if connected to shallow bedrock fracture networks, should rapidly transmit infiltrated water to the groundwater system.

Soils developed on lower slopes underlain by the Yeso Formation have siltstone, sandstone, and subordinate limestone as parent materials. They are thicker (up to 5 feet) and more strongly developed than those described above, with similar A horizons, but also B horizons showing evidence of color change and accumulation of clays. The B horizons indicate that in-situ chemical weathering and alteration of parent materials are more important soil-forming processes than down-slope movement. Similar A horizons to the San Andres-upper Yeso soils imply high potential infiltration, but the thicker profiles and B horizons imply slower subsurface transit and greater potential for evapotranspiration rather than aquifer recharge. Soils developed in small alluvium-filled basins on ridgetops are greater than 5 feet thick and contain clay-rich B horizons. They also contain buried soil horizons overlain by gravel-rich layers, which together indicate significant sediment input to the basin during a severe erosional event. The abundant clay and field observations of relatively dry soil profiles adjacent to areas of standing water in the small basins suggest that these soils have low permeability. Thus, they would have very low infiltration rates and may induce the development of local perched water tables.

Gravel is abundant within alluvial fans, in poorly sorted, matrix-supported layers with gravel contents often greater than 50%. Matrix materials and fine-grained layers are dominantly silt loams and loams. Buried soil horizons are common, consisting of weakly developed A horizons, similar to the surface soils.

Valley-bottom fills are alluvial deposits with little gravel (less than 10%) in poorly sorted, matrix supported layers. The deposits are dominantly composed of silt loam and sandy loam. Again, surface soils and abundant buried soils are weakly developed, with A horizons only. Poorly developed soils, low clay content, and locally high gravel content imply high potential infiltration through alluvial fans and valley bottom fills.

Geologic structures

The generally shallowly east-dipping Yeso and San Andres beds are complicated by faulting and folding. The Sacramento River drainage, which extends southeast of Sunspot, through Timberon, and out of the study area, is structurally controlled by a zone of west-side down normal faults and associated folds that form east-tilted structural blocks, or half-grabens (Fig. 10). These faults are probably of Tertiary age and related to uplift of the Sacramento Mountains.

The northeast–trending segment of the Rio Peñasco drainage near Mayhill follows the Mayhill Fault, which has minor west-side down displacement. This fault and valley segment is aligned with the Border Buckle, one of several right-lateral strike-slip fault zones that extend for tens of miles to the northeast across the Pecos Slope (Havenor, 1968, Kelley, 1971). The Mayhill Fault may be an extension of this regional structure and have some component of right-lateral slip. This fault appears to die out in the vicinity of Denny Hill north of Weed. There are several small folds extending to the southwest and northeast along the trend of this fault that are probably due to distribution of displacement across a broad zone at the fault tip.

The southern end of the Dunken-Tinnie anticlinorium forms a linear north-south trend of ridges and low hills in the eastern third of the map area. This regional structure extends north to the eastern end of the Capitan Mountains (Kelley, 1971) and dies out within the study area just northeast of Piñon. The

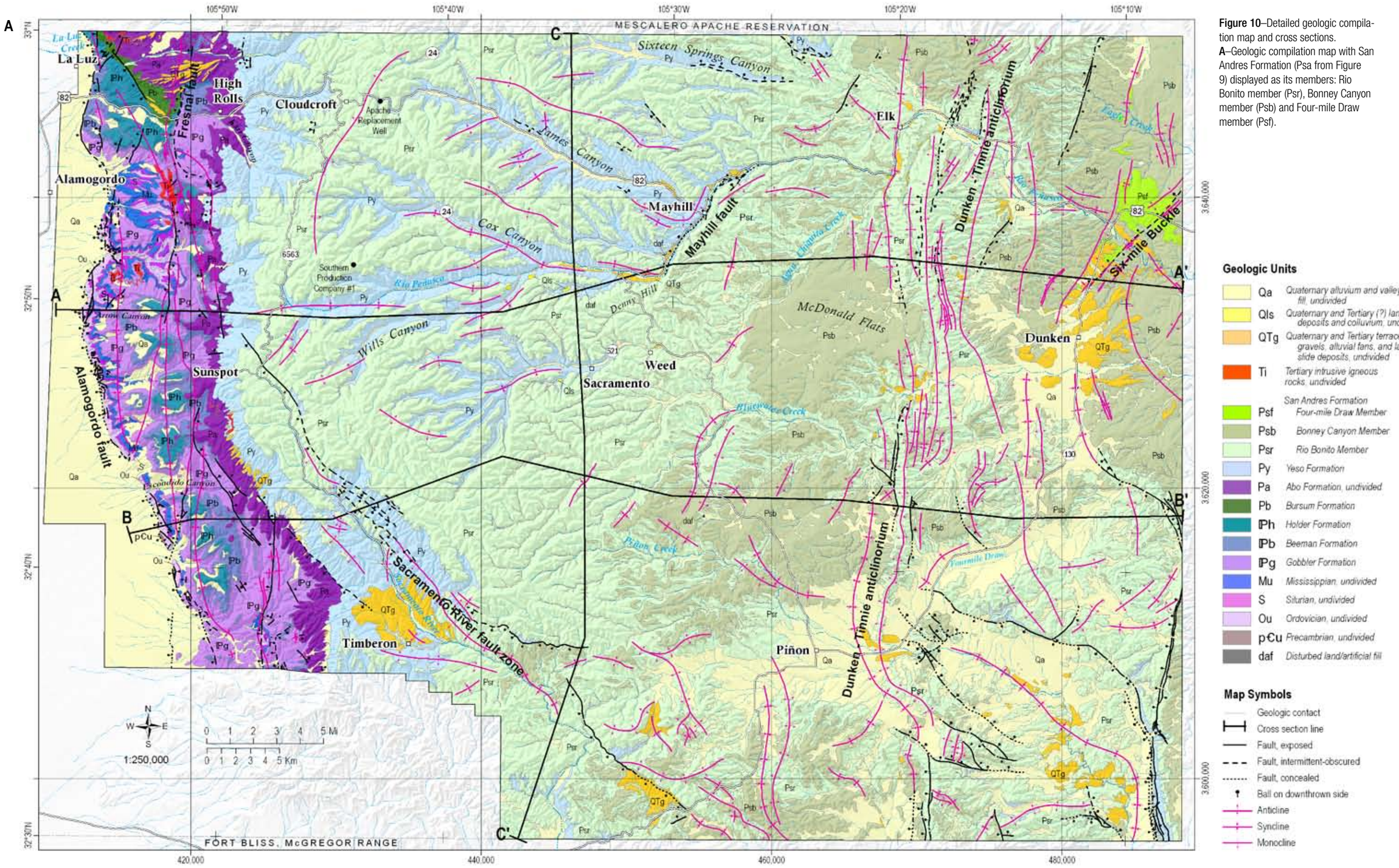

Figure 10–Detailed geologic compilation map and cross sections.
A–Geologic compilation map with San Andres Formation (Psa from Figure 9) displayed as its members: Rio Bonito member (Psr), Bonney Canyon member (Psb) and Four-mile Draw member (Psf).

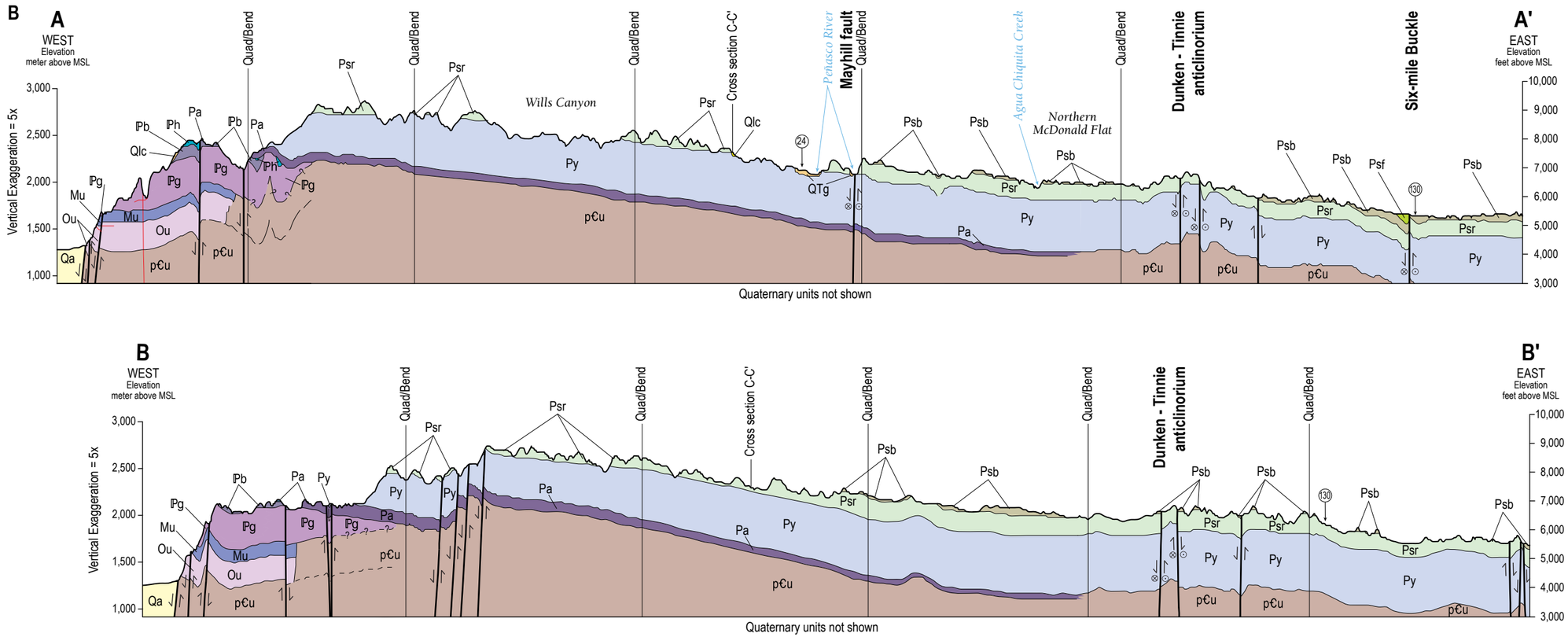

Map Symbols

Geologic contact

Fault

down up — Vertical motion

into page ⊗ out of page ⊙ — Horizontal motion

Scale 1:250,000

0 1 2 3 4 5 Mi

0 1 2 3 4 5 Km

Figure 10–Detailed geologic compilation map and cross sections.
B–Geologic cross sections along west-east transects (A-A' and B-B') and north-south transect (C-C')

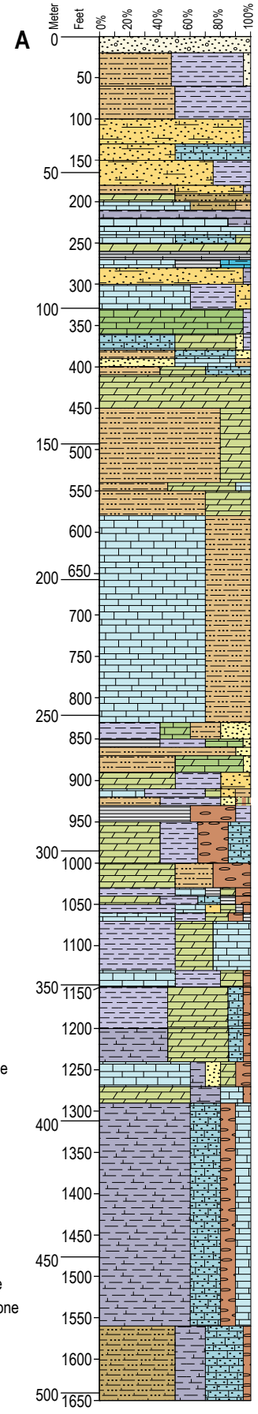

Figure 11–Stratigraphy and collapse features in the Yeso Formation.
A–A simplified lithologic log from the Village of Cloudcroft Apache replacement well illustrating the complex lithologies in the upper portion of the formation. Limestone, dolomite and claystone are the most abundant rock types. Well cutting descriptions are from Street and Peery (2007).

anticlinorium is a complex structure of sub-parallel anticlines and synclines and discontinuous east- and west-side-down faults, but overall is both a structural and topographic high where the Rio Bonito member is uplifted along the ridgeline (Fig. 10). Southeast- and north-south-trending faults of the Sacramento River valley and the northern Guadalupe Mountains east of Piñon are associated with very complex, though broad folding.

The complexity of faulting and folding in the southeast corner of the map area, near the southern termination of the anticlinorium, may be partly due to the interaction between the anticlinorium and the Six-Mile and Y-O buckles, two of the right-lateral strike-slip fault zones on the Pecos Slope (Kelley, 1971). The Six-Mile buckle enters the study area in the northeast corner, within the outcrop area of the Four-Mile Draw member. Synclinal folding associated with this buckle preserves the Four-Mile Draw member on the surface (Fig. 10). The Y-O buckle impinges on the mapped area about 15 miles to the south, where faults change trend from northwest-southeast to roughly north-south. Kelley (1971) and Black (1973) both interpreted the Dunken-Tinnie anticlinorium and the buckles as Laramide-age features. However, the deformation in the southeast corner of the mapped area may also be related to Rio Grande Rift extension, as extensional faults with Tertiary movement are present to the west in the Sacramento River valley and to the south along the west face of the Guadalupe Mountains. There are no fault scarps in the Quaternary units.

Structural contours derived from elevation points along the mapped San Andres-Yeso (Ps-Py) stratigraphic contact are illustrated in Figure 12. The elevation of the surface defining the contact between these two units decreases from more than 9,000 feet near the range crest to less than 7,200 feet on the east side of the Yeso outcrop belt. The structure contours indicate that the strata dip gently to the east from a broad anticline at the range crest. Troughs in the contoured surface along major drainages are broad folds that probably influenced the formation of the drainages and likely continue to influence local groundwater flow directions. Structural contours along the mapped contact between the Bonney Canyon and Rio Bonito members (Psb-Psr) of the San Andres Formation are also illustrated in Figure 12.

Limestone throughout the study area is deformed by joints, which are open fractures that have small displacements perpendicular to the fracture surface and negligible displacement in any other direction. Most fractures in the Sacramento Mountains are probably joints, but the terms are used interchangeably in this report. As part of this study, 170 joints at 70 sites were measured west of the Dunken-Tinnie anticlinorium in the high mountains (Walsh, 2008). Two predominant joint sets consistently orient NE-SW and NW-SE throughout the high mountain area (Fig. 13A). Outcrops containing joints occur at roadcuts, bedrock stream channels (Fig. 13B), and stream valley walls that are not covered with alluvium and/or vegetation. No consistent age relationship could be established between the joint sets.

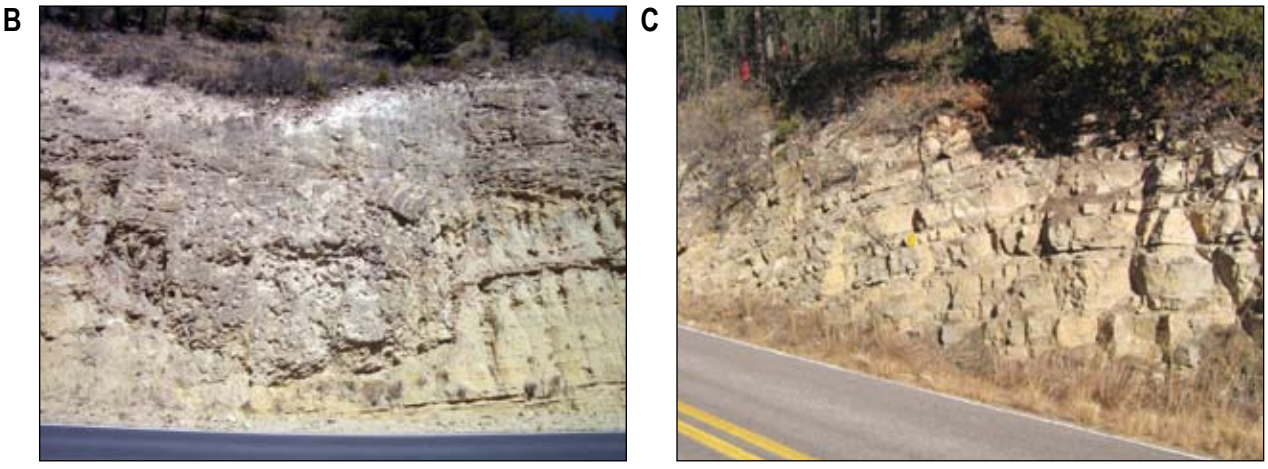

Figure 11–Stratigraphy and collapse features in the Yeso Formation.
B–Collapse feature visible in outcrop along Hwy 82 west of Mayhill. Collapse features result from dissolution of soluble rocks by groundwater, causing limestone beds to collapse, fracture, and form a chaotic breccia. Collapse breccias are common throughout the Yeso Formation and can disrupt the flow of groundwater along rock layers.
C–Rock layers in the Yeso Formation are laterally discontinuous due to faulting, folding, and dissolution of limestone, dolomite, and anhydrite. This broad fold visible in outcrop along NM 24 in Cox Canyon is typical of folding and collapse caused by dissolution of soluble rocks by groundwater over geologic time.

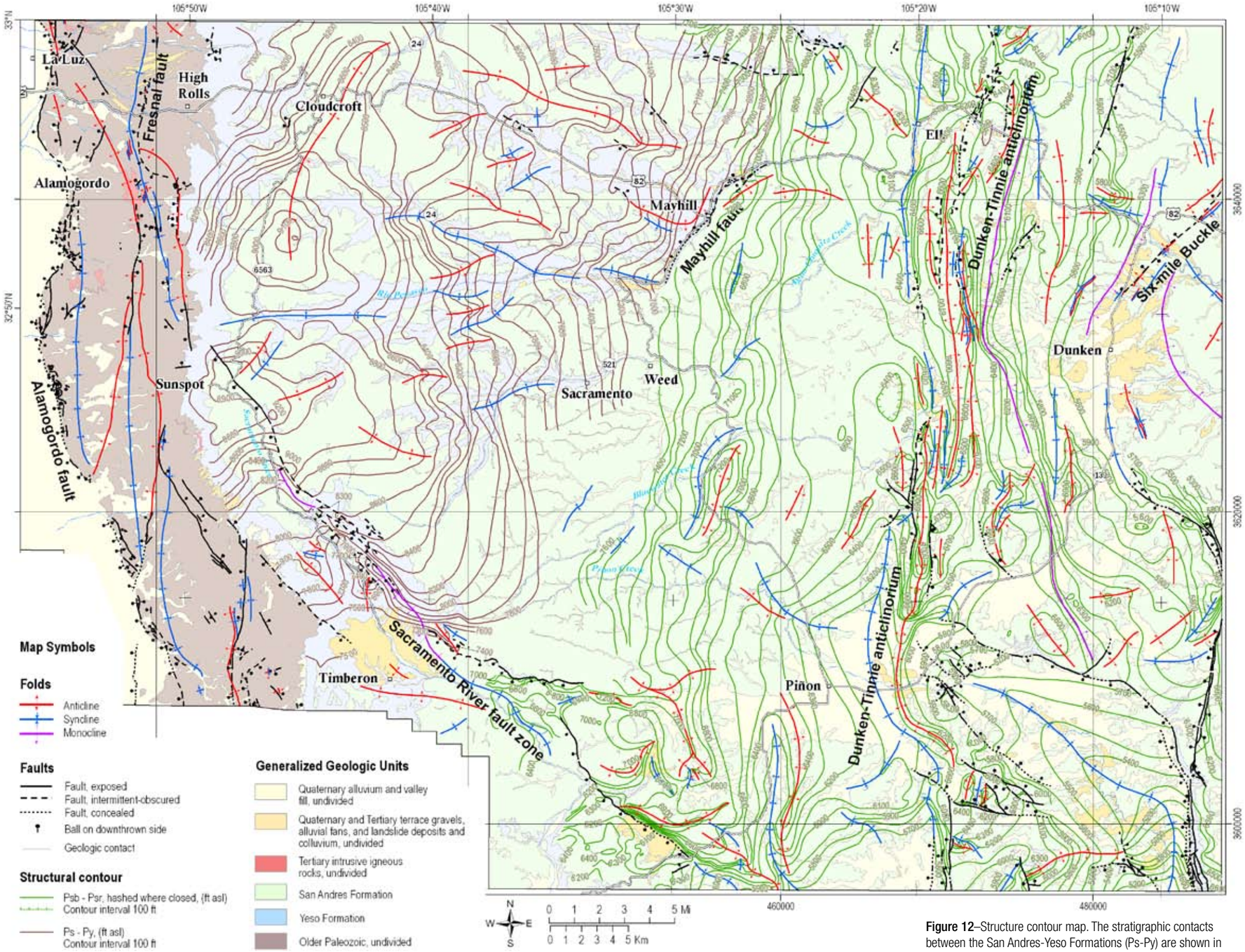

Figure 12–Structure contour map. The stratigraphic contacts between the San Andres-Yeso Formations (Ps-Py) are shown in brown. The contacts between the Bonney Canyon and Rio Bonito (Psb-Psr) members of the San Andres Formation are in green.

A

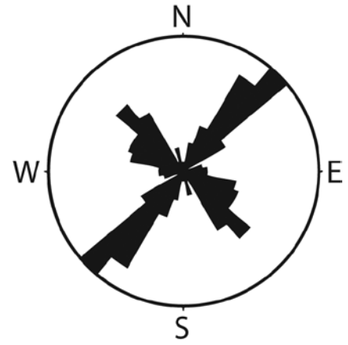

B

Figure 13–Joints in bedrock are pathways for recharge the shallow aquifer system.
A–Rose diagram of joint orientations. Each black triangle represents the number of joints within 10 degrees of an azimuth. The outer circle represents 16% of the total number of joints (27 of 170 joints). The two primary joint orientations observed are NE-SW and NW-SE.
B–Joints in bedrock exposure in Piñon Creek. The stream at this location is parallel to closely spaced joints. Joints beneath stream valleys, whether floored by bedrock or alluvium, are solution-enlarged and provide flow paths for surface water to recharge groundwater and for groundwater to discharge to streams and springs.

As part of this study, Walsh (2008) used field observations, aerial photo interpretation, and GIS analyses to document the influence of regional fracture trends and lineaments on stream valley orientations and spring locations. Several bedrock-floored stream channels have an orientation parallel to one of the fracture trends (Fig. 13), demonstrating that orthogonal NE-SW and NW-SE fractures exert a strong control on the orientation of stream valleys. These segments probably formed due to enhanced erosion and carbonate dissolution along zones of intense fracturing, which enlarges small fractures into large fissures and conduits and enhances groundwater movement.

Geomorphology

The Sacramento Mountains form a large, east dipping plateau uplifted along the steep western escarpment by the Alamogordo fault. The plateau is dissected by deep canyons, some more than 1000 feet deep, formed by the major east and south-flowing drainages of the Rio Peñasco, Agua Chiquita Creek, Bluewater Creek, Piñon Creek, the Sacramento River and their tributaries. These canyons are incised through the ridge-capping San Andres Formation into the less-resistant Yeso Formation. Valley floors are broad with alluvial deposits that are usually several feet thick. The valley floor deposits interfinger with alluvial fan deposits emanating from the numerous side canyons. Active and inactive spring mounds composed of porous calcareous tufa are common. Stream terraces are locally present, as are exposed ledges of resistant Yeso Formation limestone in stream channels. Bedrock-floored channels become more prevalent to the east in the Pecos Slope region.

Most of the upland surfaces of Pecos Slope are bare rock with thin soils, but locally there are relict gravel deposits. East of the study area, in the Roswell Artesian Basin, there are scattered low mesas capped with similar gravels, the surfaces of which project to the same plane as the western Pecos Slope. The gravel deposits have been described as correlatives of the upper Miocene to lower Pleistocene Gatuna, and/or Ogallala Formations by Kelley (1980), Frye et al. (1982), Hawley (1993a,b) and Powers and Holt (1993).

East of the Dunken-Tinnie anticlinorium, the Sacramento Mountains merge into a low-relief surface known as the Pecos Slope. The slope is broken by arroyos and canyons whose depths generally become shallower eastward toward the Pecos River. The linear, northeast-trending hills associated with the Border, Six Mile, and Y-O buckles are distinct features in an otherwise concordant upland surface that slopes to the east at 60-80 feet per mile.

Just east of Alamogordo, the western escarpment of the southern Sacramento Mountain range is characterized by numerous short, very steep canyons with steep bedrock walls and thin, gravelly fill. Bates (1961) documented numerous examples of recent and imminent stream capture along the Sacramento River drainage, wherein the much steeper west-draining canyons have beheaded east-draining canyons. Examples include the beheading of the uppermost Agua Chiquita Canyon by Scott Able Canyon and beheading of Broad Canyon by Monument Canyon.

HYDROLOGY

Precipitation

Precipitation is the primary source of groundwater recharge; thus it is important to understand regional climatic and geographic controls on the spatial and temporal variability of precipitation in the area. In this section we discuss important regional weather patterns and analyze existing local precipitation data.

Precipitation Patterns

In the Sacramento Mountains, the highest rainfall is associated with the North American Monsoon (NAM) and generally occurs during the summer months of July through September. These months usually account for about half of the annual precipitation, and in an average year, about 75% of annual precipitation will fall between the months of May to October. Monsoon rains are usually characterized by intense afternoon thunderstorms. Conversely, November through April is usually the driest period, with April typically the driest month (Malm, 2003). The spatial variability of precipitation is usually related to surface elevation. As air is forced up and over topographic features such as mountains, moisture within the air condenses and falls as precipitation. Therefore, areas of high elevation usually receive more precipitation than those at lower elevations.

The NAM is caused by northward movement of the subtropical ridge, an area of high pressure. During the summer months, as the surface is heated in the southwestern US, moisture from the eastern Pacific and the Gulf of California is transported into the region by the resulting low pressure trough. Moisture from the Gulf of Mexico is also drawn into the region at this time by easterly winds aloft (Liebmann et al., 2008, Stensrud et al., 1995, Gochis and Higgins, 2007, Ritchie et al., 2007, Ritchie and Szenasi, 2006, National Weather Service, n.d. a, National Weather Service, n.d. b, National Weather Service Southern Region Headquarters, 2006, National Weather

Service Climate Prediction Center, 2003). The strength and timing of the monsoon for any given year can be affected by factors such as sea surface temperature anomalies, large-scale circulation patterns, and land surface conditions within the monsoon region.

Tropical disturbances originating in the Gulf of Mexico or eastern Pacific can also add significant amounts of rain to southwestern US. These disturbances include tropical depressions, tropical storms, and hurricanes, and can contribute 25% to 30% of seasonal rainfall totals. Occasionally, decaying tropical storms will be caught in weakening monsoonal flows, and get swept across the southwest at the end of the monsoon season (National Weather Service Climate Prediction Center, 2003; Ritchie et al., 2007; Ritchie and Szenasi, 2006). Due to the topographic relief of the Sacramento Mountains and their proximity to the Gulf of Mexico, they are especially susceptible to these disturbances.

During the winter, frontal storms are the primary source of precipitation in the state. Mid-latitude frontal storms occur throughout the year, as relatively warm subtropical air mixes with cooler air, generating areas of high and low pressure that move eastward from the Pacific Ocean across the continent. The track of these storms shifts northward during the summer and southward during the winter as the Earth's surface heats and then cools. During the course of any given year, frontal storms lasting from 3 to 10 days move eastward from the Pacific and routinely cross New Mexico. Although frontal storms cross New Mexico frequently, their contribution to annual precipitation totals is modest. As these storms move onshore from the eastern Pacific, they are forced up and over mountains and topographic highpoints in California, Nevada, and Arizona, and by the time they reach New Mexico, they have usually lost most of their moisture (Bell, 1979).

Large-scale fluctuations in heating and cooling of the Pacific Ocean can also alter the prevailing storm track. During some years, unusually warm waters develop off the coast of South America, causing the dominant storm track to shift southward, increasing the contribution of winter storms to annual precipitation totals in the Southwest. This warm phase is called an "El Niño" event. At other times, cool water develops along the South American coast, pushing the storm track northward, thereby decreasing the contribution of frontal storm systems to precipitation totals in New Mexico. This cooler phase is called a "La Niña" event. La Niña winters typically produce only half to one-third of the precipitation dropped during El Niño winters in the Southwest (Ahrens, 2003).

Historic Precipitation

Daily precipitation amounts have been recorded in the Sacramento Mountains and vicinity for most of the past century, with some records dating back to 1895 (Table 2). These detailed records are available from the Western Regional Climate Center, National Oceanic and Atmospheric Administration (NOAA) (see http://www.wrcc.dri.edu/summary/climsmnm.html). Portions of this record have been compiled to show general trends in annual and seasonal precipitation in the study area. Average annual precipitation ranges from ~26.9 inches/year in Cloudcroft to 16.5 inches/year in Elk. Figure 14 shows a linear regression for average annual precipitation reported at weather stations listed in Table 2, as a function of elevation.

Table 2–NOAA weather stations within the region used for examination of historic precipitation.

Station	Station Number	Elev (ft)	Period of Record	Years*
White Sands National Monument	299686	3,990	1939 to 2007	68
Hope	294112	4,100	1919 to 2007	88
Orogrande	296435	4,180	1914 to 2007	93
Alamogordo	290199	4,350	1914 to 2007	93
Tularosa	299165	4,540	1914 to 2007	93
Elk	292865	5,710	1895 to 2007	112
Mayhill Ranger Station	295502	6,550	1917 to 1976	59
Mescalero	295657	6,790	1914 to 1978	64
Mountain Park	295960	6,790	1914 to 2007	93
Ruidoso	297649	6,860	1942 to 2007	65
Cloudcroft**	291927/ 291931	8,810	1914 to 2007	93

* = entire span may include gaps

** = combined record for Cloudcroft stations 291927 (1914 to 1987) and 292931(1987 to 2005).

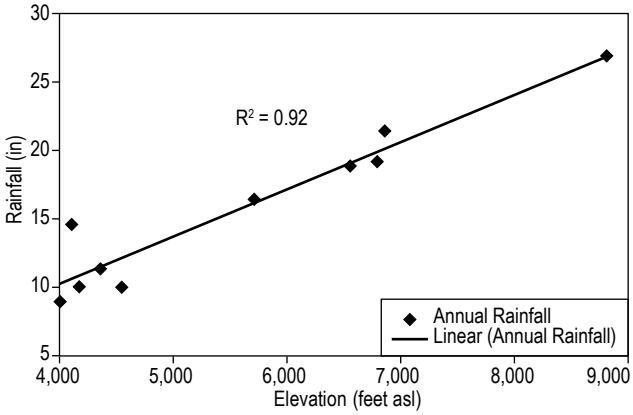

Figure 14–Average annual precipitation versus elevation. The total annual precipitation at weather stations listed in Table 2 increases linearly with elevation, indicating that there is more precipitation at higher elevations than at lower elevations.

Correlation with elevation is good with an R^2 value of 0.92, indicating that elevation is a strong predictor of average annual rainfall in the study area.

Extreme rainfall events and seasons can and do occur that significantly alter annual precipitation totals for a given location. Extreme rainfall years can be the result of a single storm event, season-long conditions such as those which accompany a major El Niño event, or a confluence of both seasonal factors and individual storm events. During this study, the Sacramento Mountains experienced above-average summer precipitation during 2006 and 2008. Figure 15 shows the probability of exceedance curves for annual and monthly precipitation amounts recorded at Cloudcroft between 1914 and 2008. The total annual precipitation at Cloudcroft in 2006 exceeded 40 inches with a probability of exceedance of about 3% and an average recurrence interval of 33 years (Fig. 15A). During the summer of 2006, an exceptional monsoon season produced high precipitation amounts between July and September. The total annual precipitation in 2008 was approximately 30 inches with a probability of exceedance of 24% and an average recurrence interval of 4.2 years. When looking at the total annual precipitation amounts, 2008 does not stand out as much as 2006. However, July of 2008 was the wettest month on record with a probability of exceedance of 1% and an average recurrence interval of 95 years (Fig. 15B). The remnant of Hurricane Dolly was responsible for approximately half of the annual precipitation that fell in July 2008, and produced locally heavy rains in the Sacramento Mountains for a few days (Pasch and Kimberlain, 2009).

Extreme rainfall events or seasons are of particular importance in terms of their potential impact on groundwater recharge, especially when topography is considered. High elevation areas receive more rain and snow, and the lower temperatures characteristic of these locations increase the length of time that snow remains on the ground and help minimize evaporation of monsoon rainfall. Taken together, these climatic factors suggest that 1) high elevation areas are important to groundwater recharge, and 2) extreme rainfall events or seasons impacting high elevation portions of the study area will significantly influence groundwater recharge and the local water table.

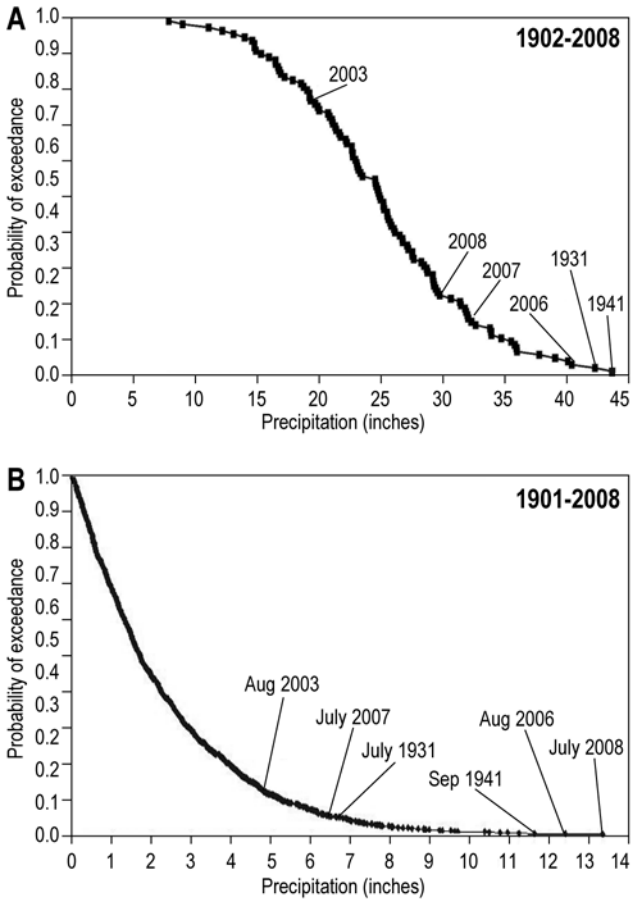

Figure 15–Probability of exceedance curves for annual precipitation and monthly precipitation in Cloudcroft.
A–Probability of exceedance curve for annual precipitation in Cloudcroft (1902–2008) shows the probability of the total annual precipitation exceeding a specific value. During this study, from 2005 to 2009, several years had exceptionally high annual precipitation, particularly 2006, which had over 40 inches.
B–Probability of exceedance curve for monthly precipitation in Cloudcroft (1902–2008) shows the probability of the total monthly precipitation exceeding a specific value. July 2008 stands out as the wettest month on record, although 2008 did not have an extremely high annual precipitation.

Streams and drainage basins

East of the crest of the Sacramento Mountains, stream valleys generally drain eastward toward the Pecos River (Fig. 2). The orientations surface water drainages are strongly affected by the regional dip of bedrock and regional fracture systems (Walsh, 2008). Figure 16 shows surface water drainage basins and perennial stream reaches in the study area. Valley bottoms have approximately the same overall dip as the San Andres - Yeso geologic contact (2-3°). However, short stretches are steep, even approaching vertical, and others are nearly horizontal. Small wetlands are common in the flat sections of stream valleys, especially around springs and at the heads of perennial reaches of streams. Saturated soil and single or multiple coalescing drainages characterize these wetlands. Such spring-fed wetlands typically evaporate more water than steeper, flowing stream channels because they have much larger surface area and nearly stagnant water. Both the headwaters and downstream reaches of the Sacramento River, upper

Figure 16–Surface water drainage basins and perennial stream reaches. Few streams in the Sacramento Mountains are perennial. Perennial flow, depicted in dark blue, typically only occurs over short distances before infiltrating to shallow groundwater.

and lower Rio Peñasco, Wills Canyon, and Agua Chiquita Canyon have these types of wetlands.

Very few streams in the Sacramento Mountains are perennial (Fig. 16). Perennial flow only exists over relatively short distances before infiltration to the shallow groundwater system. Base flow is the portion of streamflow that is attributable to groundwater discharge into the stream bed. In the arid southwestern United States, perennial streams typically approach base flow between late fall, after cessation of monsoons, and spring, before snowmelt runoff begins. During the extremely dry winter of 2007-08 and spring 2008, streamflow rates and the extent of perennial reaches decreased throughout the Sacramento Mountains between November and April (Table 3). Stream discharge measurements are presented in Appendix 5.

Near Mayhill, the Rio Peñasco has a 4-mile perennial reach that coincides with the Mayhill fault (Figs. 10A and 16). This fault appears to affect streamflow. Flow measurements in November 2007 showed a steady increase in discharge from 9.7 cubic feet per second (cfs) upstream of the fault, to 13.5 cfs about 1 mile upstream of Mayhill, to 15.7 cfs approximately four miles downstream of Mayhill. We attribute much of this inflow to Posey Spring (SM-1076), which is located on the fault trace (Fig. 17B).

Table 3—Repeat stream flow measurements and reduction in flow length of three perennial streams between November 2007 and April 2008. Measurements are made in cubic feet per second (cfs).

Stream	Flow rate (cfs) November, 2007	Flow rate (cfs) April, 2008	Reduction in stream length between Nov. and April (miles)
Wills Canyon	0.6	0.4	2
Agua Chiquita	4.1	2.0	>2
Sacramento River	2.17	0	3

Springs

Springs are common throughout the southern Sacramento Mountains and are the primary source for all perennial and ephemeral streams (Fig. 17). Of the 93 springs that we inventoried, 80% of them are located above 7,400 feet (west of Mayhill). The largest density of springs is located along the upper Rio Peñasco and in Wills Canyon. Springs are found on both hillsides and canyon floors and are stratigraphically controlled. Most springs discharge from perched aquifers in fractured limestone beds overlying relatively impermeable red mudstones in the upper 200-230 feet (60-70 meters) of the Yeso Formation (Walsh, 2008).

Many springs discharge into stream beds that convey water along the surface for some distance, while others discharge water that almost immediately infiltrates into the stream bed downstream. Springs are preferentially located along stream reaches parallel to regional fracture trends and decrease in abundance away from these streams (Walsh, 2008). These observations indicate that bedrock fractures are preferential groundwater flow paths and influence surface water patterns as well.

Spring discharge rates are generally low, less than about 0.04 cfs (20 gallons per minute (gpm)), but a few springs discharge more than 0.22 cfs (100 gpm). Two examples of high-discharge springs are Posey Spring (SM-1079) near Mayhill and Monument Spring (SM-1076) near Timberon (Fig. 17B, C). Posey Spring discharges into a large pond and contributes significant

flow to the Rio Peñasco. There is a nearly 4-foot high boil of turbulent sediment over the spring outlet on the floor of the pond. Total discharge has been estimated to be approximately 3.8 cfs (1700 gpm) (R.L. Posey, personal communication). Monument Spring discharges turbulent water from a cavernous solution-enlarged fracture in limestone of the San Andres Formation, at the contact with the underlying Yeso Formation.

Many springs in the study area show evidence of calcareous tufa precipitation, and many are located on or near large tufa mounds (Fig. 17C, D). In addition, there are numerous fossil spring mounds composed of tufa overgrown with vegetation, which suggest ongoing dynamic fluctuations in the shallow groundwater system as spring outlets progressively dry and/or plug with precipitated carbonate minerals.

Groundwater

Hydrostratigraphic units

Based on surface geologic mapping, spring surveys, and lithologic logs in water well records, the Yeso Formation, a heterogeneous unit of limestone, shale, siltstone, and sandstone, is the primary source of groundwater west of Mayhill. Water-bearing zones are distributed vertically and laterally throughout the formation and connected by local and regional fracture systems. Most springs discharge from discontinuous, perched aquifers in the Yeso Formation, but distinguishing between these local perched aquifers

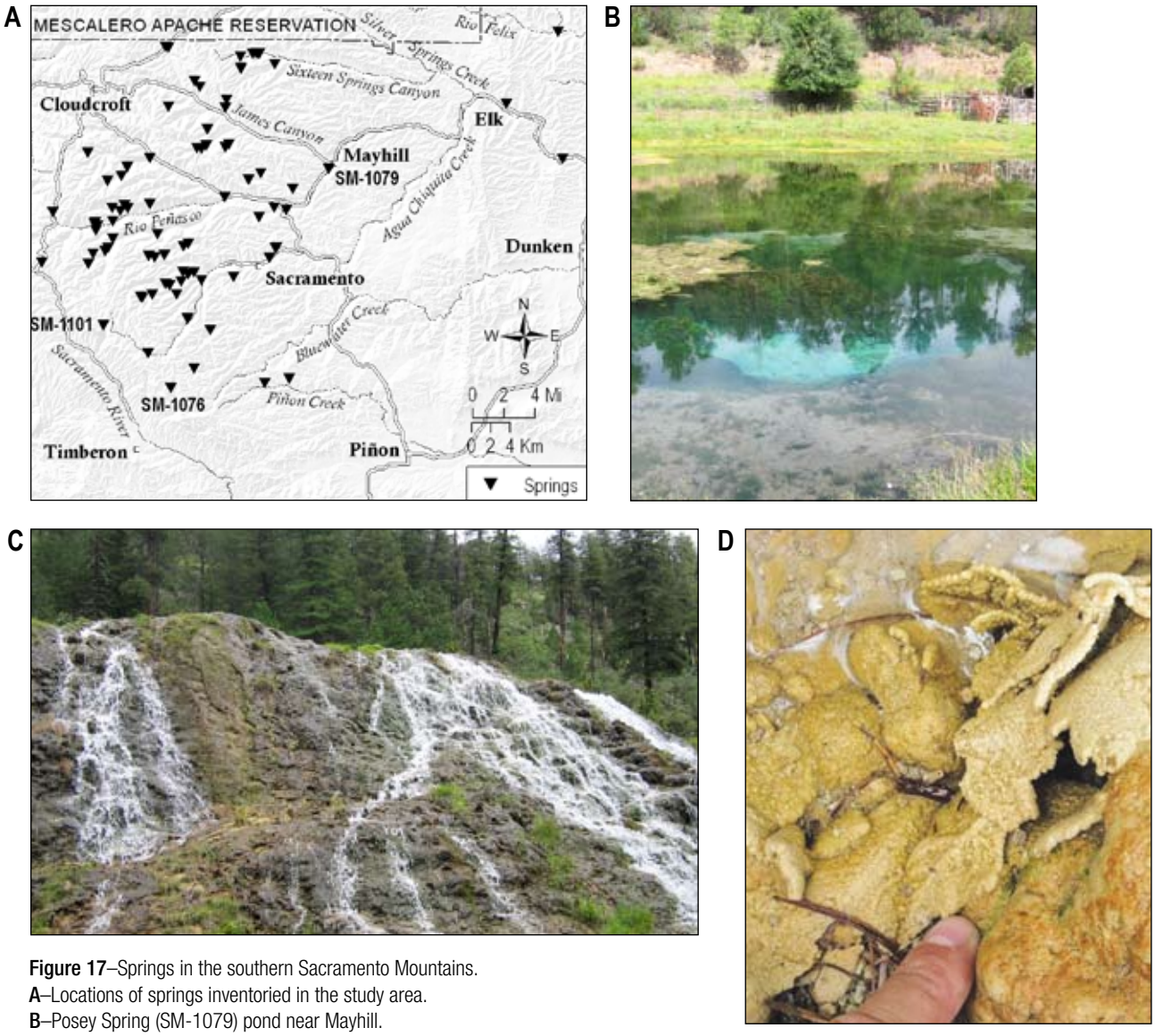

Figure 17–Springs in the southern Sacramento Mountains.
A–Locations of springs inventoried in the study area.
B–Posey Spring (SM-1079) pond near Mayhill.
C–Monument Spring (SM-1076) tufa mound near Timberon.
D–Tufa precipitation on leaves and rocks from spring discharge in Scott Able Canyon (SM-1101).

and the regional aquifer is often difficult. Subsurface correlations of individual beds within the Yeso Formation are tenuous due to complex stratigraphic variation and dissolution-induced collapse (Fig. 11B). In approximately 80% of wells with lithologic logs (Appendix 2), the water producing intervals are composed of either fractured limestone or collapse breccias within the Yeso Formation. The remaining wells are completed in shallow valley-bottom alluvium or spring deposits.

To the East of Mayhill, along the Pecos Slope, wells are completed in both the Yeso and San Andres Formations. In the subsurface, the Yeso Formation is still the primary aquifer, as saturated zones of the San Andres occur in only the lower portions of the formation. In contrast to the groundwater system in the high mountains, along the Pecos Slope, the saturated zone in Yeso Formation likely occurs in the bulk formation, rather than in specific rock types. The San Andres Formation becomes more important as a regional aquifer in the eastern portion of the study area. The saturated zones in the San Andres Formation are often karstic, characterized by large conduits and sink holes. The Glorieta Sandstone in the San Andres Formation is not a significant water-bearing interval because it is thin in the study area and generally lies above the zone of saturation, except perhaps east of the Dunken-Tinnie anticlinorium where water-levels rise into the lower San Andres Formation.

Groundwater flow conditions

We created a map of the regional water table in the southern Sacramento Mountains (Fig. 18), which is available as NMBGMR Open-file Report 542. Data used to contour the water elevations are presented in Figure 19 and Appendix 6. Contours of the regional water table elevation in the study area were drawn by hand based on water-level measurements made between 2005 and 2009. The water-level elevations from wells were combined with spring elevations and valley floor elevations along the reaches of perennial streams. In locations where these data were not available, static water-levels were used from selected, recent (year 1995 or newer) New Mexico State Engineer Office well records. No attempt was made to distinguish between perched and regional aquifers for contouring.

Regional groundwater flow is driven by the topographic gradient from high to low elevations (Fig. 18). Water elevation contours range from 9,000 feet, near the crest of the Sacramento Mountains, to 3,600 feet, near the eastern margin of the study area. The groundwater mound enclosed by the 8,200-foot water table elevation contour delineates the primary recharge area along the crest of the mountain range. By assuming that hydrologic properties of the aquifers are isotropic on a regional scale, we approximate horizontal groundwater flow perpendicular to groundwater elevation contours and down gradient to the east, west, and south. Locally, groundwater flow velocity and direction are influenced by geology (rock type, bedding dip, and geologic structures) and hydrologic characteristics such as porosity, permeability, and aquifer thickness. In reality, local groundwater flow directions may differ from that indicated by the regional groundwater surface (Fig. 18). The water table at lower elevations on the Pecos Slope is a subdued reflection of the regional topography and indicates that groundwater generally flows east toward the Pecos Valley and southeast toward the Salt Basin.

Spacing of the groundwater elevation contours on Figure 18 defines the hydraulic gradient, which is the vertical change in water table elevation over a lateral distance. The water table is steepest west and southwest of the crest of the Sacramento Mountains, with gradients close to 500 feet/mile, or about 5 degrees. These steep gradients are associated with the steep topography of the western escarpment, and strongly folded and faulted strata, which form low permeability zones that likely impede or restrict horizontal groundwater movement.

East of the crest, hydraulic gradients range from approximately 150 to 220 feet/mile and are greater than the stratigraphic dips in Yeso and San Andres Formations. Groundwater flows across bedding planes and permeable rock layers, enhanced by fractures. East of Mayhill, on the Pecos Slope, the hydraulic gradient flattens to about 100 feet/mile in the vicinity of Dunken, and to less than 50 feet/mile west of the village of Hope. Stratigraphic dip is generally steeper than the hydraulic gradient beneath the Pecos Slope. Eastward-flattening of the water table indicates areas where groundwater flows through high-transmissivity limestone in the San Andres Formation, which contains large cavernous fractures and sinkholes. This is particularly noticeable across McDonald Flats, where the slope of the water table is less than 48 feet/mile. Geologic structures such as the Dunken-Tinnie anticlinorium also produce a local steepening of the hydraulic gradient east of McDonald Flats.

A depth-to-water map was also created based on our extensive data set of wells and springs (Fig. 20). The hydrology of the aquifer system above about 7,400 feet land surface elevation, east of Mayhill, is very complex (large, dark blue region, Fig. 20). This region of the high mountains is where the majority of springs are located. It is complicated due to: 1) high topographic relief in canyons and watersheds, 2) the

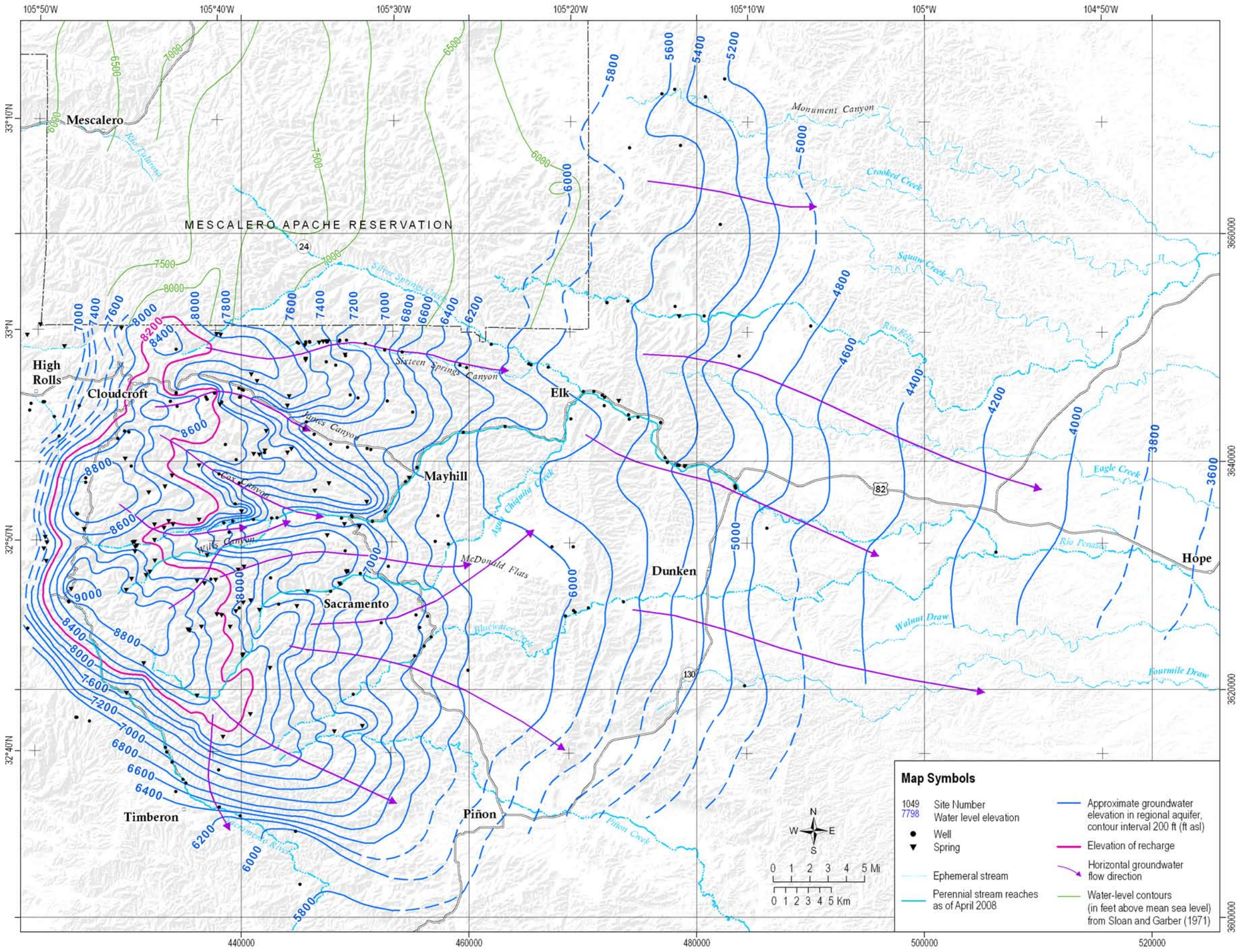

Figure 18–Water table surface map for the Sacramento Mountains. Average water-level elevation contours (in feet) show that regional groundwater movement is controlled by topography. Groundwater flows from the crest of the mountains to lower elevations east, west and south. Contours do not distinguish between perched and regional aquifers. The actual direction of groundwater flow at a local scale, particularly in the high mountains, may differ from that indicated by the regional elevation contours due to lithologic heterogeneities of the Yeso Formation, the presence of regional fracture systems, and variation in topographic relief. Most groundwater recharge occurs near the crest of the Sacramento Mountains above the 8,200-foot water-level contour (pink-line).

presence of local and regional fracture systems, and 3) the lateral and vertical distribution of different lithologies in the Yeso Formation. Depth to water in shallow (less than 300-foot) wells ranges from 4 to 233 feet and averages 99 feet. Wells completed in deeper aquifer zones (greater than 300 feet) generally have deeper water-levels that range from 65 to 420 feet and average 260 feet in depth. This observation suggests that an overall downward hydraulic gradient exists, in addition to a strong horizontal gradient. Areas with depths to water of 100 to 500 feet occur at high elevation, most prominently in James Canyon along US Highway 82 between Cloudcroft and Mayhill (Fig. 20). Depth to water on the Pecos Slope, which is generally deeper than in the high mountains, ranges from 4 to 900 feet, with an average of 297 feet.

Water-level changes and hydrographs

By comparing changes in water-levels, in wells of various depths and completions, to the timing and magnitude of local precipitation events, we can broaden our understanding of the hydrodynamics and physical properties of the various aquifers. To evaluate water-level responses to precipitation, continuous water-level records from four wells and hydrographs from 11 selected wells that were measured monthly and bimonthly are plotted with daily precipitation recorded at NOAA weather stations near Cloudcroft (Figs. 21A and 22A). These wells range in depth from 30 feet (SM-0026) to over 700 feet (SM-0055), and are distributed from the crest of the mountain block to just east of Mayhill (Figs. 21B and 22B). Monthly and bimonthly water-level data are presented in Appendix 3, and continuous water-level records are available electronically in Appendix 4.

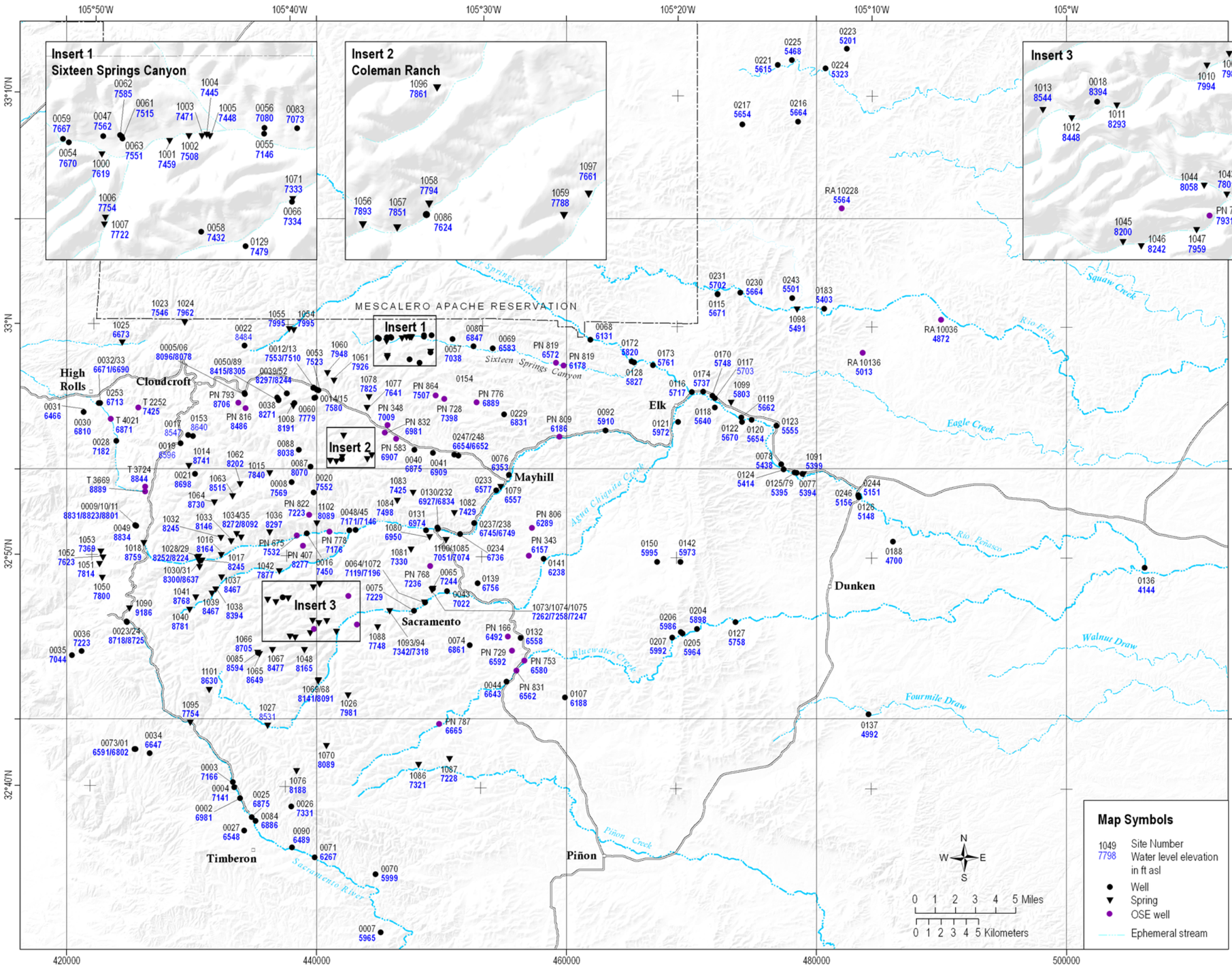

Figure 19–Control points for water-level elevation contours. Contours were drawn by hand based on water-level measurements made for this study between 2005 and 2009 (see also Appendix 6). The water elevations measured in wells were combined with spring elevations and valley floor elevations at perennial reaches of streams. Static water-levels from select well records (year 1995 or newer) on file in the New Mexico Office of the State Engineer were used to fill data gaps.

The water-level trends are quite varied. However it is clear from the data that the extremely wet summers of 2006 and 2008 produced significant recharge events, as did the winter of 2006-07 to a lesser degree. Infiltration of rain and snowmelt during these time periods induced water-level rises in most wells in the study area. Two general trends in timing of water-level rises and subsequent declines are observed from the well hydrographs (Figs. 21 and 22).

(1) Short-Term Response (STR)—With few exceptions, these wells are less than 300 feet in depth and located above about 8,000 feet in elevation in the high mountains west of Mayhill. The well hydrographs (Fig. 21A) demonstrate rapid water-level rises that correlate directly with large summer monsoon precipitation events during 2006 and 2008, and reach peak levels within one to three months. In the case of SM-0049, the first water-level rise in response to the 2006 summer monsoon takes a mere 3 hours from the base to the peak of the rising limb. The falling limbs show protracted water-level declines along exponential recession curves. Water-level rises ranged from 4 to 70 feet in 2006 and 2 to 35 feet in 2008 (Table 4). Larger rises during the 2006 monsoon season reflect the larger volume of rain and the more gradual precipitation rate. These

Table 4–Water level increases from well hydrographs in response to recharge events in 2006 and 2008.

	Total water level increase (feet)			
	2006		2008	
	Min.	Max.	Min.	Max.
Short-Term Response wells	4	70	2	35
Long-Term Response wells	20	116	5	45

shallow wells are completed in the perched and shallow regional aquifer systems in the high mountains, except for SM-0026 and SM-0044, which are located in the upper Salt Basin and Pecos Slope, respectively.

(2) Long-Term Response (LTR)—All of these wells are completed in the deeper horizons of the regional aquifer west and north of Mayhill; most are greater than 300 feet in depth. The well hydrographs (Fig. 22A) generally show slow water-level rises starting in late summer and fall of 2006 that leveled off before increasing again in response to precipitation events during the summer 2008. At the end of the monitoring period in June 2009, water-levels in these wells remained at or near peak magnitudes, with no defined hydrograph recession. Water-level increases during the 2006 monsoon season ranged from 20 to 116 feet and for 2008 ranged from 5 to 45 feet (Table 4).

Recharge to a fractured or karst aquifer via infiltration of precipitation or streamflow can produce a rapid increase in spring discharge and water-levels in wells. The shape of the hydrograph – the form and rate of recession, in particular – provides significant information on the storage and structural characteristics of the aquifer system sustaining the spring or producing water to the well, including quantitative and qualitative information on aquifer properties (transmissivity (T), storativity (S), and diffusivity (T/S)) and the hydrodynamics of the aquifer (matrix versus conduit flow) (Powers and Shevenell, 2000; Bailly-Comte et al., 2010). The various forms of spring discharge hydrographs have long been used as indicators of the role of conduit versus matrix flow in karst aquifers (Bonacci, 1993; Ford and Williams,1989, 2007). Recently, Bailly-Comte et al. (2010) interpret spring and well hydrographs in terms of water exchange and pressure transfers between conduits and matrix. Qualitative interpretations of the hydrodynamics of the perched and shallow aquifers based on STR well hydrographs are discussed below. A quantitative analysis of aquifer properties in a shallow zone of the high mountain aquifer based on the SM-0049 well hydrograph is presented in Appendix 9.

A rapid water-level rise from low water table conditions, followed quickly by an exponential recession curve, as observed in the SM-0049 hydrograph in August 2006 and July 2008 (Fig. 21A), follows the shape of an ideal well or spring hydrograph from a karst aquifer and reflects the movement of infiltration and recharge from the storm event through the unsaturated and saturated aquifer zones (Ford and Williams, 2007, 1989). The August 1, 2006 storm event hydrograph (Fig. 23) nicely demonstrates fast percolation of rainfall and displacement of storage water from various zones of a karst aquifer. A rapid water-level rise of 17 feet over a 3-hour period (from 11:00 to 14:00) indicates recharge occurring through conduit flow that likely involved no water exchange between conduits and matrix. Water transfer from the conduits to the matrix occurred over the next 1.5 hours (14:00 to 15:30) as the rising limb flattened to its peak level.

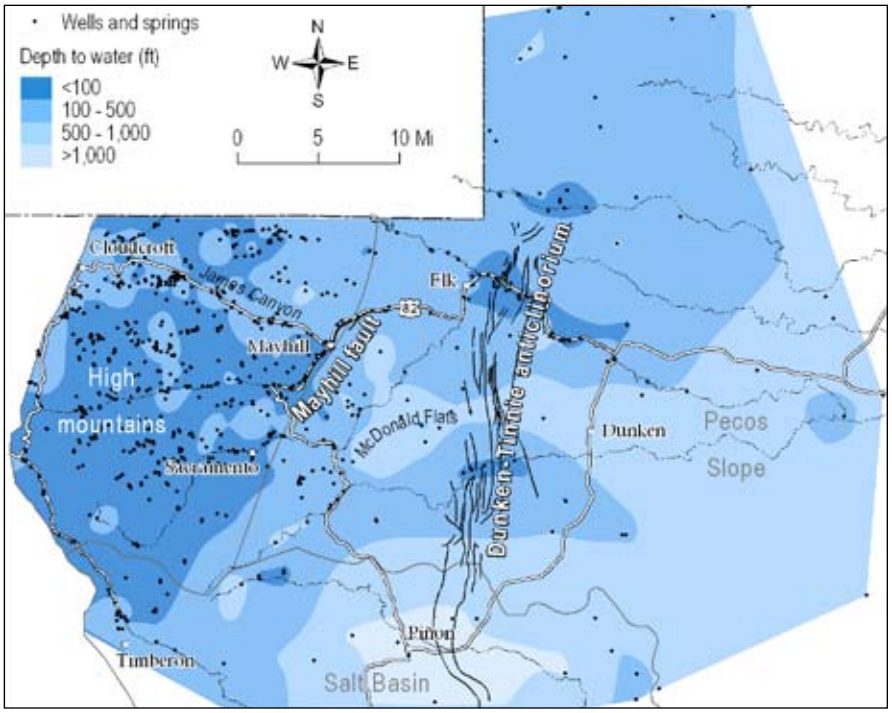

Figure 20–Map of depth to groundwater created from spring locations and depth-to-water measurements in wells. Static water-levels from well records on file with NM State Engineers Office drilled after 2000 were used to supplement this study's well monitoring network to create this map.

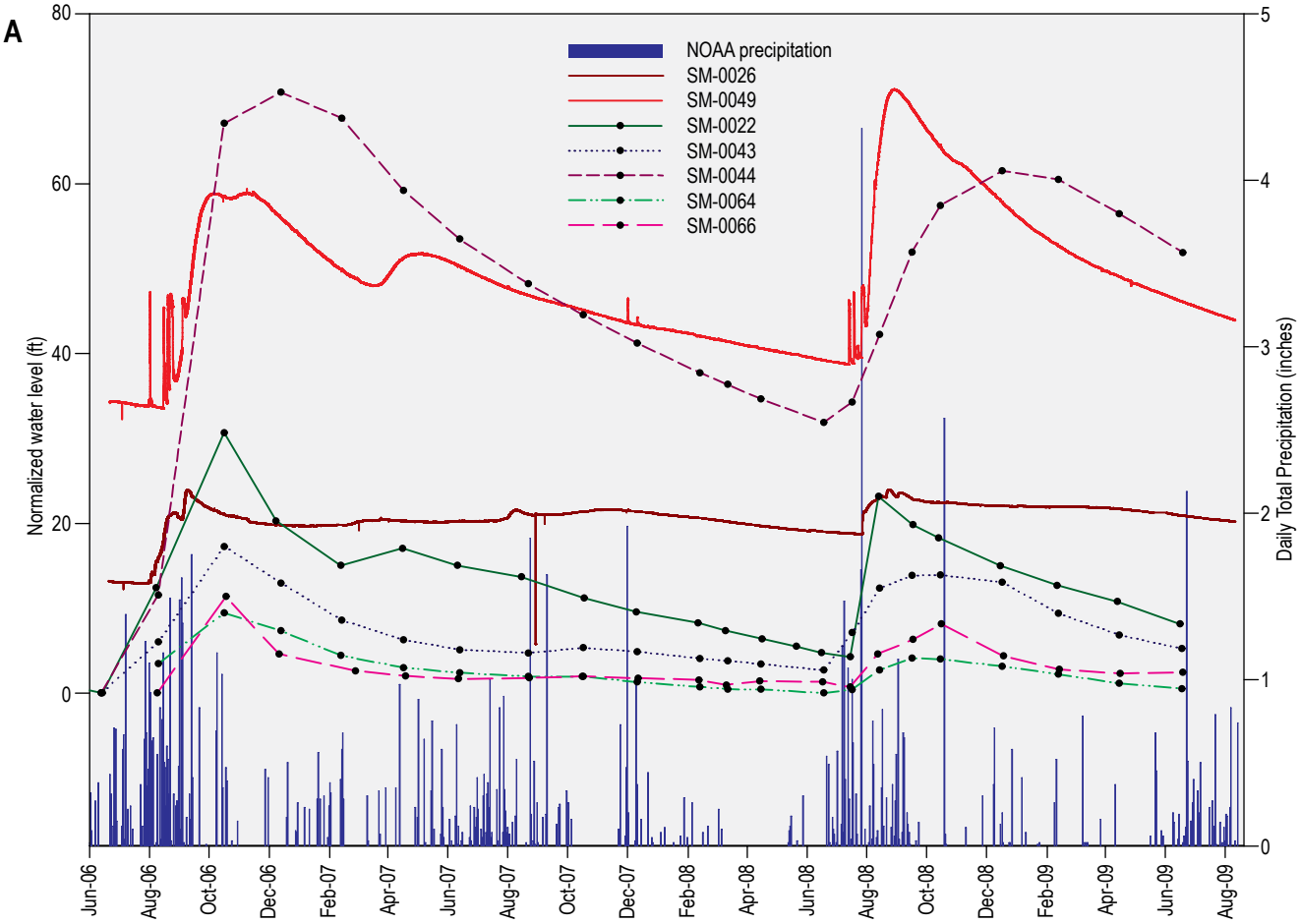

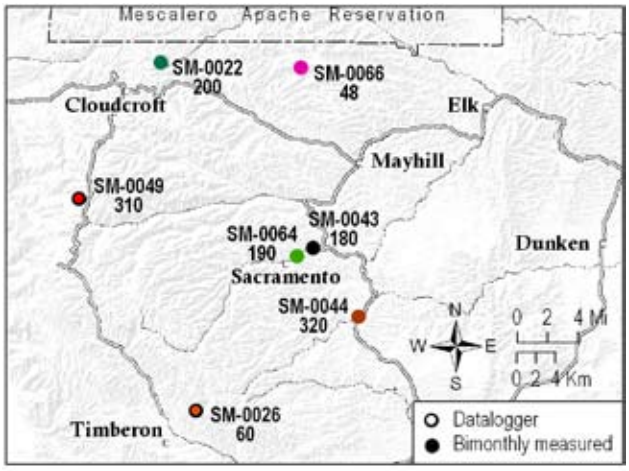

Figure 21–Hydrographs showing a short-term water-level response to precipitation.
A–The hydrographs (curves) show rapid water-level responses to precipitation in five wells with monthly and bimonthly measurements and two wells with continuous water-level recorders. The vertical bars show total daily precipitation at several weather stations near Cloudcroft
B–Locations of short-term-response (STR) wells shown in the hydrograph, with total well depth (in feet) below point label.

The hydrograph peak occurs when the storage in the system is at its maximum. In a karst or fractured system, the exponential decrease in hydraulic head (e.g. Aug 1, to about Aug 2, 10:00) observed in all STR wells when recharge ceases or becomes negligible, generally indicates slow drainage from a saturated porous matrix (intergranular and/or fracture porosity) into higher transmissivity fractures. The exponential shape of the recession curve is characteristic of a matrix-dominated flow regime and is explained by slow transfer of water from the saturated matrix back to fractures and/or conduits, which either discharge to the numerous springs or recharge deeper levels of the regional aquifer.

Hydrographs from LTR wells (Fig. 22B), which show a slow water-level rise and little or no decline, cannot be interpreted through hydrograph separation techniques as water-level monitoring did not capture flow recession. Persistent high water-levels following the hydrograph peak usually indicate a flow constriction or low-permeability barrier down gradient in the aquifer that prevents the aquifer from draining quickly. In this case, it may simply reflect convergence between the deeper regional

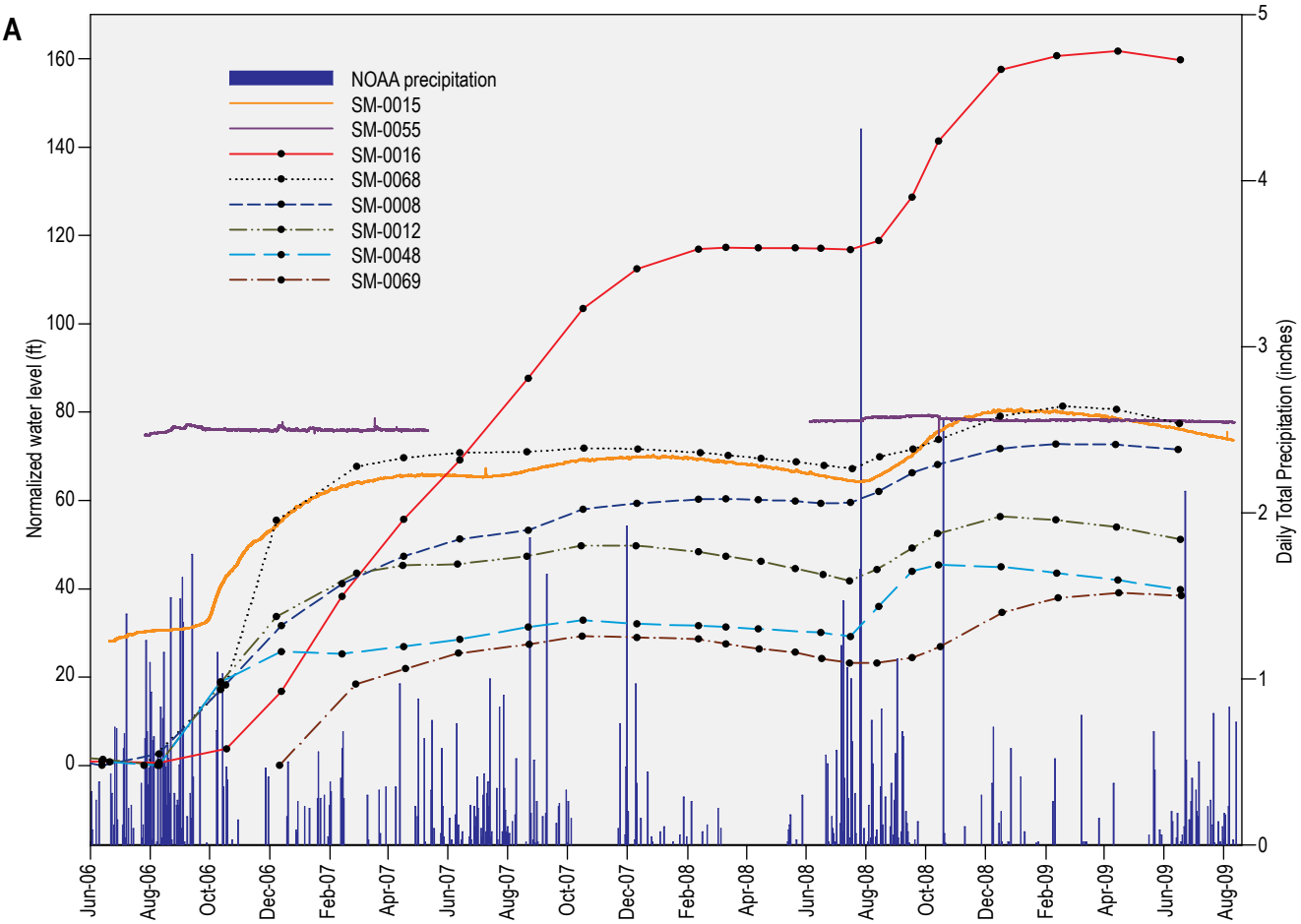

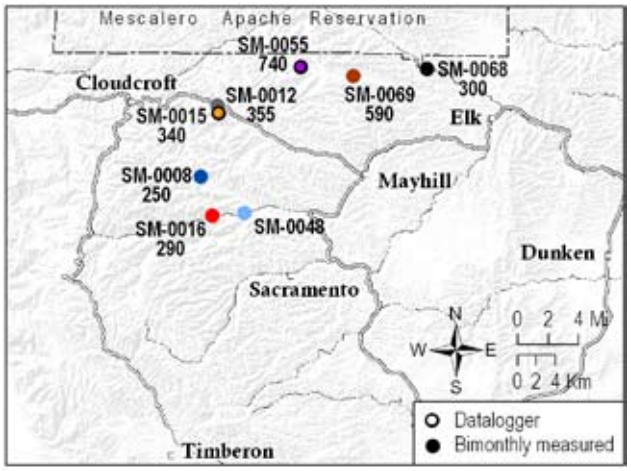

aquifer in the high mountains with the regional Pecos Slope aquifer. The deep LTR wells are completed across large aquifer intervals and are more representative of deep regional flow conditions than the shallower STR wells. The similarity in hydrographs between wells in proximity to one another (for example, STR wells SM-0043, SM-0044, SM-0049, SM-0064, SM-0066 (Fig. 21), and LTR wells SM-0008, SM-0012, SM-0015, SM-0048, SM-0068 and SM-0069 (Fig. 22)) indicates hydraulic connection through the portion of the aquifer represented in the wells. In general, the hydrographs for deep wells that respond slowly to precipitation input are quite similar throughout the highlands west of Mayhill.

The well hydrographs (Figs. 21 and 22) also show that mild monsoon seasons do not have a significant effect on groundwater-levels. The monsoon season of 2007 was above average (Fig. 15), but stimulated little or no response in water-levels. This indicates that summer precipitation events must have a volume threshold in order to recharge the aquifer system. It is fortuitous that water-level

Figure 22–Hydrographs showing a long-term water-level response to precipitation.
A–The hydrographs (curves) long-term water-level responses to precipitation in six wells with monthly and bimonthly measurements and two wells with continuous water-level recorders. The vertical bars show total daily precipitation near Cloudcroft.
B–Locations of long-term-response (LTR) wells, with total well depth (in feet) below point label.

monitoring captured the two large recharge events of 2006 and 2008.

Although most continuous water-level records indicate that the wells being measured penetrate unconfined aquifers, there is evidence that some aquifers in the high mountains are confined. The hydrograph of well SM-0015 shows small (approximately 5 cm or less) water-level fluctuations, superimposed on the rising limb of the hydrograph. These fluctuations were inversely correlated with atmospheric pressure changes, which is indicative of a confined aquifer (Ramussen and Crawford, 1997). Additional evidence of confined aquifer behavior was found in three wells that were installed on private property near James Canyon with depth to water ranging from 35 to 400 feet. For all of these wells the water-level increased significantly shortly after reaching groundwater.

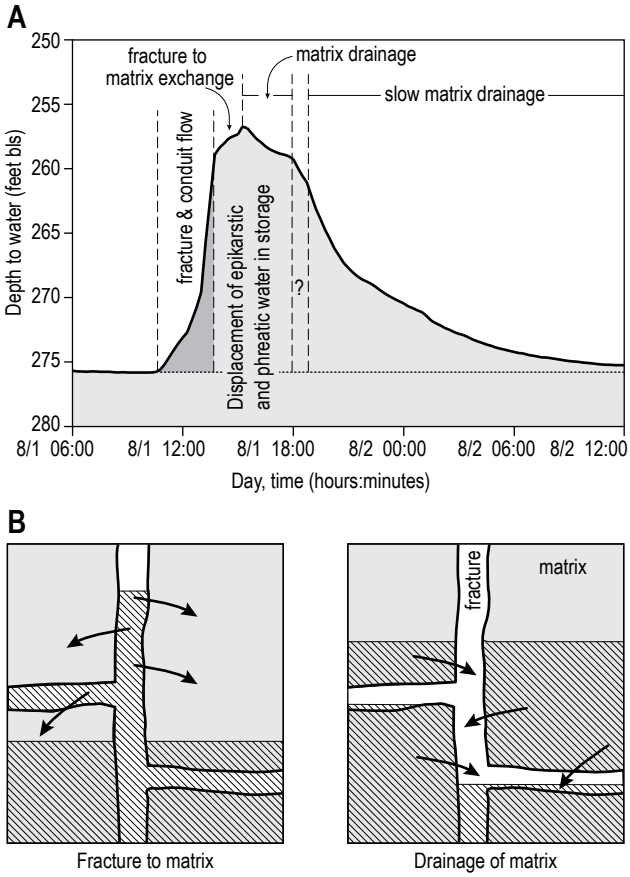

Figure 23–Well hydrograph from SM-0049 and fracture-matrix interactions.

A–During the August 1, 2006 storm event, the rapid increase in water-level on the rising limb demonstrates conduit flow. The exponential water-level decrease on the recession limb demonstrates matrix drainage.

B–Fracture matrix interactions are controlled by the total head gradient between the matrix and fractures (conduits). Arrows indicate groundwater (hatched pattern) flowing from conduits into matrix on the left, compared to groundwater draining from the matrix on the right.

These water-level increases indicate confined conditions in these aquifers.

Regional aquifer systems

The Sacramento Mountain area is comprised of four regional aquifers or aquifer systems: the high mountain aquifer system, the Pecos Slope aquifer, the Tularosa Basin mountain front aquifer and the Salt Basin aquifer (Fig. 24). The aquifer divisions are based on drainage divides, depth to water, the regional water table surface, and geologic boundaries. This study focuses on the high mountain aquifer system and the Pecos Slope aquifer, which are separated by the Mayhill Fault. The Mayhill Fault marks the location where the Yeso Formation dips beneath land surface and the San Andres Formation becomes a significant hydrostratigraphic unit, generating a change in flow characteristics and a decrease in the number of springs. Chemical and stable isotope data (discussed in the following section) also indicate differences in water chemistry and isotopic characteristics across this hydrogeologic boundary.

Surface water drainage divides do not always coincide with groundwater divides, for example the boundary between the Pecos Slope and Salt Basin aquifers. Here, the water table dips gently to the east and southeast, perpendicular to the surface water boundary. The disparity between the groundwater and surface water divides may partly reflect the limited number of data points or wells in the area. But our water table surface also includes existing data to the south on Otero Mesa (Sharp et al., 1993; Mayer and Sharp, 1998), and is thus broadly representative of the regional hydraulic gradient. Discrepancies between drainage divides and groundwater divides are common in karst terrains and reflect substantial subsurface flow through solution-enlarged regional fracture systems and karst conduits that cross local drainage divides.

High mountain aquifer system—From the crest of the southern Sacramento Mountains to just east of Mayhill, groundwater primarily resides in the Yeso Formation. The combination of lateral and vertical heterogeneity in Yeso strata, karst collapse and solution features, regional fracture systems, and deeply incised canyons creates a complex karst/fractured hydrologic system. This system consists of multiple, discontinuous, shallow and perched aquifers with recharge and discharge zones that function on the scale of a single watershed to a composite of watersheds. Deep wells within this aquifer system also demonstrate the presence of a deep aquifer of more regional extent. Shallow and perched aquifers discharge to a multitude of springs that may be interconnected through shallow, regional fracture networks and local streams, and also appear to allow downward leakage and recharge

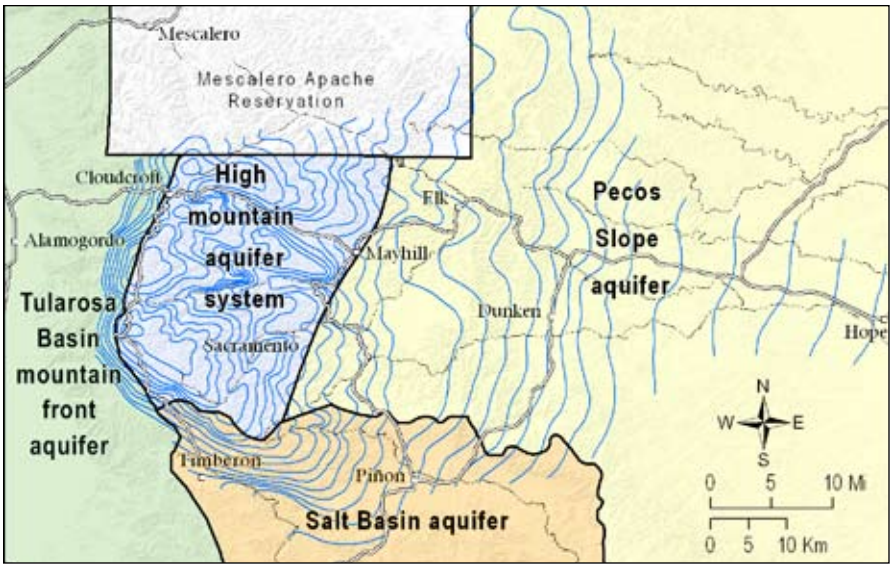

Figure 24–Map of regional aquifer systems in the Sacramento Mountains. Blue lines are water-level elevation contours shown in Figure 18.

to a deeper, more regional aquifer that coalesces with adjacent aquifers in the Salt Basin and the Pecos Slope. Because of these characteristics, we identify the high mountain aquifers as a system rather than a single aquifer.

Pecos Slope aquifer—The Pecos Slope aquifer occupies a broad area on the eastern slope of the Sacramento Mountains, east of Mayhill, with elevations below about 7,000 feet. Wells here average 600 feet and depth-to-water is generally greater than in the high mountains (Fig. 24). Although the Yeso Formation remains the principal water-bearing zone, in some areas the water table rises into the lower part of the overlying San Andres Formation. These areas are characterized by a flatter hydraulic gradient (Fig. 18), reflecting the higher transmissivity of the large cavernous fractures and sinkholes in the San Andres Formation. The Pecos Slope aquifer eventually merges with the aquifer system in the Roswell Artesian Basin to the east, where the San Andres Formation is the principal water-bearing zone. The Yeso Formation contributes a significant component of old groundwater to the Roswell Artesian Basin by subsurface groundwater flow into the San Andres Formation (Morse, 2010).

Tularosa Basin mountain front aquifer—The Tularosa Basin mountain front aquifer is located along the western escarpment of the Sacramento Mountains. The geology, topography, and hydrologic conditions, as well as physical and chemical characteristics of the aquifer, differ markedly from other regions to the east and southeast. Groundwater discharges through alluvium and colluvium overlying deeper water-bearing formations including parts of the Abo Formation, the Yeso Formation or Paleozoic limestone beneath the Yeso Formation. The water table is steep and mimics the steep topography of western flank of the mountains. Strongly folded and faulted strata form low permeability zones that likely impede or restrict horizontal groundwater movement.

Salt Basin aquifer—The Salt Basin aquifer encompasses the southern margin of the mountain block and extends north up the Sacramento River drainage to include Timberon. The northern boundary east of Timberon coincides with the surface drainage divide separating east-flowing and south-flowing drainages. The San Andres Formation and a carbonate facies of the Yeso Formation make up the principal aquifer in the Salt Basin, and the karst character of the aquifer beneath Otero Mesa is well-documented (Mayer and Sharp, 1998). Wells in the vicinity of Timberon are completed in the Yeso Formation and range from 86 to 1200 feet deep. South and east of Timberon, wells in the Salt Basin range from 500 to 1638 feet deep and are completed in both the Yeso and San Andres Formations. Groundwater flows south and southeast from the Sacramento Mountains to Otero Mesa and the Salt Basin under steep hydraulic gradients resulting from steep topography, faulting, and heterogeneity in the Yeso Formation. Shallow gradients reflect high-transmissivity fractures and cavernous zones in the San Andres Formation.

Hydrogeologic framework

Geologic mapping, lineament analyses (Walsh, 2008), and water-level data have helped us to characterize the hydrologeologic framework and identify important features that control the transport of water

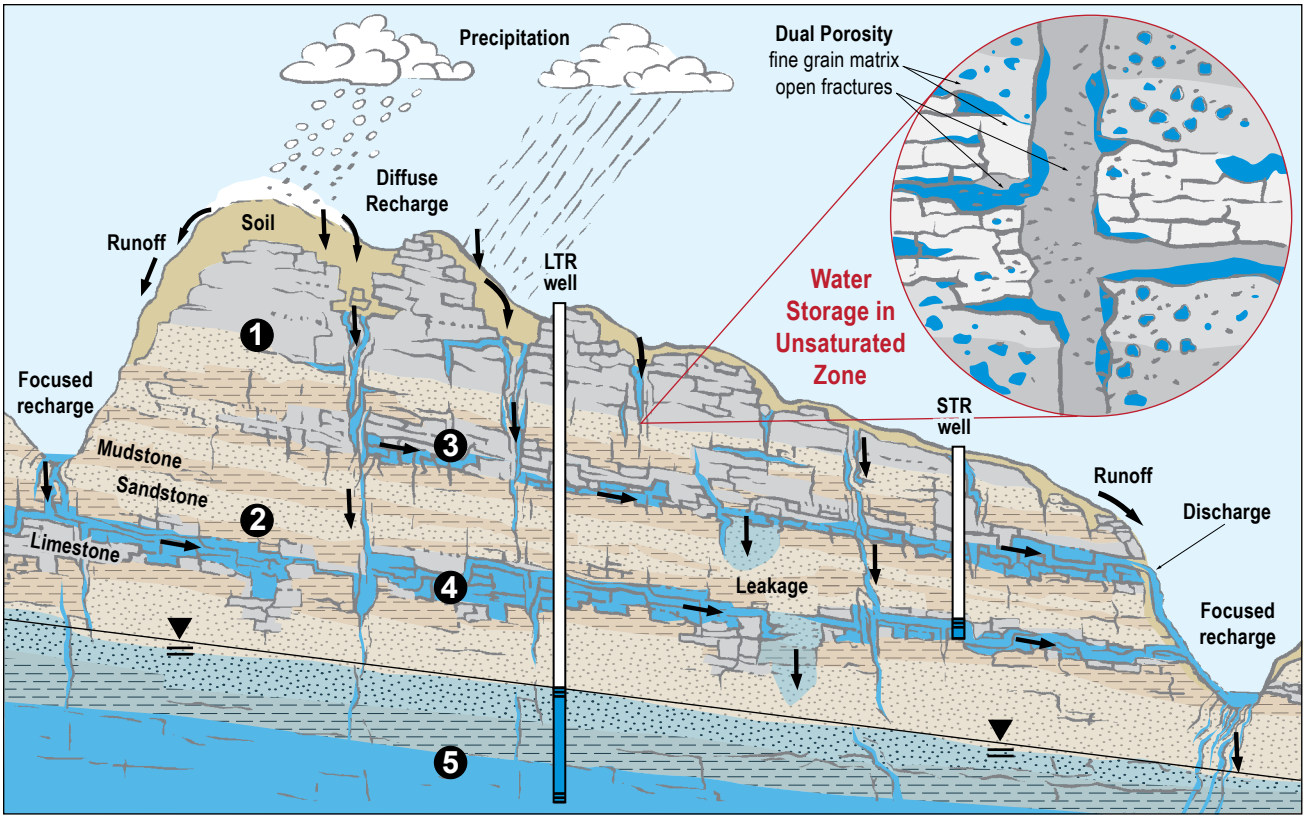

Figure 25–Watershed-scale conceptual model aquifers in the Yeso Formation of the Sacramento Mountains.
1–An upper vadose zone is the unsaturated bedrock that exists above local perched aquifers. Water can be stored in fractures, epikarst, and pores in this zone.
2–An intermediate vadose zone is unsaturated bedrock located between two saturated carbonate aquifers.
3–A local perched aquifer is the upper-most perched aquifer that is recharged by infiltration from directly above and discharges at a spring in the local watershed.
4–An intermediate perched aquifer is located beneath at least one other perched aquifer and is recharged by focused recharge from one or more watersheds and leakage from above aquifers. This aquifer discharges to springs. Most STR wells are likely completed in these aquifers.
5–A regional aquifer is primarily recharged by focused recharge from several streams and leakage from perched aquifers. These aquifers are deep enough to avoid groundwater/surface water interactions and likely merge with the Pecos Slope aquifer. Some LTR wells are likely completed in these aquifers.

through the high mountain aquifer system and the Pecos Slope aquifer. Hydrogeologic characteristics for different rock types can greatly affect the amounts, rates, and direction of groundwater flow. Depending on the rock type, the rock (or matrix) will have intergranular or matrix porosity, which is the volume of water that occupies the pore spaces in the rocks. Different rock types are also characterized by different permeabilities (the ability of a rock to transmit water). Fractures and conduits are referred to as secondary porosity and generally have higher permeabilities than the rock matrix. The following discussion identifies important features, based on the observed geology, that control groundwater flow. The resulting conceptual model provides a framework, under which water chemistry, stable isotope, and age dating data will be interpreted.

High mountain aquifer system—The most significant aspect of the regional and local aquifers in the high mountains is the extreme heterogeneity with respect to permeability. The different rocks that make up the Yeso Formation range from shale with very low permeabilities to limestone with intermediate permeabilities (Freeze and Cherry,1979). The vertical distribution of limestone beds that overlie rocks of lower permeabilities largely influences the locations of springs on hill slopes and valley bottoms. Rocks of low permeability that overlie more permeable, saturated rocks can act as local confining beds, resulting in some locally confined aquifers, which has been observed. The lateral distribution of rock types due to the spatial and temporal variability of depositional environments (Zeigler et al., 2010), folding, and the dissolution of soluble minerals affect the location and extent of local and regional aquifers in the study area.

In addition to the spatial distribution of different rock types, the presence of regional fractures systems

greatly increase the heterogeneity of the hydrologic system. Fracture permeability is significantly higher than the intergranular or matrix permeabilities. However, total water storage in fractures is minor compared to that in the matrix. This contrast in porosity and permeability between matrix and open fractures (called "dual porosity," Fig. 25) results in a complex interchange of water between fractures and matrix as described above. Vertical fractures or joints allow water to move quickly from the surface into the bedrock and across stratigraphic boundaries. Therefore, fracture controlled stream reaches, which represent zones of high fracture density (Walsh, 2008), are likely areas of high recharge rates.

Karst processes within limestone and dolomite beds add more complexity to the high mountain hydrologic system. Carbonate dissolution enlarges fractures to form conduits, which increases the secondary porosity and permeability in these rocks. Karst features observed in the high mountains west of Mayhill include solution enlarged fractures (Fig. 13B), sinking streams, and tufa mounds. A well-developed karst system is characterized by an interconnected network of pipe-like solution enlarged conduits that localize the transport of groundwater (White, 1988). The hydrograph for well SM-0049 (Fig. 23) shows evidence of conduit flow and several well records report voids where the circulation of drilling fluids was lost, providing more evidence of the presence of conduits. However, the scale and extent of an interconnected network of conduits is not known. The lateral flow of groundwater through limestone and dolomite beds is likely enhanced by the formation of conduits. However, the vertical movement of water is limited by the permeability of fractures in less soluble rocks (siltstones, shales), which are not significantly affected by karst processes. Therefore, the karsitification of limestone and dolomite does not necessarily enhance vertical groundwater flow. These perched carbonate aquifers are similar to the "Sandwich Aquifer" described by White (1969). This type of carbonate aquifer is perched and capped by rocks of lower permeability and recharge from overlying beds is limited.

In the uppermost unsaturated layer of a karst aquifer, called epikarst, a large proportion of the fractures have been enlarged into fissures and pipe conduits by erosion and dissolution. These features have very high permeability and porosity that allow rapid percolation of rainfall and temporary storage of large quantities of water in an unsaturated state (Fig. 25). This karst feature is present on upper hill slopes and ridge tops where soil overlies the San Andres Formation.

In a fractured or karst aquifer system, recharge occurs by two mechanisms, diffuse and focused recharge. Diffuse recharge is the infiltration of local precipitation through soils, epikarst, and fractured bedrock on hill slopes and ridges, while focused recharge occurs in perennial and ephemeral streams and rivers (Fig. 25). In the high mountains, water in streams, derived from base flow, spring discharge, and runoff, infiltrates quickly through valley bottom alluvium and fractured bedrock to recharge local and regional aquifers.

Figure 25 shows a conceptual model of local, intermediate, and regional aquifer systems in the Yeso Formation at the watershed scale. Water makes its way through the mountains to adjacent regional aquifers by traveling through five main domains or zones:

(1) Upper vadose zone—This unsaturated zone includes soil and underlying bedrock that overlies the shallowest aquifer in the area of interest. All water enters this zone by infiltration of local precipitation. Water is stored in pores, fractures and conduits in epikarst and other rocks.

(2) Intermediate vadose zone—This unsaturated zone includes fractured bedrock that lies between two aquifers. Water enters this zone by leakage from the above aquifer. Water is stored in pores and fractures in rock.

(3) Local perched aquifers—A perched aquifer that is recharged purely from diffuse recharge within the watershed. Water percolates through soils, epikarst and other fractured rocks and pools in karstified limestone or dolomite that overlies less permeable mudstones or shales. These shallow aquifers discharge at one or more springs in the local watershed. These aquifers are relatively small and may dry up during long periods of little or no precipitation.

(4) Intermediate scale perched aquifers—Recharged by a combination of leakage from other aquifers in overlying strata and focused recharge through higher elevation stream beds. If no aquifer lies above it, diffuse infiltration of local precipitation can also recharge this aquifer. Overlying rock of low permeability may act as a confining bed, resulting in local artesian pressures. Most STR wells are likely completed in these aquifers.

(5) Regional aquifers—These aquifers are located deep enough below the surface that they do not discharge at springs or streams, and eventually merge with the Pecos Slope aquifer. These aquifers are recharged primarily by leakage from perched aquifers at higher stratigraphic elevations. These aquifers can be under confined conditions. Most LTR wells are likely completed in these aquifers.

Pecos Slope aquifer—Down slope and east of the Mayhill fault in the Pecos Slope aquifer, Yeso strata dip below the surface and are entirely overlain by thick, resistant limestone beds of the San Andres Formation. Karstification of the San Andres limestone manifests in large cavernous fractures and sinkholes. Many wells east of Mayhill produce from fractured and cavernous limestone in the San Andres, particularly east of the Dunken-Tinnie anticlinorium. However, the Yeso Formation is still the primary water bearing formation. Unlike, the high mountains aquifer system, the Pecos Slope aquifer appears to be one regional aquifer that transports groundwater to the east and south.

CHEMICAL COMPOSITION OF GROUNDWATER

In this section, we present geochemical data, including field parameters that were measured during sample collection, and major ion concentrations in spring and well samples. Locations of sampled springs and wells are shown in Figure 26. Water chemistry results from this study are available in Appendix 7.

Field parameters

Chemical and thermal parameters collected in the field during sample collection reveal general spatial trends in water chemistry and geochemical conditions. The pH measurements of spring and well water are typically around neutral with mean values of 7.5 and 7.4, respectively. There does not appear to be any significant spatial variability in pH. Specific conductance (SC) of spring water (135 to 956 µS/cm, mean of 611 µS/cm) is lower than for well water (399 to 3269 µS/cm, mean of 808 µS/cm). These trends in SC suggest that water discharging at springs has undergone slightly less water/mineral interaction than water collected from wells. A spatial trend in SC measured in springs and wells was also observed. Box plots (Fig. 27A) show that SC for wells and springs in the high mountain aquifer system is generally lower than in the Pecos Slope aquifer. Similar trends are observed for temperature (Fig. 27B). The spatial trends for SC and temperature suggest groundwater in the high mountains has undergone less water/mineral interaction than water in the Pecos Slope aquifer. Oxidation reduction potential (ORP) and dissolved oxygen (DO) were variable. In general, ORP was positive, indicating oxidizing conditions, which is supported by DO values generally greater than 5 mg/L.

Major ions

A statistical summary of chemical parameters measured in spring and well samples is presented in Table 5. In most water samples, total dissolved solids (TDS) are below 1000 mg/L and are therefore defined

Table 5–Statistical summary for chemical parameters for springs and wells. The standard deviation of the dataset is indicated in the column labeled "SD." In the parameters, specific conductance is abbreviated as "SC" and total dissolved solids as "TDS."

		Springs				Wells			
Parameter	**Unit**	**Mean**	**Min**	**Max**	**STD**	**Mean**	**Min**	**Max**	**STD**
Temperature	°C	10.0	6.3	18.4	3.0	15	7.3	22	3.7
pH	pH units	7.4	6.8	8.5	0.34	7.5	6.89	8.6	0.29
SC	µS/cm	623	135	956	176	791	399	3269	357
TDS	mg/L	406	260	634	85	529	240	3072	341
Calcium	mg/L	112	58	140	18	120	56	515	55
Magnesium	mg/L	18	9.9	39	7.8	34	8.8	272	31
Sodium	mg/L	10	2.2	76	12	13	2.6	42	6.5
Potassium	mg/L	0.48	0.3	1.1	0.16	0.75	0.20	3.0	0.39
Bicarbonate	mg/L	361	195	455	55	309	200	445	54
Sulfate	mg/L	58	12	250	57	178	16	2090	257
Chloride	mg/L	11	2	107	18	12	2.3	38	6.8
Nitrate	mg/L	2.0	0.19	11	1.9	4.4	0.46	17	3.7
Bromide	mg/L	0.028	0.0090	0.064	0.013	0.047	0.02	0.11	0.017
Silicon	mg/L	4.8	3.1	7.1	0.97	5.5	3.3	12	1.5
Fluoride	mg/L	0.15	0.078	0.28	0.056	0.40	0.11	1.8	0.33
Iron	mg/L	0.44	0.015	3.1	0.90	0.36	0.0040	1.7	0.50
Boron	mg/L	0.012	0.0040	0.039	0.0077	0.040	0.0070	0.58	0.078
Barium	mg/L	0.036	0.019	0.086	0.013	0.032	0.010	0.064	0.0091
Nickel	mg/L	0.0024	0.0010	0.006	0.0010	0.014	0.00080	0.058	0.016
Strontium	mg/L	0.48	0.18	1.4	0.30	1.1	0.14	11	1.4
Zinc	mg/L	0.0030	0.0010	0.029	0.0056	0.32	0.0060	1.5	0.42

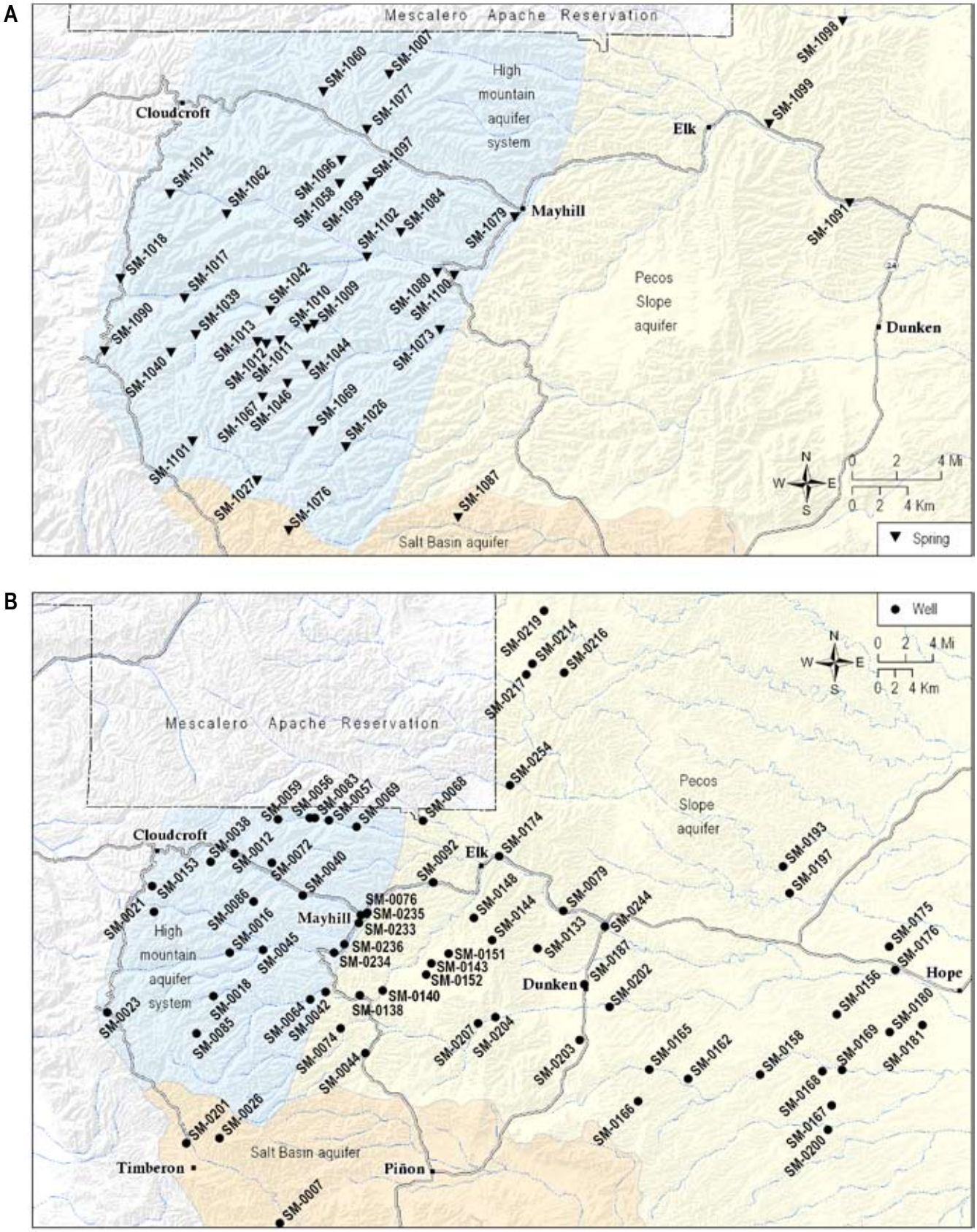

Figure 26–Locations of sampled springs and well. **A**–Springs sampled. **B**–Wells sampled.

as "fresh water" (http://ga.water.usgs.gov/edu/dictionary.html). Calcium, magnesium, bicarbonate and sulfate (Ca, Mg, HCO_3, and SO_4) are the dominant ions. This section presents chemistry data for well and spring samples, identifies spatial and temporal trends, and provides interpretations of these trends.

Spatial variability

Groundwater generally flows from west to east, from high to low elevations (Fig. 18); therefore, surface elevation can be used as a spatial proxy for down-gradient groundwater flow. Any observed trends in water chemistry that correlate to elevation can help assess processes that control water chemistry as groundwater flows from recharge to discharge areas. TDS

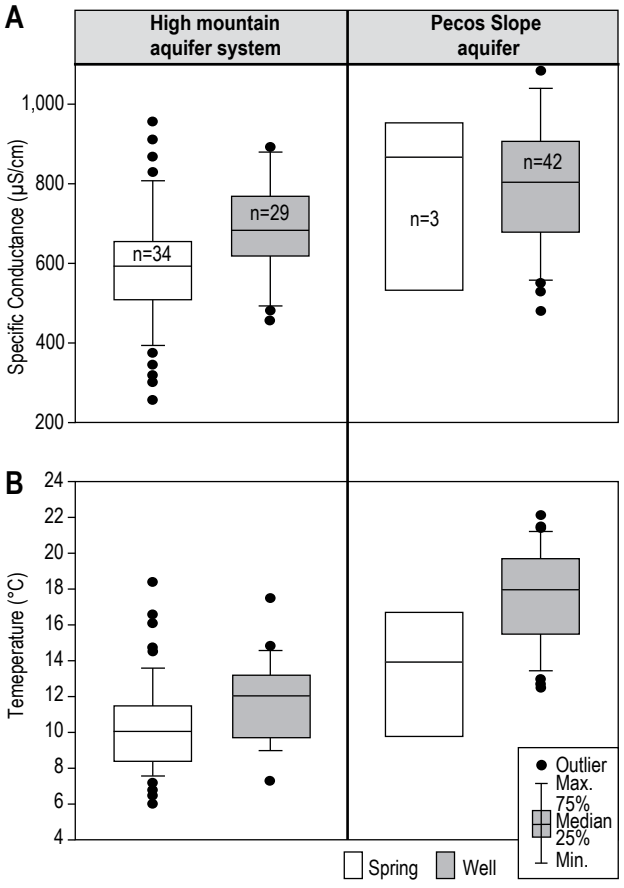

Figure 27–Water temperatures and specific conductance box plots. **A**–Specific conductance in springs and wells in the high mountains and Pecos Slope regions.
B–Temperature in springs and wells in the high mountains and Pecos Slope regions. Box plots graphically represent the range of each dataset. On these plots, the number of samples in each group is "n," which is the same for both specific conductance and temperature. The bar in the middle of each box represents the median of the dataset, and the top and bottom of the box represent the upper and lower quartiles respectively. The "T" bars extending from the box indicates the maximum and minimum values. The points represent statistical outliers.

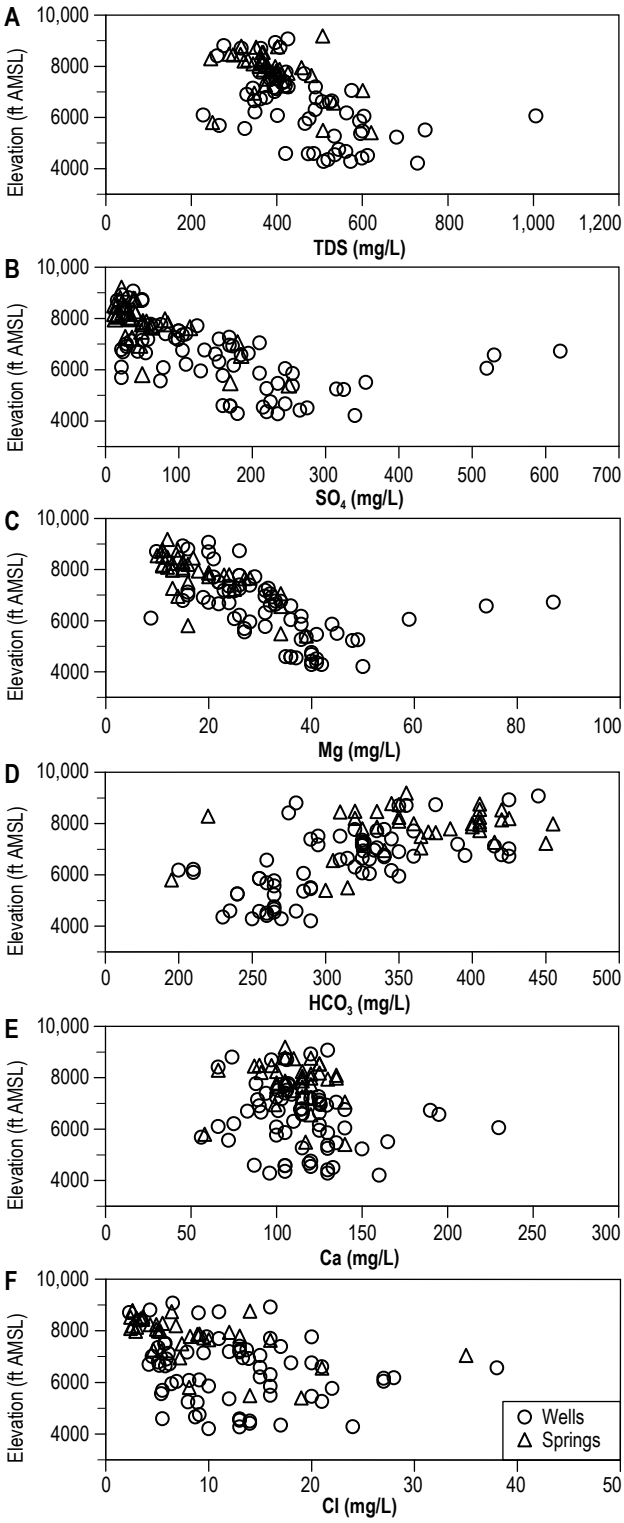

Figure 28–Water chemistry variations plotted with surface elevation. The change in concentrations for different ions as a function of elevation for springs (triangles) and wells (circles). Elevation is a proxy for regional flow direction. **A**–Total dissolved solids, **B**–Sulfate, **C**–Magnesium, **D**–Bicarbonate, **E**–Calcium, and **F**–Chloride.

concentrations show a rough inverse correlation with elevation (Fig. 28A), with lower TDS values at higher elevations. Similar but more pronounced trends are observed for SO_4 and Mg (Fig. 28 B, C). HCO_3 shows an opposite trend, with values decreasing down gradient (Fig. 28D). Calcium and chloride (Cl) show little or no correlation with elevation (Figs. 28 E and F).

This spatial trend for SO_4 in springs and wells (Fig. 29) increases from west (high mountains) to east (Pecos Slope), and also appears to increase from south to north in the high mountain aquifer system. These south-to-north and east-to-west trends of increasing concentration are also found with other constituents, including chloride, strontium, sodium, magnesium, silica, and TDS (data not shown).

Temporal variability

Several springs and wells were sampled multiple times to assess temporal or seasonal variability in water chemistry. Figure 30 shows the change in

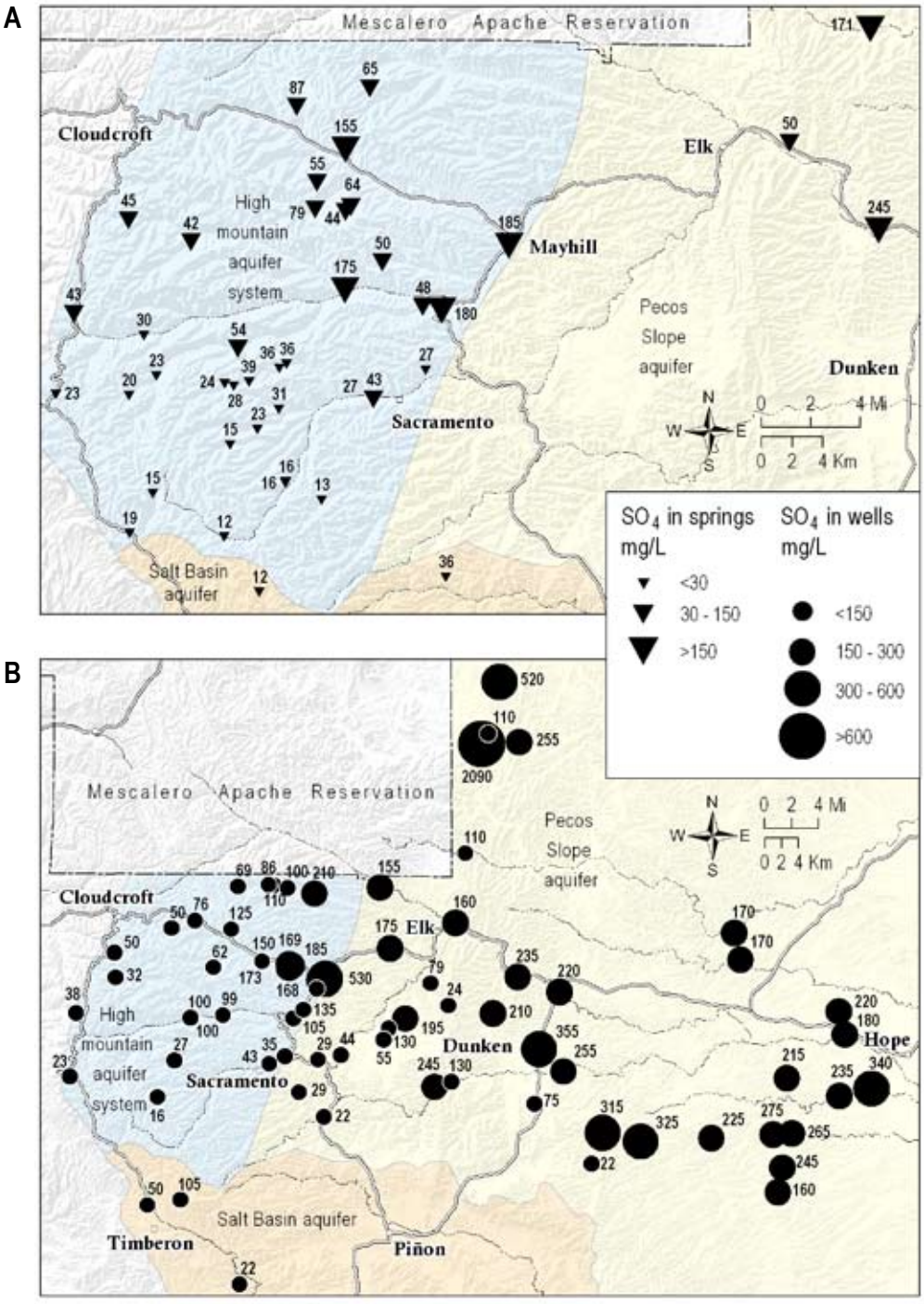

Figure 29–Maps of sulfate concentrations.
A–SO_4 concentrations (noted in mg/L) in springs in the high mountain aquifer system increase from south to north.
B–SO_4 concentrations (noted in mg/L) in wells in increase from west to east in the Pecos Slope aquifer and from south to north in the high mountain aquifer system.

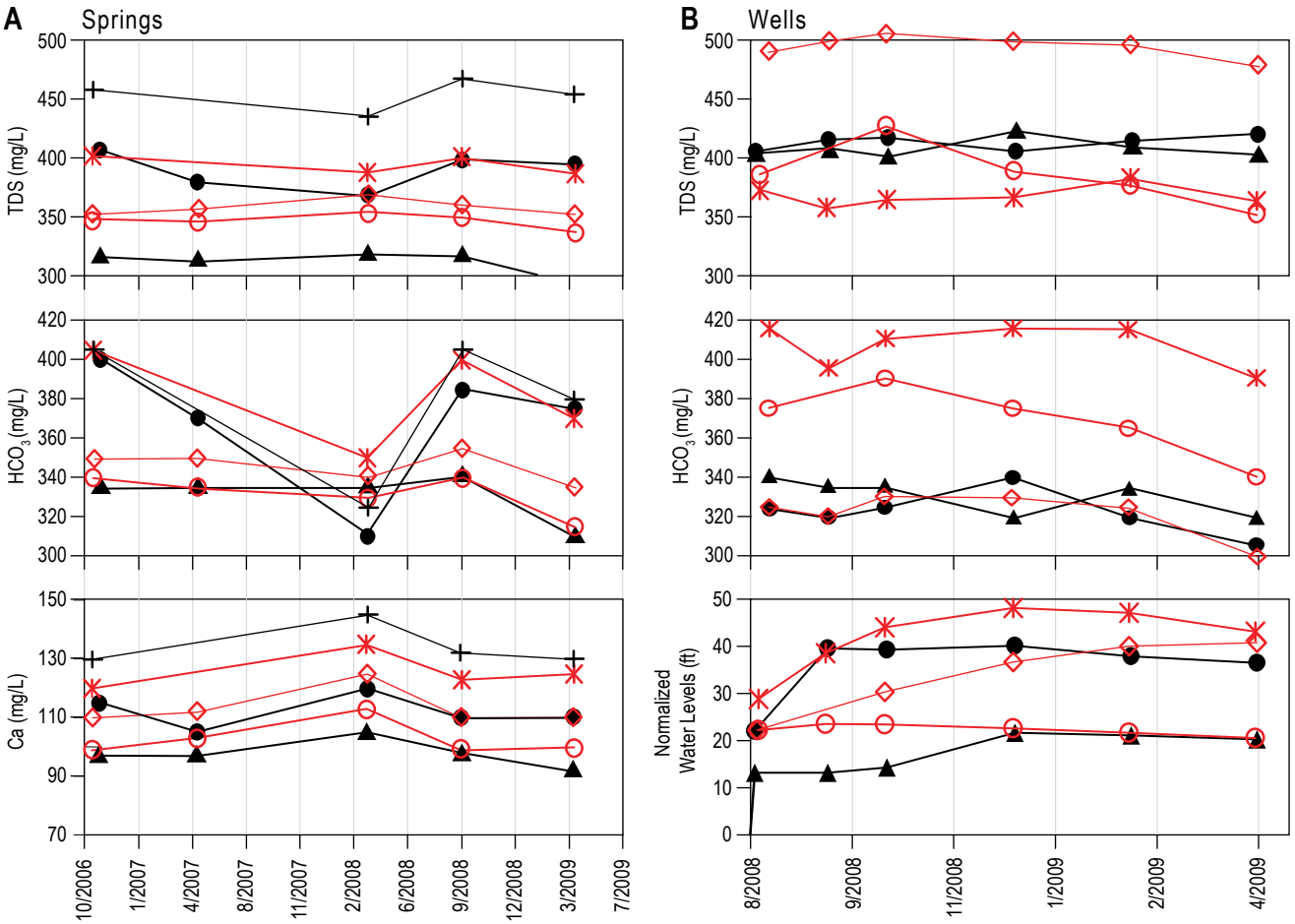

Figure 30–Temporal variation in water chemistry.
A–Spring chemistry changes for total dissolved solids (TDS), bicarbonate (HCO_3) and calcium (Ca) between 2006 and 2009.
B–Chemistry (TDS and HCO_3) and changes in water-levels in wells between August 2008 and April 2009.
C–Locations of wells and springs with repeated samples.

C

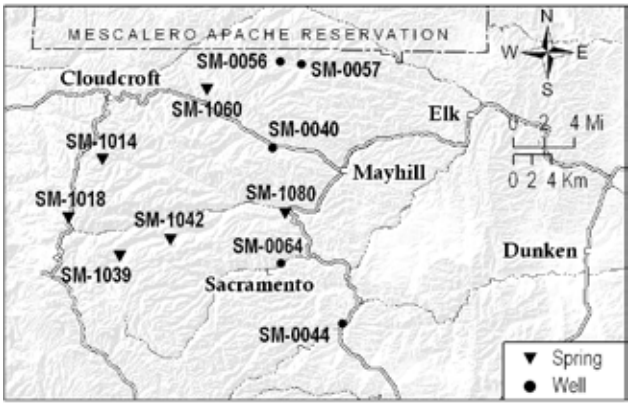

concentration over time for selected ions and TDS in five wells and six springs distributed throughout the study area. There was very little variability in ion concentrations between fall 2006 and spring 2009. The slight fluctuations observed do not correlate with seasonal climate fluctuations or groundwater-levels.

Water type

The Piper diagram shown in Figure 31 categorizes water samples into four water types based on the dominant cations and anions: 1) Ca-HCO_3, 2) Ca-Mg-HCO_3, 3) Ca-Mg-HCO_3-SO_4, and 4) Ca-Mg-SO_4-HCO_3. All water samples, with the exception of SM-1090, fall along linear trends of increasing Mg and increasing SO_4. The spatial distribution of the four water types, shown as hydrochemical zones in Figure 32, illustrates that the high mountain aquifer system is characterized as type 1, 2, or 3 waters, while the Pecos Slope aquifer consists of type 3 and 4 waters. Springs and wells producing type 1 water are located near the crest of the mountain range, and the water type progresses from type 1 to type 4 as surface elevation decreases to the east. Groundwater gradually changes from Ca-HCO_3

(type 1) to Ca-Mg-SO_4-HCO_3 (type 4) as it flows down gradient from the high mountains into and through the Pecos Slope aquifer.

Controls on water chemistry

The chemical characteristics of groundwater in the Sacramento Mountains may be affected by several processes such as, dissolution of minerals and mixing between chemically different water sources. In this section we evaluate the effect of rock-water interactions and possible mixing of chemically different sources using the data, plots and maps described above, and by evaluating mineral saturation through speciation modeling with the geochemical model PHREEQC (Parkhurst and Appelo, 1999).

Carbonate and gypsum dissolution

Most springs and wells discharge water from fractured limestone and dolomite in the Yeso Formation. The dominance of Ca and HCO_3 ions is due to dissolution of limestone. The second most abundant cation, Mg, likely originates from dissolution of dolomite. Most water samples have a moderate to high molar ratio of bicarbonate to silica (HCO_3:SiO_2, median value of 32), which indicates that carbonate dissolution, rather than silicate weathering, is the dominant process influencing chemical characteristics of groundwater (Hounslow, 1995). The most common source of SO_4 is gypsum or anhydrite, both of which are present in the Yeso Formation. Water chemistry data suggest that gypsum, calcite and dolomite dissolution are dominant processes affecting water chemistry.

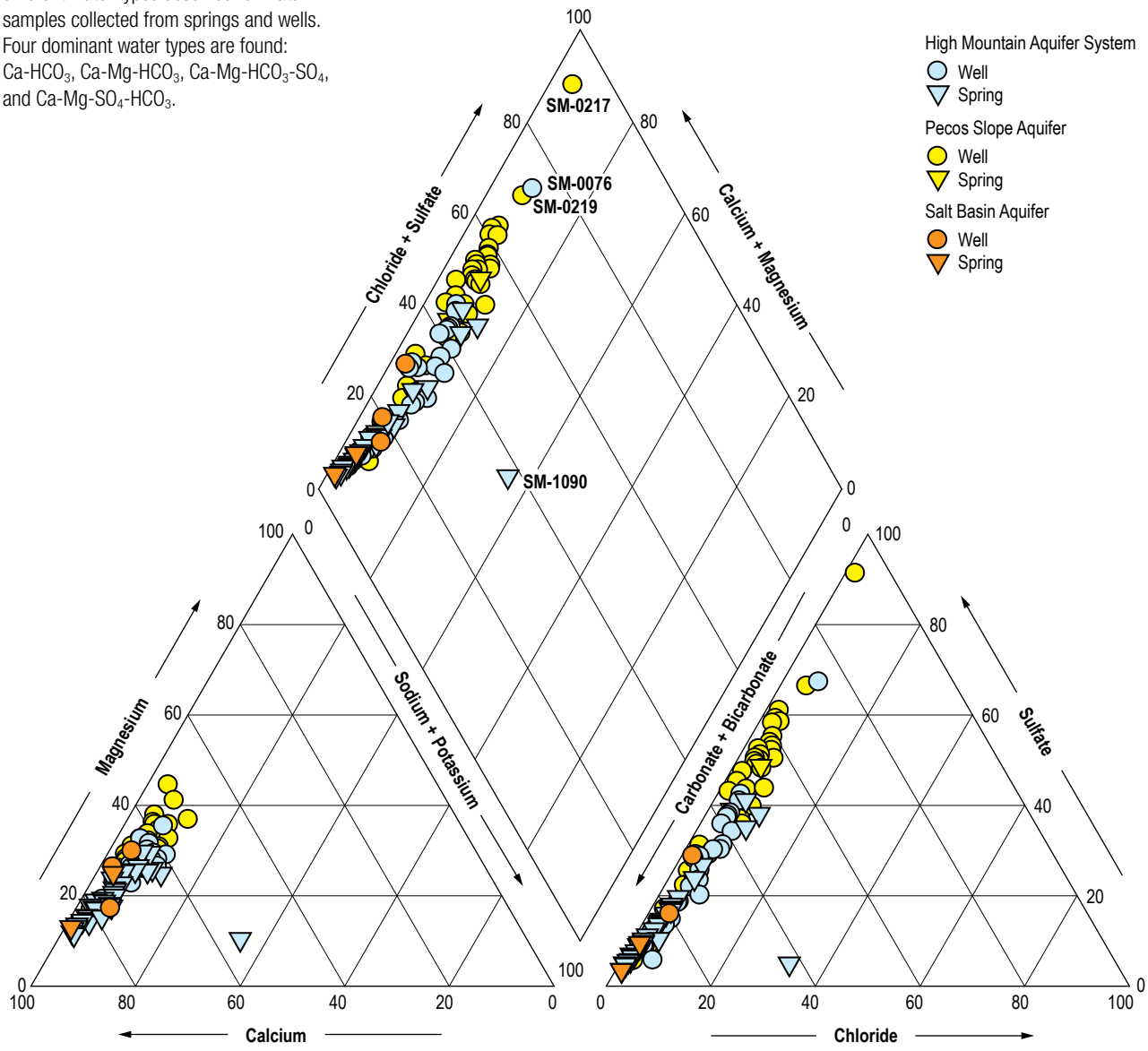

Figure 31–Piper diagram showing different water types observed for water samples collected from springs and wells. Four dominant water types are found: Ca-HCO_3, Ca-Mg-HCO_3, Ca-Mg-HCO_3-SO_4, and Ca-Mg-SO_4-HCO_3.

Mineral saturation

Mineral saturation was assessed to better understand thermodynamic controls on the composition of spring and well water and the degree to which the groundwater has equilibrated with various mineral phases. The state of saturation is expressed as the Saturation Index (SI). Super-saturation (SI >0) indicates that precipitation of a specific mineral is thermodynamically favorable. Under-saturation (SI <0) signifies that dissolution of that mineral is favored. Figure 33 shows SIs for calcite ($CaCO_3$), dolomite ($CaMg(CO_3)_2$) and gypsum ($CaSO_4$) as a function of SO_4 concentration in springs and wells. In general, waters are under-saturated with respect to gypsum and saturated or super-saturated with respect to calcite. For dolomite, most samples with low SO_4 concentrations are slightly under-saturated. This trend is most obvious in spring water. As sulfate concentrations increase, waters quickly become saturated with respect to dolomite.

Dedolomitization

The spatial trends for water chemistry (Fig. 32) and the relationship between mineral saturation indices and SO_4 concentrations can best be explained by a process called dedolomitization. Dedolomitization occurs when the dissolution of gypsum or anhydrite, and the associated increase in SO_4 concentration, causes dissolution of dolomite and precipitation of calcite. A solution in equilibrium with calcite and in the presence of gypsum and dolomite will become saturated to super-saturated with respect to calcite due to the addition of Ca ions from the dissolution of gypsum. As the dissolution of gypsum continues, the common ion effect will cause calcite to precipitate, which removes carbonate from the system, and forces the dissolution of dolomite. This process is well documented in the Madison aquifer in parts of Montana, Wyoming, and South Dakota (Plummer et al., 1990; Back et al., 1983).

Observed increases in SO_4 and Mg concentrations in down-gradient flow (Fig. 28) and the evolution of water chemistry from Ca-HCO_3 to Ca-Mg-SO_4-HCO_3 (Fig. 32) are a reflection of ongoing dedolomitization along the groundwater flow path. The water chemistry data is consistent with groundwater that is primarily recharged at high elevations in the mountains, where interactions with limestone and dolomite control the water chemistry signature. As groundwater flows down gradient through the high mountain

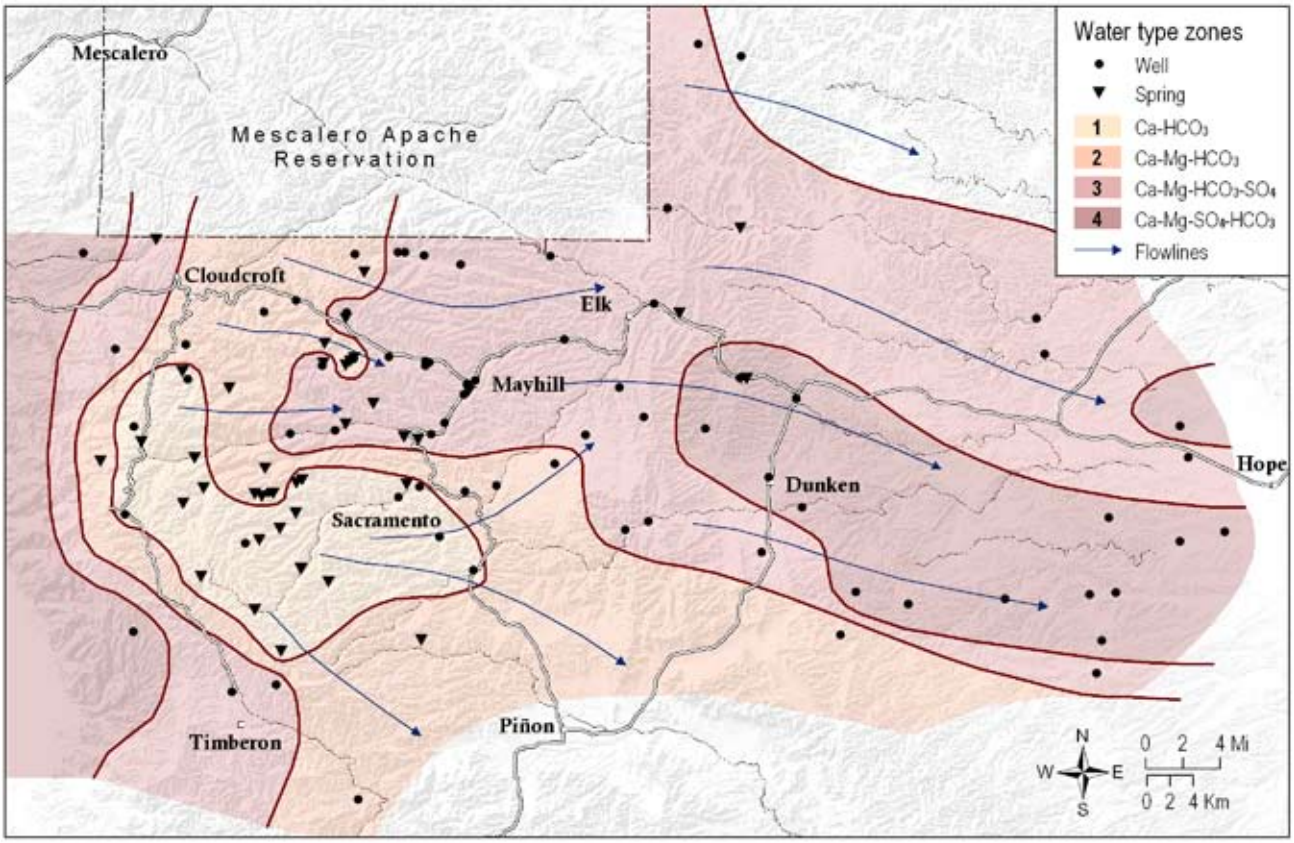

Figure 32–Hydrochemical zones inferred from water types from sampled wells and springs. Grouping water types into contoured zones generally mimics water-level elevation contours. The blue arrows represent general flow direction from type 1 to type 4 water.

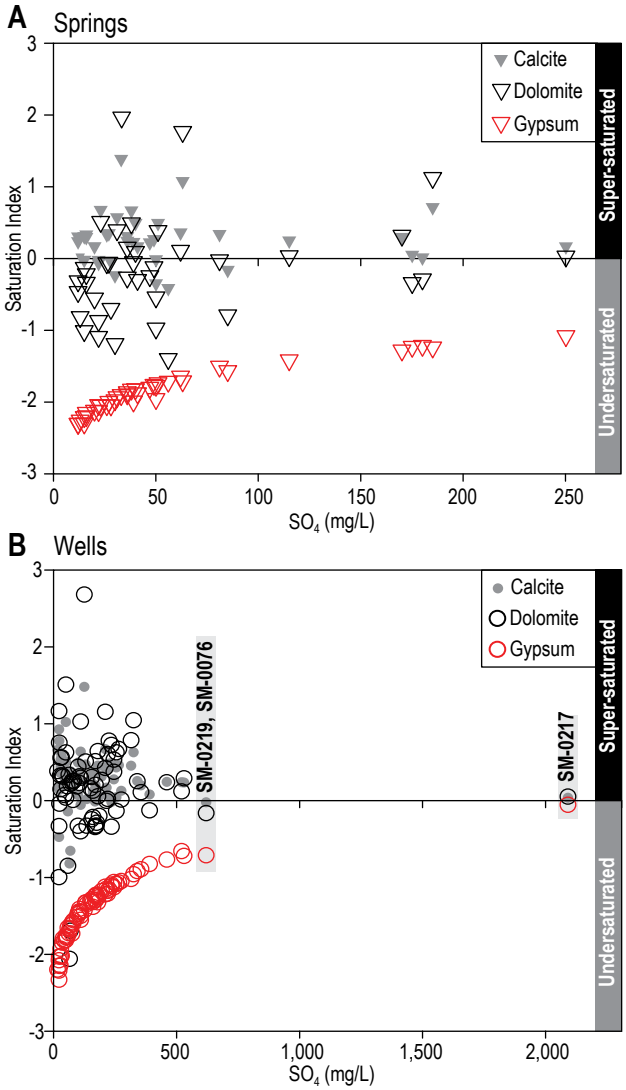

Figure 33–Saturation indices for calcite, dolomite and gypsum.
A–Saturation indices from spring water samples.
B–Saturation indices from well samples. The state of saturation is the Saturation Index (SI). Super-saturated (SI >0) indicates that precipitation of a specific mineral is thermodynamically favorable. Undersaturated (SI <0) indicates that dissolution of that mineral is favored.

aquifer system and into the Pecos Slope aquifer, the ongoing dissolution of gypsum and anhydrite drive the process of dedolomitization, causing the water chemistry to evolve. During dedolomitization, there is no gain or loss of HCO_3. Therefore, the down-gradient decrease of HCO_3 (Fig. 28D) is not due to this process, but instead is probably a result of calcite precipitation driven by increasing water temperatures associated with deeper, longer circulation pathways (Fig. 27B). The solubility of calcite decreases as water temperature increases.

The chemical end member in dedolomitization is represented by sample SM-0217, the uppermost point in the Piper diagram (Fig. 31), which along with SM-0219 was collected near the northern end of the Dunken-Tinnie anticlinorium (Fig. 10). Waters that have undergone complete dedolomitization and are in equilibrium with dolomite and gypsum have a molor ratio of $(Ca+Mg)/SO_4$ approaching one (Richter and Kreitler, 1986). Molar ratio values for SM-0217 and SM-0219 are 1.1 and 1.5, respectively, and the waters are in or approaching equilibrium with gypsum, calcite and dolomite (Fig. 33). Well SM-0076 located along the Mayhill fault zone has a similar molar ratio of 1.4. These waters are relatively warm (16.9 to 17.5°C) and have high concentrations of sulfate, total dissolved solids, and magnesium. The mix of chemical signatures – dolomite-gypsum equilibrium, high TDS, and warm temperatures – and proximity to faults suggests that these structures may act as barriers or partial barriers to flow at depth, and provide vertical conduits that facilitate upward movement of regional groundwater.

In general, water chemistry from springs at lower elevations and down gradient in the flow system is more evolved than that at high elevations, which indicates that water discharging from low elevation springs has a longer residence time. This suggests that most springs below about 8,200 feet elevation discharge from an intermediate or regional aquifer rather than a local, system. This trend also indicates interconnectivity between perched aquifer systems in the high mountains.

Mixing of different water sources

The mixing of high-chloride brines with fresh groundwater was assessed using chloride/bromide (Cl/Br) ratios. The analyses confirm that some mixing of high-Cl waters does occur. This mixing is apparent in SM-1090, but it is volumetrically insignificant (Appendix 8).

Summary

The dissolution of limestone and dolomite is the primary process that controls the water chemistry in groundwater. Dedolomitization results in the gradual geochemical evolution from Ca-HCO_3 to Ca-Mg-SO_4-HCO_3 water type as groundwater flows down gradient from high elevations to low elevations. This gradual change in water type is also observed in springs in the high mountains aquifer system, indicating inter-connectivity between springs. Spring discharge at higher elevations recharges shallow perched aquifers that discharge at lower elevation springs. This trend also suggests that most water initially enters the system at high elevations that likely correlate to the 8,200 water-level elevation contour in Figure 18.

STABLE ISOTOPES OF HYDROGEN AND OXYGEN

Precipitation

Figure 34 shows locations of precipitation collection sites. The linear regression of stable isotope data from precipitation defines a local meteoric water line (LMWL) for the Sacramento Mountains (Fig. 35) with an equation of:

$$\delta D = 8.4\delta^{18}O + 23.4$$

The seasonal variability of the isotopic composition of precipitation is shown in the shaded areas of the LMWL (Fig, 35) as winter precipitation (October to March) and summer precipitation (April to September).

Variations in the stable isotopic composition of precipitation are due to three seasonal factors (Rozanski et al., 1993): 1) changing temperature, 2) modulated evapotranspiration flux, and 3) changing source areas of vapor and/or different storm trajectories. All three of these factors play a role in the observed seasonal variability in stable isotopic composition of precipitation in the Sacramento Mountains. In this area, the average temperature difference between summer and winter is approximately 15°C. The Sacramento Mountains are heavily vegetated compared to surrounding areas, and during the summer, a significant amount of water vapor is returned to the atmosphere due to an increase in evapotranspiration rates. This addition of water vapor to the atmosphere effectively reduces the extent of isotopic depletion of precipitation during the summer (Rozanski et al., 1993). As discussed previously, the dominant source area of winter storms is the Pacific Ocean, while summer storms associated with the North American Monsoon originate from the eastern Pacific and the Gulf of California.

Occasionally an individual storm event will result in precipitation with an isotopic composition that plots outside the expected seasonal range. During July 2008, a remnant disturbance of Hurricane Dolly, which traveled overland in southern Texas and northern Mexico, produced heavy rainfall in the Sacramento Mountains (Pasch and Kimberlain, 2009). Cloudcroft received 13 inches of rain within a few days in late July. Stable isotope values for precipitation that fell during this period plot along the LMWL within the range of winter values (Fig. 35). An anomalously light isotopic composition associated with hurricanes has been observed by other researchers (Lawrence et al., 2002), and is mainly attributed to high condensation efficiency and long storm duration, which produces an extreme rain-out effect.

The volume-weighted mean isotopic compositions of samples collected at four sites (SM-2005,

Figure 34–Locations of precipitation collectors. Rain and snow were collected at a range of elevations.

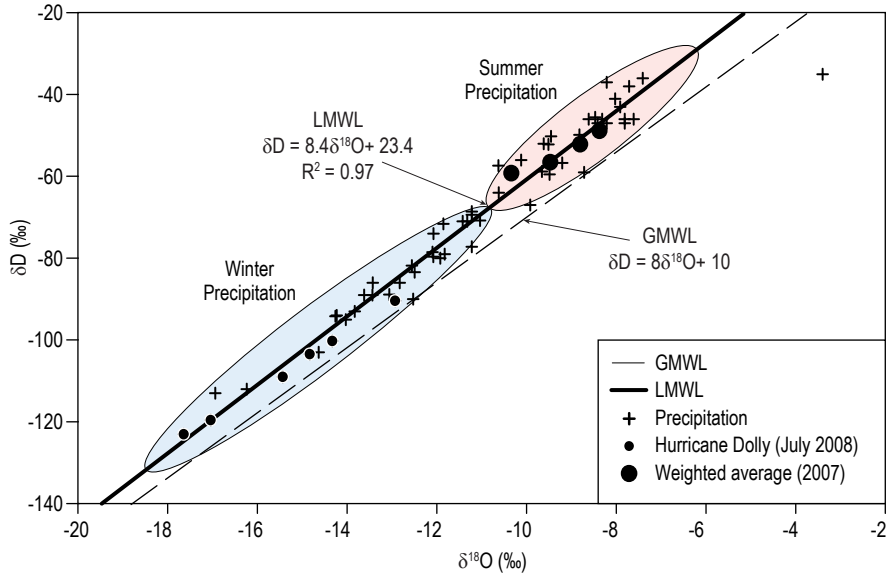

Figure 35–Precipitation samples used to construct a local meteoric water line (LMWL). In the Sacramento Mountains, there is a distinct difference between the Global Meteoric Water Line (GMWL) and the line produced from this study for the local meteoric water line (LMWL) due to local climatic conditions. Red and blue shaded areas represent the average range of isotope values for summer and winter precipitation, respectively.

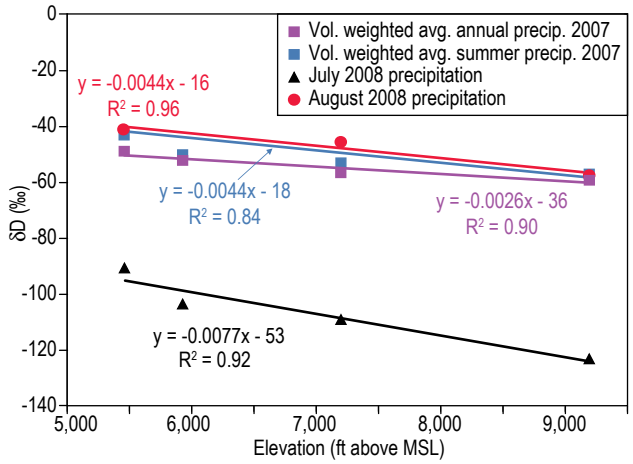

Figure 36–Volume weighted average stable isotopic composition of annual and summer precipitation as a function of elevation. The isotopic composition of precipitation is generally more depleted at higher elevations. The four precipitation collection stations shown here are SM-2009 (5461 ft elevation), SM-2005 (5935 ft), SM-2006 (7204 ft), and SM-2009 (9203 ft).

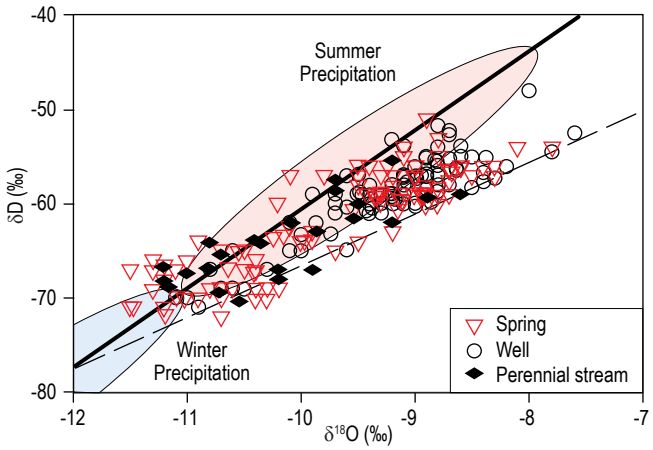

Figure 37–Stable isotope data for all stream, spring and well samples. Stable isotope water samples were collected between 2006 and 2009 and are shown here plotted along the local meteoric water line, also with the local evaporation line. Several springs and wells were collected multiple times.

Figure 38–Monthly precipitation data for Cloudcroft between 1998 and 2005 shows that monsoon precipitation amounts over this time period were usually significantly below those that caused the 2006 and 2008 recharge events. 2007 monsoons did not result in a significant increase in groundwater-levels, and therfore it is unlikely that monsoon rains between 1998 and 2006 resulted in signicant rechage events.

SM-2006, SM-2008, SM-2009, Fig. 34) in 2007 plot within the range of summer values (Fig. 35), which reflects the large proportion that summer precipitation contributes to the annual total. The variability in the volume-weighted mean isotopic composition observed for collection sites is due to elevation (Fig. 36). Weighted mean δD values for annual precipitation from 2007 and for summer precipitation for 2007 and 2008 become lighter with increasing elevation. Similar trends are observed for $\delta^{18}O$ (data not shown). The elevation effect is attributed to the progressive condensation of atmospheric vapor and rainout of the condensed phase as air masses rise up mountain slopes and cool because of adiabatic expansion (Gonfiantini et al., 2001). Interestingly, we did not observe an elevation effect for winter precipitation. The fact that we see the elevation effect for summer precipitation but not for winter precipitation reflects the different physical characteristics of the two primary weather patterns – frontal storms in the winter and the North American Monsoon in the summer – that contribute precipitation to the Sacramento Mountains.

Surface water and groundwater

Figure 37 shows stable isotope data for all spring, well and stream samples from this study collected between 2006 and 2009, with some repeat samples. The data are plotted along with the LMWL and an evaporation line that was defined by groundwater and surface water samples collected in 2003 by Eastoe (2005) (Newton et al., 2008). The isotopic composition of many of these water samples plot along this evaporation line or between it and the LMWL.

Monthly precipitation data at Cloudcroft (Fig. 38) show that monsoon precipitation amounts between

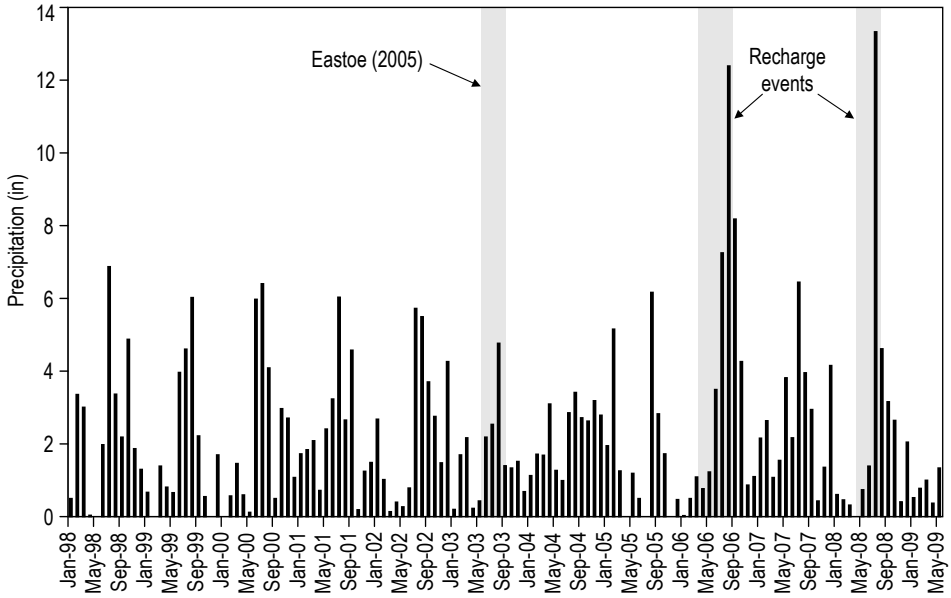

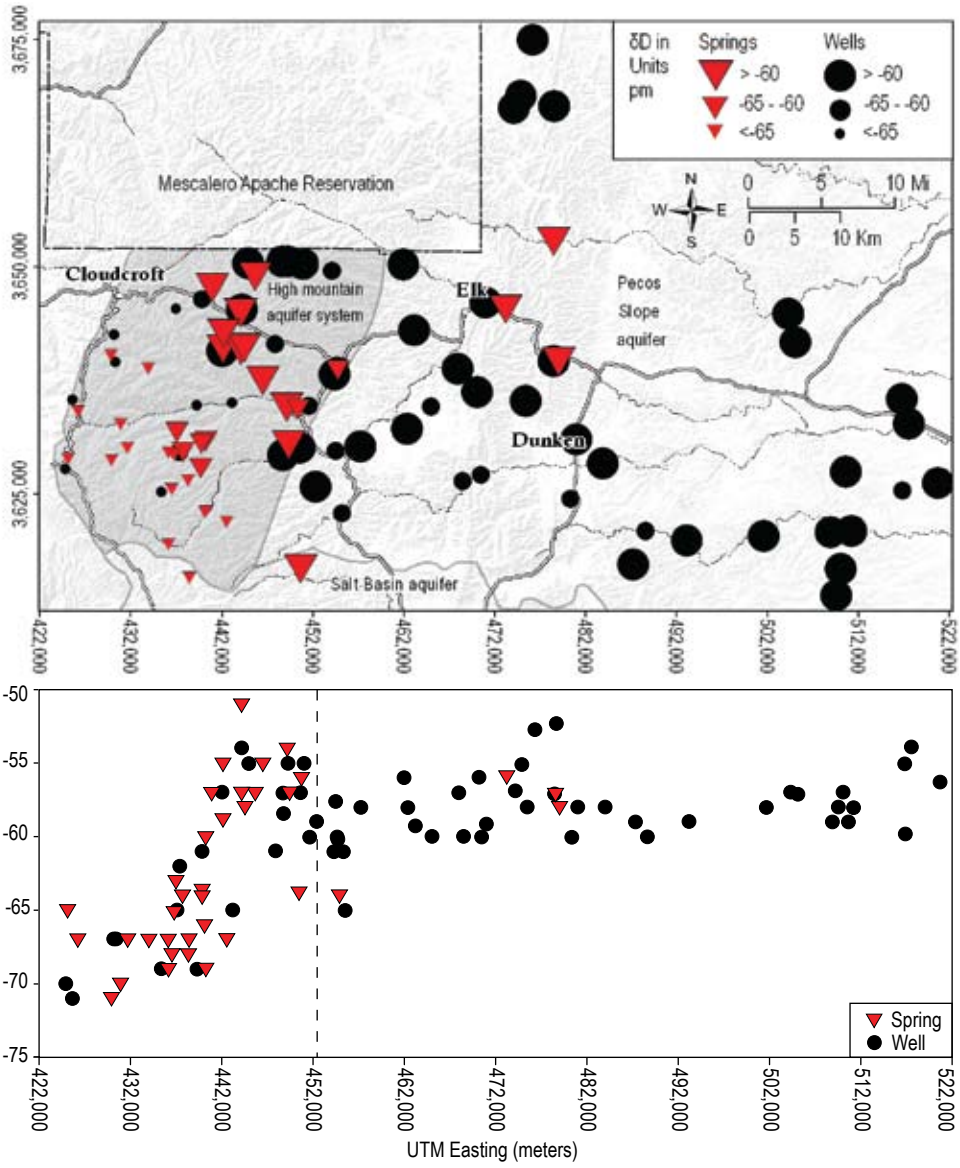

Figure 39–Stable isotopic compositions of wells and springs as a function of easting. As groundwater flows from west to east, stable isotope values (δD shown here) generally increase as elevation decreases. The dashed vertical lines represent the approximate UTM easting or elevation boundary between the high mountain aquifer system and the Pecos Slope aquifer, which are approximately aligned with map.

Figure 40–Springs sampled in March 2008 at lower elevations plot farther along the evaporation line than those at higher elevations.

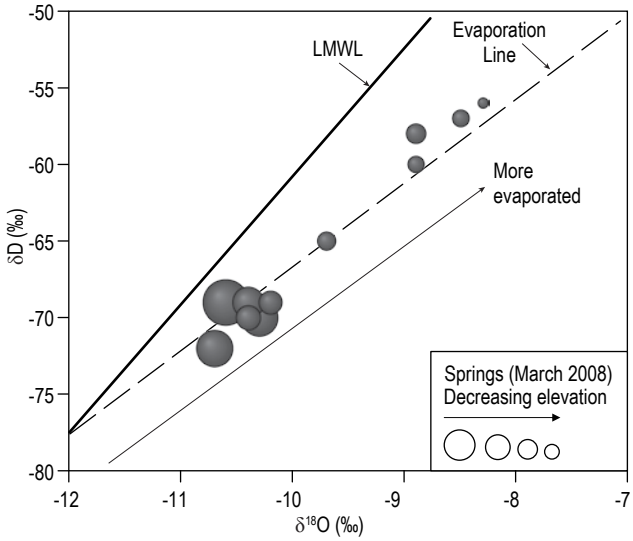

1998 and 2005 were similar to those observed in 2007 but significantly lower than those during 2006 and 2008. The fact that no significant increases in groundwater-levels were observed during or shortly after the monsoons in 2007 suggest that summer recharge events such as those observed in 2006 and 2008, did not occur within 5 years prior to 2003 when samples were collected by Eastoe (2005). Data from our study plot along this evaporation line during certain time periods. This section discusses the temporal and spatial variability of the stable isotopic composition of surface water and groundwater and their implications for recharge processes.

Spatial Distribution

δD values for spring and well samples (Fig. 39) range from -71 to -51‰, and generally increase from

west to east and as elevation decreases. In the Pecos Slope aquifer, δD values are relatively uniform and range from -65 to -52‰. Isotope values for Pecos Slope aquifer are similar to those observed at the eastern boundary of the high mountain aquifer system (Fig. 39). This implies that recharge to the Pecos Slope aquifer system flows directly from the high mountain aquifer system. Similar spatial trends were observed in $\delta^{18}O$ values. Stable isotope results for springs in the high mountain aquifer system sampled in March 2008 plot along the evaporation line (Fig. 40), with samples from springs at lower elevations plotting further along the evaporation line, indicating that water discharging from springs at lower elevations has undergone more evaporation than springs at higher elevations.

Temporal variability

Figures 41 and 42 demonstrate that over the time period of data collection (2006–2009), the isotopic compositions of springs, wells, and perennial streams varied. The fluctuations can be examined in terms of proximity to the LMWL. Data points that plot significantly below the LMWL represent water that has undergone evaporation. Figure 42 shows the δD offset from the LMWL, where positive values indicate that the data point plots above the LMWL and negative values indicate that the data point plots below the LMWL (evaporation).

Springs sampled in 2006 are tightly grouped around the LMWL. Wells and springs sampled in 2007 plot close to, but beneath the LMWL. Springs sampled before the 2008 recharge event plot significantly below the LMWL and close to the evaporation line, while those sampled after the 2008 recharge event have shifted away from the evaporation line and back toward the LMWL. Springs, wells, and perennial streams sampled in 2009 plot similarly to those from 2007 and early 2008.

Trends seen in Figures 41 and 42 suggest that the stable isotopic compositions of springs, wells and streams are related to the timing of the 2006 and 2008 recharge events. It appears that during time periods with no significant groundwater-level

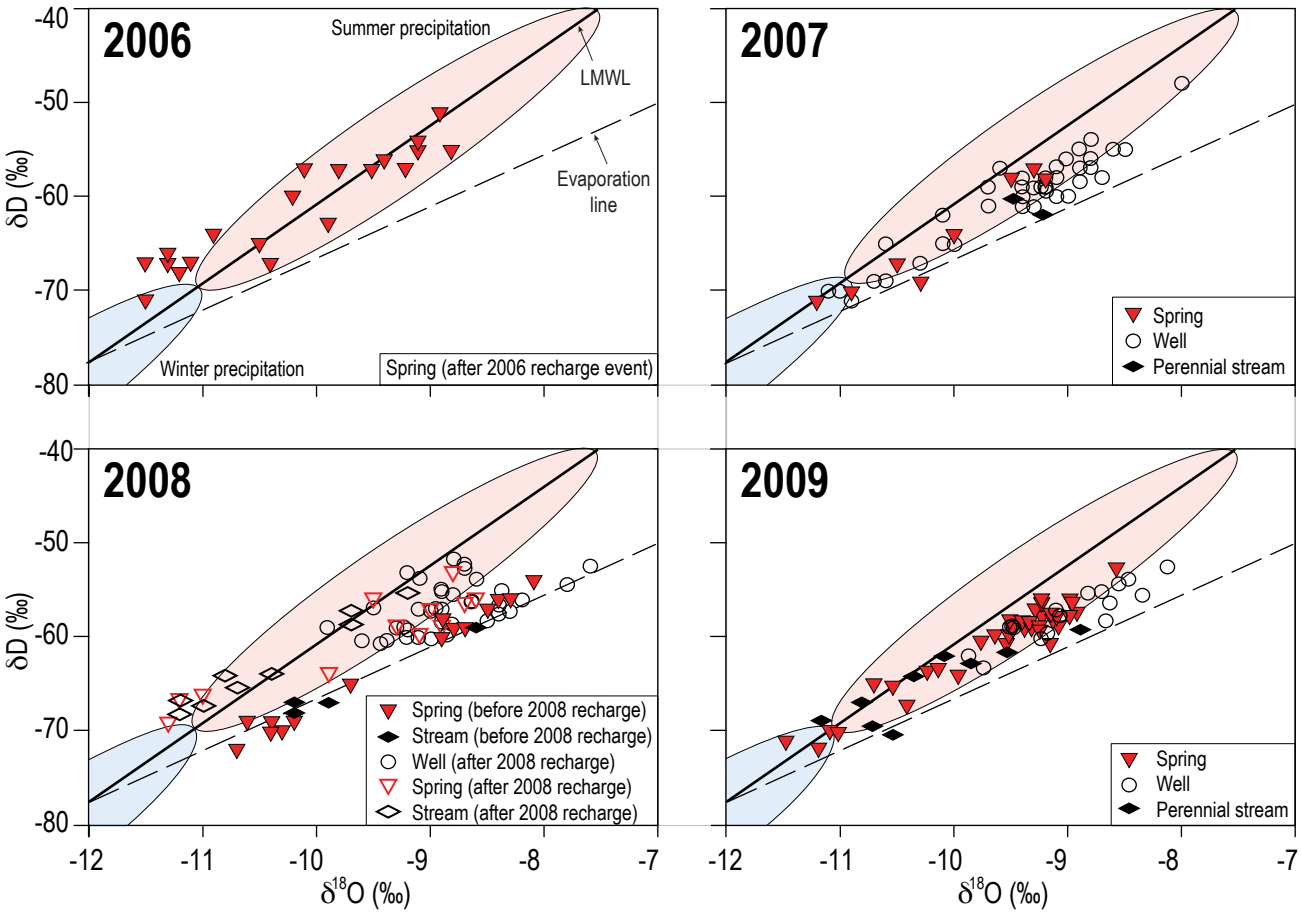

Figure 41–Temporal variations in stable isotopic compositions of streams, springs, and well samples from 2006 to 2009. Isotope values for samples collected shortly after 2006 and 2008 recharge events generally plot near the LMWL. Isotope values appear to drift towards the evaporation line after the the recharge events.

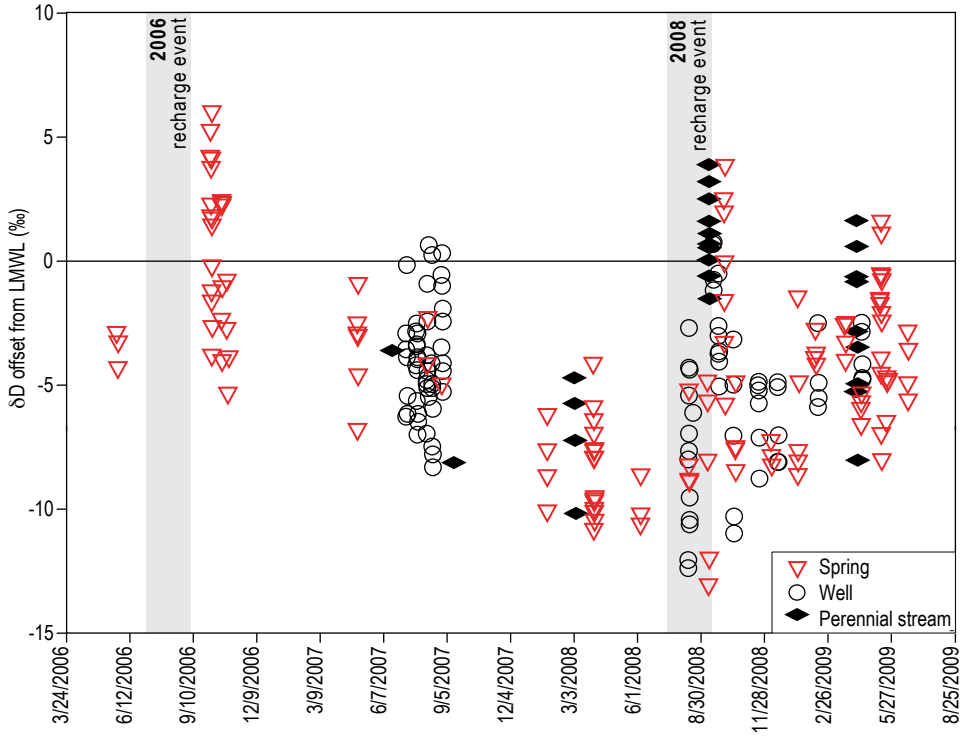

Figure 42–The δD offset from LMWL for well, spring, and stream samples. Points with positive values in this figure plot above the LMWL (as plotted in δD vs. $\delta^{18}O$ space). Points with negative values in this figure plot below the LMWL and indicate that the water has undergone evaporation. The extreme summer recharge events (2006 and 2008) cause the stable isotope composition of spring and stream samples to shift closer to the LMWL.

increases, most springs, streams, and wells will have an evaporative signature and plot close to the evaporation line. Water entering the hydrologic system in the high mountains as a result of these recharge events in 2006 and 2008 appear to shift the isotopic composition of springs, wells and streams toward the LMWL. This effect on the isotopic composition of surface water and groundwater decreases with time after the occurrence of these recharge events, with isotopic compositions slowly shifting back towards the evaporation line.

Controls on isotopic composition

Focused and diffuse recharge

As discussed above, we observed a shift of the stable isotopic composition of groundwater from the evaporation line toward the LMWL as a result of the 2006 and 2008 recharge events. This observed temporal variability in the isotopic composition of groundwater and surface water indicates that recharge occurs by two different mechanisms that result in two different isotopic trends:

(1) Water that plots along a single evaporation line—This trend indicates that the hydrologic system within the recharge area is a well-mixed system and that the water has undergone evaporation. The point at which the LMWL and the evaporation line intersect represents the isotopic composition of a mixture of summer and winter precipitation that percolates past the root zone. As can be seen in Figure 41, this initial isotopic composition plots within the range of expected values for winter precipitation, indicating that snowmelt contributes more to this recharge component than summer rains. The evaporative signature suggests that some of this recharge occurs as focused recharge in mountain streams. This water likely originates as high-elevation precipitation that infiltrates quickly through fractured bedrock to recharge local and intermediate perched carbonate aquifers and runoff in mountain streams that infiltrates through streambeds. Mixing of waters from different aquifers happens quickly due to aquifer/aquifer interactions and groundwater/surface water interactions (Fig. 25). In the subsurface, mixing can occur due to leakage from one aquifer to another, or the merging of two or more aquifers due to the intersection of different fracture zones. Springs discharging from multiple levels in a single watershed mix in perennial or ephemeral streams that then recharge an underlying aquifer system.

(2) Water that plots near the LMWL—This water represents diffuse recharge that infiltrates quickly through the thin soils into unsaturated fractured bedrock. The isotopic composition of this water does not have an evaporative signature. The spatial variability observed for this water is controlled by elevation effects on the isotopic composition of precipitation (Fig. 36). Epikarst features in the San Andres

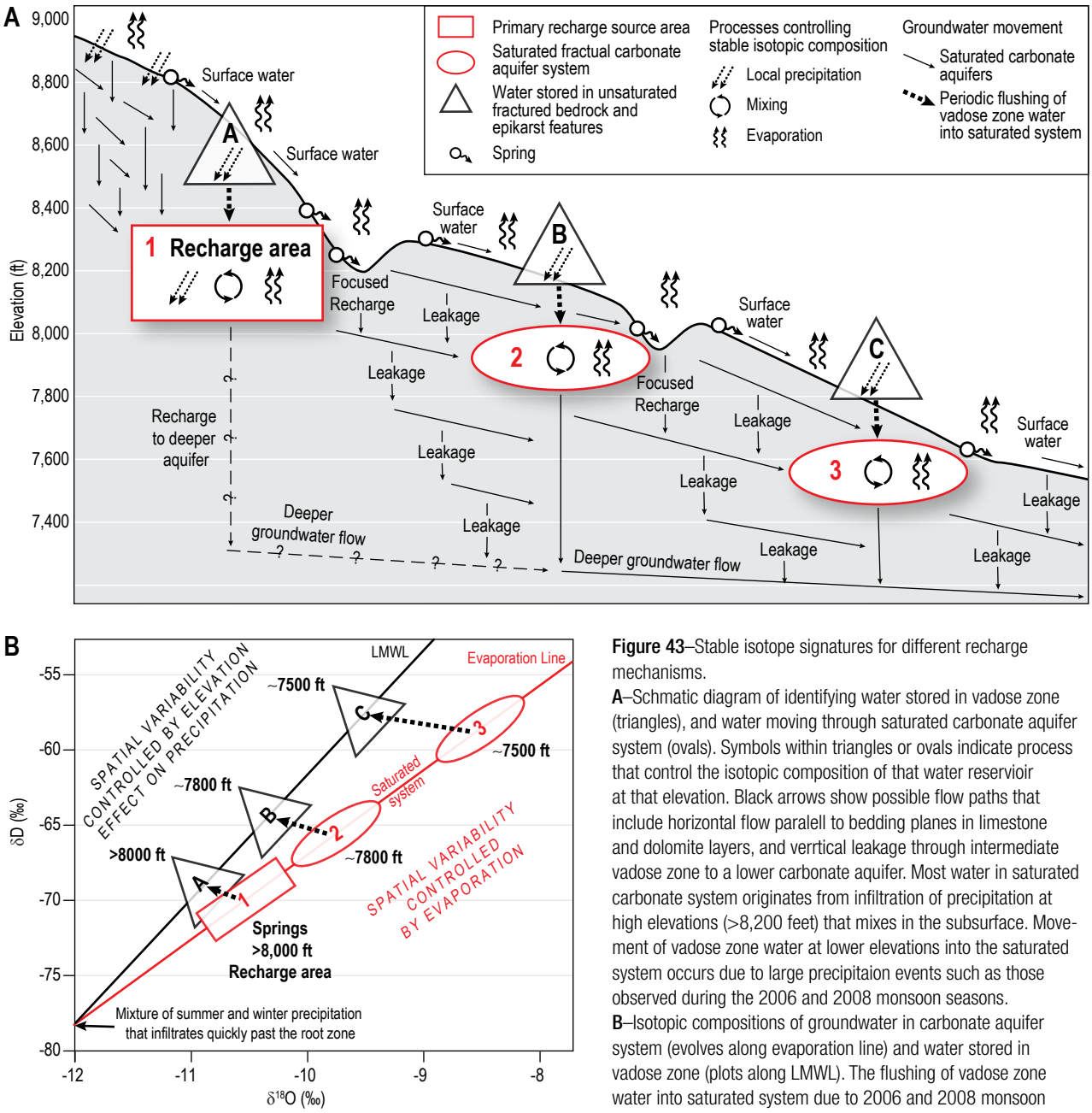

Figure 43–Stable isotope signatures for different recharge mechanisms.
A–Schmatic diagram of identifying water stored in vadose zone (triangles), and water moving through saturated carbonate aquifer system (ovals). Symbols within triangles or ovals indicate process that control the isotopic composition of that water reservoir at that elevation. Black arrows show possible flow paths that include horizontal flow paralell to bedding planes in limestone and dolomite layers, and verrtical leakage through intermediate vadose zone to a lower carbonate aquifer. Most water in saturated carbonate system originates from infiltration of precipitation at high elevations (>8,200 feet) that mixes in the subsurface. Movement of vadose zone water at lower elevations into the saturated system occurs due to large precipitaion events such as those observed during the 2006 and 2008 monsoon seasons.
B–Isotopic compositions of groundwater in carbonate aquifer system (evolves along evaporation line) and water stored in vadose zone (plots along LMWL). The flushing of vadose zone water into saturated system due to 2006 and 2008 monsoon seasons, caused isotopic composition of groundwater to shcift towards vadose zone values.

Formation can store large volumes of this water in the unsaturated zone. Extreme monsoon rains, such as those observed in 2006 and 2008 flush this vadose zone water into the saturated system.

Groundwater-surface water interactions

Springs in the Sacramento Mountains are the source for most perennial and ephemeral stream reaches, many of which subsequently infiltrate back to the shallow groundwater system. This observation in the high mountains region, along with the observed trend of increasing isotope values (higher degree of evaporation) with decreasing elevation (Fig. 40), indicates a circular "recycling" relationship and interconnection between surface water, springs, and shallow groundwater. Water that recharges a shallow perched aquifer may discharge at a spring that flows into a stream where it undergoes evaporation. This stream water, with an evaporated signature, can recharge another shallow aquifer and discharge at a spring at a lower elevation. This cycle may occur several times as the water flows down gradient. Therefore, the

isotopic composition of water evolves as it makes its way through the high mountain groundwater system due to these groundwater/surface water interactions. Earman (2004) identified a similar process in the Chiricahua Mountains, which he termed "re-recharge". This recycling process does not occur beyond the high mountain aquifer system.

Summary

Two primary recharge mechanisms identified based on the stable isotopes of oxygen and hydrogen are depicted on Figure 43. Snow and rain enter the system in primary recharge area (denoted by the rectangle), via fractures and losing mountain streams, where water undergoes evaporation. The extreme heterogeneity of the Yeso Formation combined with the regional fractures systems results in the mixing of groundwater through aquifer/aquifer and groundwater/surface water interactions described above. Groundwater (wells and springs) in the recharge area is characterized by an isotopic signature that plots on the evaporation line close to where it intersects with the LMWL (Fig. 43B). As this water moves through the high mountain aquifer system, shallow groundwater is exposed to the atmosphere repeatedly due to groundwater/surface water interactions. Evaporation of this water in mountain streams causes its isotopic signature to evolve along the evaporation line, with groundwater at lower elevations being more evaporated. Isotopic compositions that plot along the evaporation line were observed in springs sampled in March 2008, and spring and well samples collected in and around the study area in 2003 (Eastoe, 2005; Newton et al., 2008). It appears that isotope values for most groundwater plots along this evaporation line during dry climatic conditions, such as those observed in the early 2000's.

Water residing in unsaturated bedrock (triangles in Fig. 43) originates as local precipitation that infiltrates through soils into fractures and pores with little or no evaporation occurring. The isotopic composition of these waters is controlled by the elevation effects on the isotopic composition of local precipitation (Fig. 36). Therefore, the isotopic composition of this water plots along the LMWL with heavier isotopic compositions at lower elevations. On ridge tops and upper hill slopes where the San Andres Formation underlies shallow soils, large quantities of water can be stored in epikarst features. This water was flushed into the saturated carbonate aquifer system by large rainfall events during 2006 and 2008 monsoons, causing the isotopic composition of well and spring samples to shift towards the LWML. This recharge mechanism appears to occur as a response to extreme precipitation events.

GROUNDWATER AGE AND RESIDENCE TIME

When conducting large-scale groundwater tracer investigations, it is important to understand the residence time of groundwater within an aquifer. The residence time of groundwater is often inferred from its "isotopic age", based on interpretation of environmental tracers such as tritium (^{3}H), chlorofluorocarbons (CFCs), or carbon-14 (^{14}C). The isotopic age relates to the time elapsed between groundwater recharge and collection of a sample at a discharge point such as a well or spring (Mazor and Nativ, 1992). The heterogeneous nature of the Yeso Formation aquifer system can result in very different groundwater flow velocities and groundwater ages. Tracer ages will also be influenced by mixing of waters due conduit/fracture/matrix interactions and by mixing of groundwater from multiple sources. Such aquifer heterogeneities complicate studies of groundwater flow rates in large, regional-scale investigations such as this study. Figure 44 shows sample locations for various age-dating analyses collected in the study area.

Tritium

Tritium levels collected from precipitation samples in the southern Sacramento Mountains range from 3 to 10 TU, reflecting typical seasonal variations (Appendix 7). Tritium concentrations in well and spring samples from the study area range from zero to 7.82 TU (Table 6). The highest tritium concentrations, indicating shorter residence times (younger water), generally occur in the high mountains region (Fig. 45), and there is a rough correlation between sample elevation and ^{3}H concentration. In general, tritium values decrease from west to east (down gradient), and the lowest concentrations of ^{3}H, less than about 1 TU, are found in wells sampled on the Pecos Slope, in the eastern part of the study area (Fig. 45B).

Water samples from wells in the study area tend to have lower tritium concentrations than spring samples. The average ^{3}H concentrations from all well samples is 1.6 TU, compared with 3.7 TU for springs. This observation reflects the fact that wells are accessing deeper, older water than springs in the high mountains, many of which discharge from perched aquifers.

Several springs from the high mountains, and one from the Pecos Slope, were sampled twice to assess changes in the groundwater age and potential age effects from recharge events. From springs sampled in the high mountains, the first samples were collected after the monsoons of 2006, while

Table 6–Compiled age data for all wells and springs.

	Point ID	Collection Date	Site Type GW = well SP=spring	Tritium (TU)	$^{3}H:^{3}He$ Age (yrs)	R/Ra^	$\delta^{13}C$ (‰)	^{14}C (pMC)	CFC113 (yrs)	CFC12 (yrs)	CFC113/12 ratio (yrs)	Avg % young in mix from CFC113/12**
High Mountain aquifer system	SM-0011	23-Jul-07	GW	3.18					30	34	26	65.7
	SM-0012	25-Jul-07	GW	2.12								
	SM-0016	24-Jul-07	GW	2.86								
	SM-0018	28-Aug-07	GW	4.06	1.9	1.02			23	26	20	76.5
	SM-0021	10-Jul-07	GW	3.56	0	1.00			20	22	19	93.5
	SM-0023	10-Jul-07	GW	0.01	>50	1.25			29	Cont	NA	25.2*
	SM-0038	09-Jul-07	GW	2.41	0	0.97			19	18	19	69.3*
	SM-0040	09-Jul-07	GW	0.88	>50	0.18			26	21	29	NA
	SM-0042	24-Jul-07	GW	2.35					21	Cont	NA	NA
	SM-0045	10-Aug-07	GW	3.02	6.7	1.00			27	Cont	NA	NA
	SM-0056	26-Jul-07	GW	2.59					28	34	22	49.7
	SM-0057	26-Jul-07	GW	2.26	0	0.96			24	30	20	66.8
	SM-0059	11-Jul-07	GW	2.86					22	Cont	NA	NA
	SM-0069	11-Jul-07	GW	1.67								
	SM-0072	28-Aug-07	GW	2.52								
	SM-0076	25-Jul-07	GW	0.13	>50	0.16			38	47	17	6.5
	SM-0085	24-Jul-07	GW	7.2	14.9	1.04			21	23	21	94.9
	SM-0086	25-Jul-07	GW	0					23	26	21	83.7
	SM-0153	25-Jul-07	GW	1.85					24	27	22	82.5
	SM-1007	24-Oct-06	SP	4.42			-12	91.84	21	25	19	81.6
	SM-1009	23-Oct-06	SP	4.32			-12.9	92.65	20	24	18	81.5
	SM-1013	20-Jun-06	SP	6.11					20	24	17	76.3
	SM-1014	25-Oct-06	SP	4.52					21	24	19	86.1
	SM-1017	20-Jun-06	SP	4.05					21	25	19	76.9
	SM-1018	**18-Mar-08**	**SP**	**4.33**								
	SM-1018	**24-Oct-06**	**SP**	**4.52**					23	26	21	83.4
	SM-1026	20-Jun-06	SP	4.28					28	34	21	43.4
	SM-1027	21-Jun-06	SP	5.09								
	SM-1039	07-Nov-06	SP	4.92					22	25	21	87.7
	SM-1042	07-Nov-06	SP	1.92					21	24	20	90.6
	SM-1044	23-Oct-06	SP	4.3					20	23	19	84.9
	SM-1058	**15-Nov-06**	**SP**	**4.16**					20	22	19	89.7
	SM-1058	**20-Mar-08**	**SP**	**4.61**								
	SM-1059	**20-Mar-08**	**SP**	**1.85**								
	SM-1059	**15-Nov-06**	**SP**	**2.17**			-11	82.72				
	SM-1060	**20-Mar-08**	**SP**	**4.53**								
	SM-1060	**25-Oct-06**	**SP**	**5.04**					19	20	18	93.9
	SM-1062	25-Oct-06	SP	3.68					22	26	20	82.2
	SM-1067	23-Oct-06	SP	4.26					21	25	20	84.8
	SM-1069	**23-Oct-06**	**SP**	**5.25**					21	24	20	85.6
	SM-1069	**19-Mar-08**	**SP**	**5.32**								
	SM-1073	24-Oct-06	SP	3.49			-11	82.93	24	28	21	75.8
	SM-1077	24-Oct-06	SP	4.27					21	26	17	67.8
	SM-1079	**09-Aug-07**	**SP**	**0.87**								
	SM-1079	**12-Nov-08**	**SP**		problems	NA			31	29	34	20.8*
	SM-1080	24-Oct-06	SP	3.64								
	SM-1084	25-Oct-06	SP	3.2			-11.8	86.62	24	25	23	94.3
	SM-1090	14-Nov-06	SP	4.53					21	25	19	78.3
	SM-1097	28-Aug-07	SP	1.88					24	27	21	80.5
	SM-1101	12-Nov-08	SP	4.69								
Pecos Slope	SM-0044	09-Jul-07	GW	2.75					23	25	22	92.5
	SM-0068	10-Aug-07	GW	1.71					31	36	24	44.7
	SM-0074	24-Jul-07	GW	1.97	0	0.97			22	22	22	93.6
	SM-0079	25-Sep-08	GW	1.11								
	SM-0092	26-Sep-08	GW	1.86	mixed	0.98						
	SM-0092	13-Aug-08	GW						26	26	26	25.9
	SM-0133	14-Aug-07	GW	0			-7.4	49.35				
	SM-0138	16-Aug-07	GW	2.01			-8.9	85.76				
	SM-0140	16-Aug-07	GW	2.18			-8.9	80.89				
	SM-0144	07-Aug-07	GW	0.89			-8.3	70.54				
	SM-0151	07-Aug-07	GW	0.99			-7.9	58.67				
	SM-0152	07-Aug-07	GW	0.75			-8.5	65.71	38	38	38	19.1*
	SM-0156	20-Nov-08	GW	0.53								
	SM-0158	08-Aug-07	GW	0.68	29.1	1.01	-7.4	52.91	27	23	30	43.4*
	SM-0162	08-Aug-07	GW	0.42			-6.7	48.92				
	SM-0165	08-Aug-07	GW	0.17			-6.3	14.81				
	SM-0167	15-Aug-07	GW	0.41			-6.9	47.95				
	SM-0174	25-Sep-08	GW	1.63	mixed	0.50			23	17	25	55.1
	SM-0176	25-Sep-08	GW	1.08								
	SM-0193	20-Nov-08	GW	0.7	mixed	1.04			22	33	NA	38.9*
	SM-0197	20-Nov-08	GW	0.7								
	SM-0200	15-Aug-07	GW	0.26			-7.6	43.9				
	SM-0202	30-Aug-07	GW	0.34	0	0.96	-7.2	53.44	25	24	25	96.3
	SM-0203	30-Aug-07	GW	0			-7.4	45.57				
	SM-0207	30-Aug-07	GW	0.86			-8.2	62.75	Cont	29	NA	NA
	SM-0214	24-Sep-08	GW	0.05								
	SM-0217	24-Sep-08	GW	0.03					>40	59	NA	NA
	SM-0219	24-Sep-08	GW	0.58								
	SM-0244	26-Sep-08	GW	1.52								
	SM-1091	**09-Aug-07**	**SP**	**1.04**								
	SM-1091	**12-Nov-08**	**SP**	**1.1**	mixed	1.02			23	24	23	98.9
	SM-1099	19-Aug-08	SP	1.21					23	24	22	88.5
Salt Basin	SM-0007	23-Jul-07	GW	3.99	10.4	1.00			19	22	17	84.1
	SM-0026	29-Aug-07	GW	2.72	0.5	1.01			27	32	22	59.9
	SM-0201	29-Aug-07	GW	2.06	0	0.98			27	33	23	55.7
	SM-1076	24-Oct-06	SP	5.11			-12.2	89.03	24	27	22	85.7
	SM-1087	07-Nov-06	SP	4.23			-14.9	104.9	23	26	21	86

* % young in mix calculated from CFC113/11 ratios.

** Where there is no age for $^{3}H:^{3}He$ calculated, % young mix was based on "0" value for excess air.

^ R/Ra represents the following ratio: ($^{3}He/^{4}He$ for the sample)/($^{3}He/^{4}He$ from atmosphere)

NA = Not available

Cont = Contamination of CFC species

Bold = Spring with repeat tritium samples

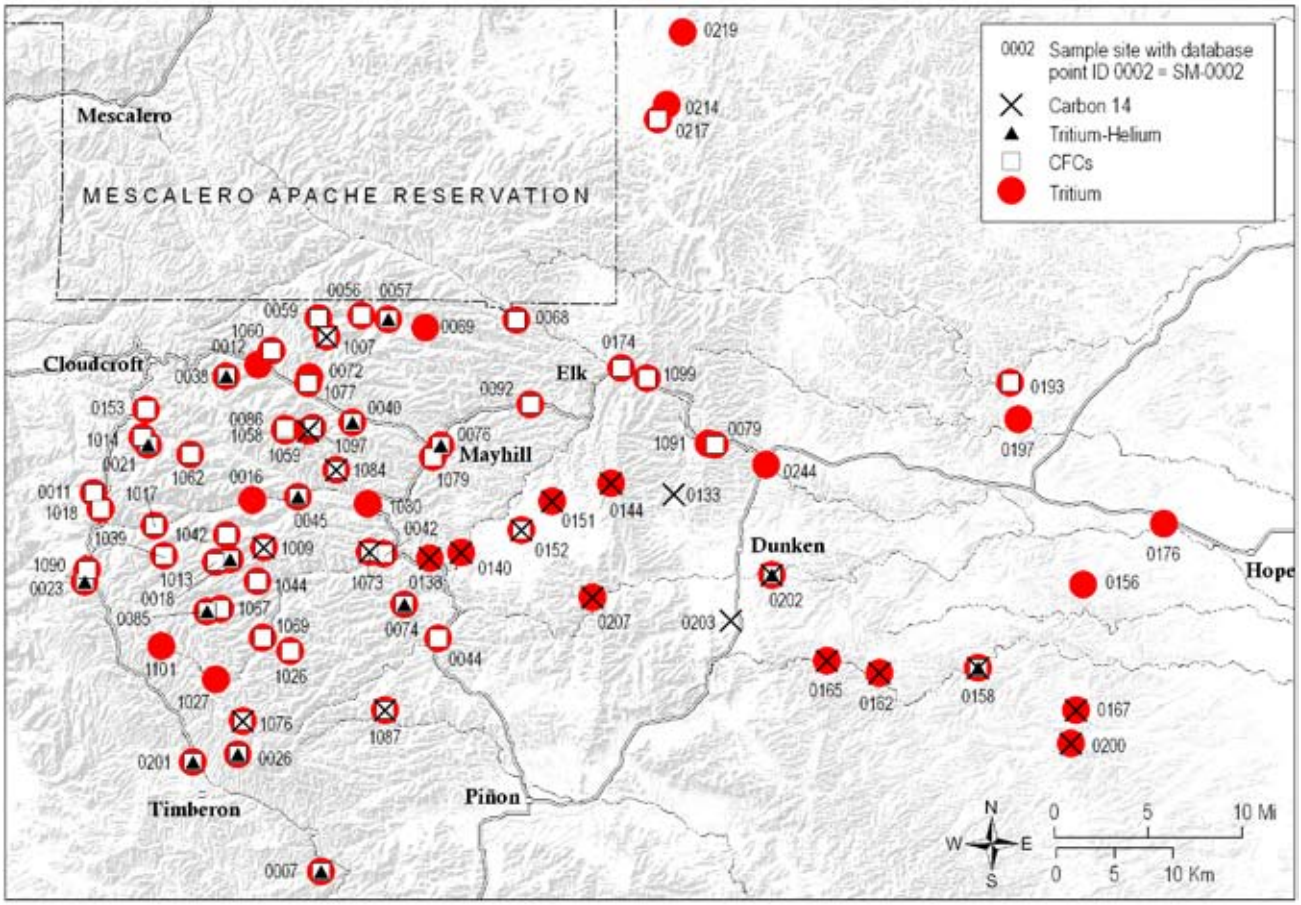

Figure 44–Map showing sample locations for age-dating analyses. Environmenal tracers used for age-dating include CFCs, tritium (^{3}H), tritium-helium (^{3}H:^{3}He), and carbon-14.

the second set of samples were collected in March of 2008 before winter snowmelt. The data are displayed in bold in Table 6. Samples collected in 2008 indicate the tritium values are nearly the same, suggesting that the tritium ages in the high mountains are largely unchanged by large precipitation events.

In the high mountains, samples with surprisingly low tritium concentrations (less than 1 TU) include SM-0023, SM-0086, SM-0040, SM-0076, and SM-1079 (Fig. 44, 45). SM-0023 is located at the crest of the mountain range where we would expect young groundwater; however, this well is along a fault which may affect groundwater flow and contribute older water. Wells SM-0086 and SM-0040 are not near any known faults, but the older age may reflect circulation of deeper, older water along a particularly well-developed joint system along the James Canyon drainage or the presence of low velocity flow paths through lower permeability rock. Well SM-0076 and spring SM-1079 are both located along the Mayhill fault zone, and also have anomalous water temperatures and chemical characteristics, which makes it likely that older water is circulating from depth along the Mayhill fault zone.

In the Pecos Slope region, the trend of young water along the margins of the high mountain aquifer indicates that this is the primary recharge zone for the Pecos Slope aquifer. Additional recharge likely occurs proximal to the Rio Peñasco where slightly higher tritium concentrations are found. Well samples collected in areas distal to the eastern margin of the high mountain aquifer system and the Rio Peñasco are older, with lower concentrations of tritium. Presumably these areas with older water and low tritium concentrations are not receiving significant surface recharge.

Tritium-helium and noble gases

Noble gas analyses were performed on 20 groundwater sample locations within the study area. Many of these analyses were used to derive tritium-helium (^{3}H/^{3}He) groundwater ages, which vary from zero (± 3 years) to greater than 50 years (Table 6). A sample with an age greater than 50 years indicates that the age is off the ^{3}H/^{3}He scale, and the true age of the groundwater sample is too old to be determined using noble gas systematics.

Most of the tritium-helium ages in the study area are quite young, in several cases less than one year old, with an average age of approximately 13 years. Although the youngest $^{3}H/^{3}He$ dates were found in the high mountains, some very old waters were also sampled in that region. Three well samples in the study area that dated at greater than 50 years, SM-0023, SM-0040, and SM-0076, also had very low measured tritium concentrations, as discussed above (Figs. 44, 45).

Most groundwater samples from the southern Sacramento Mountains yielded $^{3}He/^{4}He$ ratios similar to that observed for atmospheric gases, making it unlikely that mantle-derived helium is contributing to the ^{3}He component. Sample SM-0023, located near the crest of the Sacramento Mountains, has a high $^{3}He/^{4}He$ ratio, but a very low tritium level, making this the only site where there may be a source of mantle derived helium-3.

By contrast, low $^{3}He/^{4}He$ ratios may result from elevated levels of ^{4}He in groundwater samples.

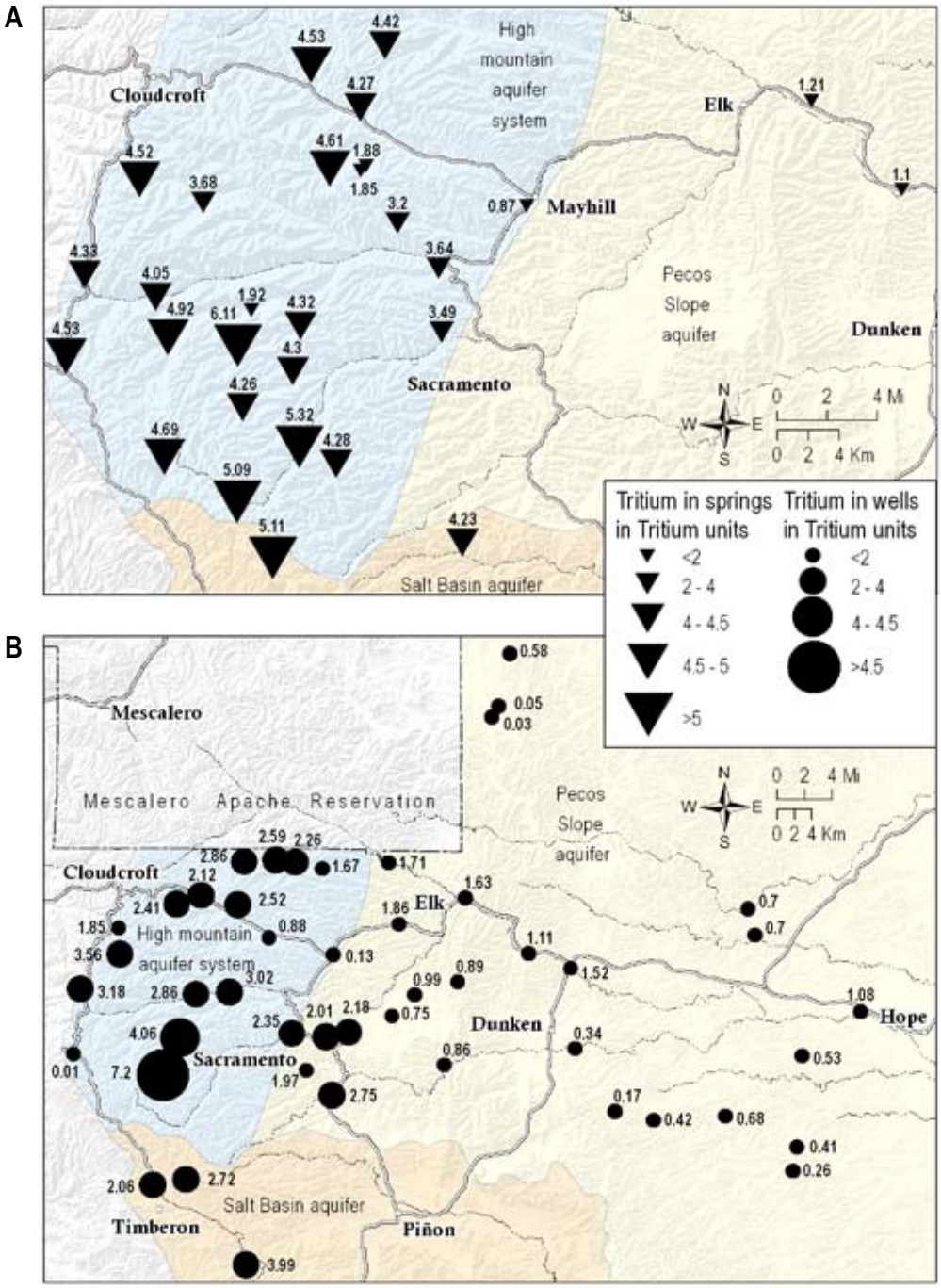

Figure 45–Spatial variation of tritium in samples. Points are labeled with tritium concentrations in tritium units (TU). Larger symbols indicate water that is younger relative to smaller symbols.
A–Tritium content in spring samples.
B–Tritium content in well samples.

Helium-4 is the most common isotope of helium in the atmosphere, and is also a product of radioactive decay of uranium and thorium nuclides in the earth's crust. Wells SM-0076 and SM-0040 yielded tritium-helium ages greater than 50 years and have low $^{3}He/^{4}He$ ratios, indicating a possible deep crustal source of groundwater (Solomon, 2000). Well SM-0076 is located along the Mayhill fault zone, which is a probable conduit for upwelling of deeper, crustal water. It is unlikely that SM-0040 sample was entirely from a deep crustal source; however, this well may draw water that has had some degree of mixing with deeper water.

Chlorofluorocarbons (CFCs)

Calculation of apparent age based on CFC concentrations in water samples is dependent on knowledge of the input recharge elevation and recharge temperature, with temperature being the more critical variable. In many areas of the southern Sacramento Mountains these parameters are difficult to determine and must be estimated. Estimated recharge temperatures that are too cold will result in apparent CFC ages that are too old, while warmer estimated recharge temperatures will result in erroneously young apparent ages. Similarly, an overestimation of recharge elevation will result in apparent ages that are too young, and an underestimation of recharge elevation will produce erroneously old ages (Kazemi et al., 2006).

For this study, recharge elevations were estimated to be approximately the same as the elevation of the sample site. Calculated recharge temperatures were determined from eight water samples based on analysis of their noble gas concentrations (Stute and Schlosser, 2000). Recharge temperatures for the remaining samples were then estimated from a linear regression based on temperatures of those eight water samples and their noble gas-derived recharge temperatures according to the following equation:

Sampled temperature = 0.94*(recharge temperature)+5.76

Samples analyzed for chlorofluorocarbons have CFC12 ages ranging from 20 to 64 years, with an average age of 28.4 years (Table 6). CFC113 ages are generally younger, with an average age of 25.1 years. Most of the CFC apparent ages are not concordant, with discrepancies of 3 to 10 years between CFC12 and CFC113.

CFC ratio ages were determined using CFC 2005-2a, a U.S. Geological Survey spreadsheet program for preliminary analysis of CFC data (Busenberg and Plummer, 2006). Groundwater apparent ages based on CFC113/CFC12 concentration ratios range from 17 to 25 years, with an average age of 21.2 years. In every case where a ratio age could be determined, the ratio ages are younger than apparent ages based on concentrations of CFC12 alone (Fig. 46). Such a discrepancy between apparent and ratio ages usually implies that mixing of waters of different ages has occurred (Han et al., 2001; Plummer et al., 2006).

In large-scale, regional studies, it is common to encounter water samples that result from mixing of two sources of groundwater with different ages, a process referred to as binary mixing. If the mixture includes an old component that is free of CFCs combined with a younger, CFC-bearing component, the CFC ratio age represents the age of the younger fraction. Under such circumstances, the ratio method can

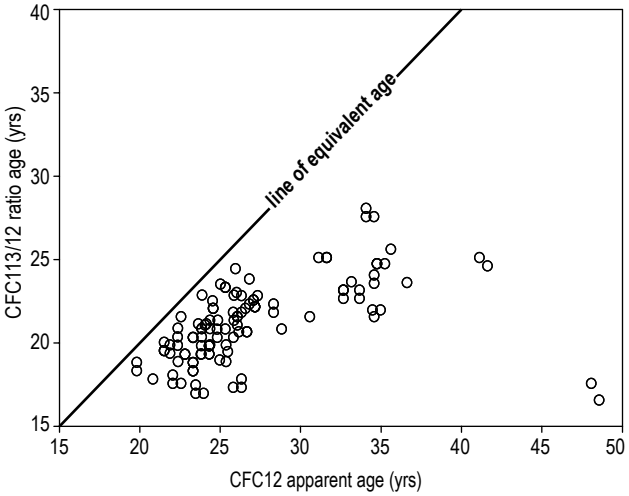

Figure 46–Comparison of apparent ages from CFC12 vs. CFC113/CFC12 ratios. CFC113/12 ratio ages are consistently older than CFC12 apparent ages.

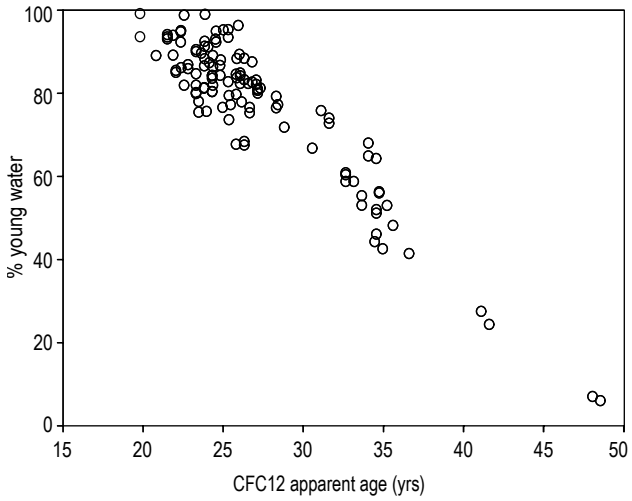

Figure 47–CFC12 apparent age of groundwater vs. percent young water in samples. Most water samples appear to be composed of >50% young water.

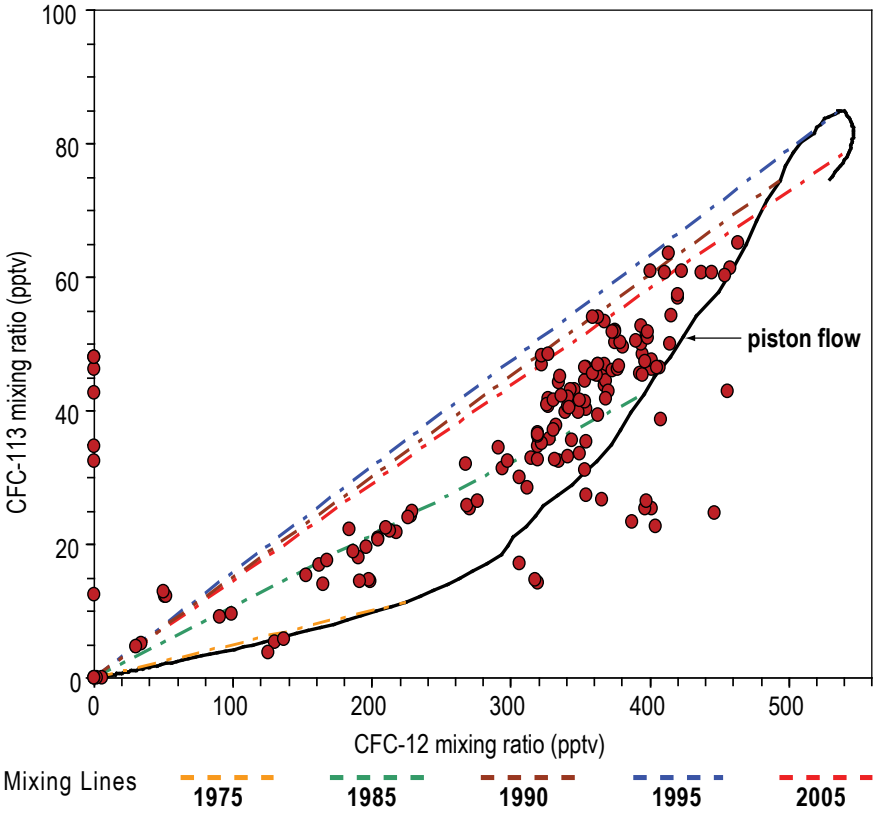

Figure 48–CFC113 and CFC12 atmospheric mixing ratios (pptv). Solid curve indicates piston flow conditions. Dashed lines are binary mixing lines for various recharge years. Any point that falls on one of the dashed lines represents linear mixing of old, CFC-free water with younger water recharged during that year. Percent young water can be estimated by location of a point on the binary mixing line. Points that fall outside the envelope defined by the piston flow curve and the binary mixing lines have been influenced by concentration-modifying effects such as CFC contamination or microbial degradation (Han et al., 2001).

also be used to determine the proportion of young water in the mix (Han et al., 2001; Plummer et al., 2006). The percentage of young water in southern Sacramento Mountains groundwater samples ranges from 99% to 6%, with an average of 77.2%. There is a correlation between the CFC12 apparent age and the fraction of young water in the mix, with the oldest samples containing the smallest percentage of young water (Fig. 47). This correlation indicates a binary mixing model is valid and that the percentage of young water is the principal factor influencing groundwater apparent age based on individual CFC species (e.g., Long et al., 2008).

A plot of CFC12 versus CFC113 mixing ratios (Fig. 48), using the method of Busenberg and Plummer (2006), clearly shows that most CFC data can be explained by a binary mixing model. The results show that the young components of groundwater recharge in the southern Sacramento Mountains occurred during the mid-to-late-1980s. The plot also shows a few samples that are significantly older, as well as evidence that microbial degradation or contamination processes have altered the CFC composition of some samples (Plummer et al., 2006). Samples with contamination issues are identified in Table 6 as "cont."

Several locations sampled for CFCs strongly indicate the presence of old water. The oldest samples based on the percent young fraction and CFCs ages include SM-0076 (with only 6.5% young water), SM-0217, and SM-0152 (Fig. 44). Well SM-0076 is located along the Mayhill fault zone, has anomalous water temperatures and chemical characteristics, and an old (greater than 50 years) tritium-helium age. It is likely that older water is circulating from depth along the Mayhill fault zone to this well. CFC concentrations in SM-0217 are very low, suggesting that much of this sample was recharged prior to the introduction of CFCs to the atmosphere. This well is located along the eastern margin of the Mescalero-Apache Reservation, and along the northern extent of the Dunken-Tinnie anticlinorium. The well also has high major ion concentrations consistent with older, more evolved groundwater circulating from depth along faults related to the structural zone. Well SM-0152 is located within the area of McDonald Flats, which is an area where the slope of the water table is noticeably flattened (hydraulic gradient less than 48 feet/mile).

Carbon–14

Most water samples collected from springs and wells in the high mountain aquifer system (above 7,000 feet elevation) are saturated with respect to calcite (Fig. 33), a fact supported by multiple field observations of tufa mounds, and springs actively

precipitating tufa at many locations. In addition, those water samples from higher elevations that were analyzed for ^{14}C show elevated levels of percent modern carbon (pMC) (Table 6). These two observations strongly suggest that the high mountain aquifer system is an open system, allowing for re-equilibration between dissolved inorganic carbon and ^{14}C-active soil and atmospheric CO_2. Therefore, conventional ^{14}C dating techniques are not likely to be useful in determining groundwater residence time. The pMC and calcite saturation data are, however, consistent with field observations and stable isotope records that suggest groundwater is recycled multiple times during its flow down gradient through the high mountain aquifer system.

Carbon-14 methods appear to have more application farther down gradient beneath the Pecos Slope, where the aquifer is a closed system (Morse, 2010). Samples collected from wells on the Pecos Slope, along an apparent flow path from the McDonald Flats area to Hope, show a systematic decrease in ^{14}C pMC from west to east, coupled with increasing $\delta^{13}C$ values. The decrease in ^{14}C pMC is due to radioactive decay of ^{14}C and the addition of "dead carbon" resulting from the dissolution of Permian carbonates. The increase in $\delta^{13}C$ values is due to the dissolution of carbonate rocks. There is also a pronounced and consistent eastward increase in Mg/Ca ratios, indicative of dedolomitization processes as groundwater moves down the flow path from west to east. Mass transfer models of the dedolomitization process have been used to adjust ^{14}C ages for groundwater in the Madison aquifer (Plummer et al., 1990; Back et al., 1983) and the Pecos Slope aquifer as a part of this study (Morse, 2010). Morse (2010) used $\delta^{13}C$ data along with dedolomitization stoichiometry to correct ^{14}C values so that they reflect the decrease in pMC values that are only due to radioactive decay. Corrected ^{14}C values beneath the Pecos Slope along this flow path, indicate that it takes groundwater approximately 1300 years to travel from the western boundary of the Pecos Slope aquifer along a flow path approximately 18 miles (35 kilometers) down gradient.

Groundwater residence time

Groundwater residence time in the southern Sacramento Mountains study based on tritium samples, and on tritium-helium and CFC methodologies, ranges from less than one year to greater than 50 years. Average residence times vary from ~13 years based on $^{3}H/^{3}He$ systematics to ~28 years based on CFC12 concentrations. CFC apparent ages derived from concentration ratios yield intermediate ages averaging 21.2 years. The spatial distribution of tritium in water samples (Fig. 45) indicates that groundwater age generally increases to the east, which is consistent with regional groundwater flow derived from mapping of the water table and water chemistry sampling in the southern Sacramento Mountains (Fig. 18, 32).

Our findings suggest that most groundwater in the southern Sacramento Mountains entered the aquifer system approximately 15 to 25 years ago. However, a distinctive feature of the sampling program is the lack of concordance among the several methods used to determine the residence time of groundwater in the study area. This discordance provides additional insight into the heterogeneous character of the high mountain aquifer system. Three main factors, discussed below, contribute to the discordance among the several methodologies employed to evaluate groundwater residence time in the southern Sacramento Mountains.

Thick unsaturated zone

Water-levels in many of the wells sampled are quite deep, in some cases several hundreds of feet below ground level. These deep water-levels imply that there is a thick unsaturated zone in many parts of the study area. The seepage of water through a thick unsaturated zone can produce conflicting results when dating groundwater using CFC and tritium-helium methodologies. Tritium in groundwater that decays in the unsaturated zone produces ^{3}He atoms that partition into the gas phase and do not continue to travel with infiltrating water (Kazemi et al. 2006). Only those ^{3}He atoms produced in the saturated zone are preserved in groundwater, which means that the $^{3}H/^{3}He$ age begins below the water table and does not account for travel time through the unsaturated zone. In areas where a thick unsaturated zone is present and vertical rates of water infiltration are low, $^{3}H/^{3}He$ ages will be much younger than the true age of the groundwater sample.

A thick unsaturated zone will have the opposite effect on groundwater age derived from CFC concentrations. If there is a thick unsaturated zone and soil water content is high, CFCs may be preferentially dissolved into the soil water, leaving the groundwater somewhat depleted in CFCs. In addition, dissolved CFCs will partition into gas phase and ultimately travel through the vadose zone at a slower rate that infiltrating water. The net effect leads to an overestimation of groundwater age. In other words, a thick unsaturated zone can result in anomalously young $^{3}H/^{3}He$ groundwater ages, and anomalously old CFC apparent ages (Kazemi et al., 2006, Happell et al., 2006).

Discrepancies between $^{3}H/^{3}He$ and CFC ages suggest the influence of a thick unsaturated zone in the southern Sacramento Mountains recharge area. The greatest difference between the two methods is

observed in five wells with water-levels ranging from 100 to 800 feet (32 to 240 meters) below ground level. These wells (samples SM-0057, SM-0201, SM-0202, SM-0038, SM-0021 and SM-0074) yield $^{3}H/^{3}He$ groundwater ages of less than one year, and CFC12 ages ranging from 20 to 33 years (Table 6). It should be noted that leakage of perched aquifers through an intermediate unsaturated zone (Fig. 25) can cause the same effects on $^{3}H/^{3}He$ and CFC apparent ages that are described above. The disparities between CFC and tritium-helium groundwater dates suggest that groundwater flow through unsaturated zones may be an important component of the total residence time of groundwater in the study area.

Recycled groundwater

A second factor influencing discrepancies among the different groundwater dating methods involves recycling of surface water to groundwater, particularly in the high mountains. Regional mapping of the water table (Fig. 18), along with water chemistry, stable isotopes and tritium data (Fig. 45), shows that the primary source of groundwater recharge is local precipitation at elevations above 8,200 feet. Stable isotope data, water chemistry and field observations suggest that water discharging from perched aquifers and springs at higher elevations undergoes evaporation as part of the surface water system. Surface water then recharges the shallow groundwater system via losing streams, and later discharges from other springs at lower elevations. This process of recycling may occur several times before the water is deep enough below the surface that it no longer interacts with the surface water system. Each time groundwater re-emerges from springs, the water partially of fully re-equilibrates with the atmosphere, resulting in the CFC and $^{3}H/^{3}He$ clocks being completely or partially reset. However, the tritium content remains the same.

Recycling of groundwater is strongly indicated by discrepancies between tritium content and $^{3}H/^{3}He$ or CFC ages of several water samples (Table 6). One example is SM-0026, with a tritium-helium age of less than one year and a tritium content of 2.72 TU. Sample SM-0026 was collected from a well adjacent to a perennial flowing stream that is spring-fed (Fig. 44). The very young tritium-helium age of the water sample coupled with rather low tritium concentration reflects recycling of groundwater. Other examples in the high mountains region, where the recycling effect is pronounced, include SM-0057, SM-0038 and SM-0021.

Previous workers have invoked groundwater recycling as a mechanism to account for discrepancies between CFC apparent ages and tritium content in the Roswell Artesian Basin farther to the east (e.g., Land and Huff, 2010). Similar discrepancies between CFC apparent ages and tritium content within springs in the high mountains are apparent in SM-1079, SM-1097 and SM-1042 (Fig. 44).

Groundwater mixing

Mixing of groundwater of different ages can also cause the discordance among the different methodologies employed to evaluate groundwater residence time in the southern Sacramento Mountains. Stable isotope data indicate that the high mountain aquifer system is a well-mixed system. The heterogeneity of the Yeso Formation, along with regional fracture systems results in a hydrologic system that can facilitate mixing of waters within flow paths at different velocities (different ages). The conceptual model shown in Figure 25 illustrates different mixing mechanisms that include leakage from one aquifer to another, the merging of two or more groundwater flow paths, and the integration of water from springs that discharge at different stratigraphic levels in perennial and ephemeral streams. Water chemistry data indicates another mixing mechanism. Water from a few wells and springs appears to be a mixture of fresh groundwater and older water that is upwelling along fault zones (Appendix 8).

Mixing of groundwater of different ages is strongly indicated by CFC data. Discrepancies in apparent CFC age among the three different CFC species suggest that some degree of mixing has occurred. In addition, apparent ages based on CFC12 concentrations are consistently older than apparent ages derived from CFC113/CFC12 concentration ratios (Fig. 46). This disparity indicates a very high probability for mixing of waters of different ages within the aquifer (Han et al., 2001). Most CFC data can be explained by a binary mixing model that assumes mixing of two principal groundwater end-members, one old source that is CFC-free (pre-1940 recharge), and one younger source of CFC-bearing groundwater. Most water samples appear to be composed of >50% young groundwater (Fig. 47), and this young component is typically 15 to 25 years old (Fig. 48). Most of these water samples are probably a mixture of groundwater of different ages as a result of the extreme heterogeneity of the high mountain aquifer system.

Four samples (SM-0076, SM-0040, SM-0023, SM-1079) are composed of <25% young water according to CFC concentrations. All of these samples show low tritium concentrations (<1TU), and the groundwater samples exhibit tritium-helium ages greater than 50 years (Table 6). Sample SM-0076

was collected near a gaining reach of the Rio Peñasco along the Mayhill fault (Fig. 44). CFC113/CFC12 ratios indicate that the sample contains only 6% young water (Table 6). High chloride-bromide ratios (Cl/Br = 1,267) and high ion concentrations (TDS = 1,025 mg/L; sulfate = 530 mg/L) are consistent with mixing of deeply sourced brines (Davis et al., 1998). Sample SM-0076 also has a low $^{3}He/^{4}He$ ratio, indicative of groundwater with a deep crustal origin (Solomon, 2000).

Approximately 3 miles upstream of well SM-0076, spring SM-1079 discharges a large volume of water with only ~20% young water in the mix (Table 6). SM-1079 also has a rather high Cl/Br ratio of 525, although the water is fresher than SM-0076, with TDS of only 546 mg/L. SM-1079 is located in the valley bottom and the low TDS may result from mixing of deeper artesian waters with younger, fresher groundwater derived very locally from Rio Peñasco valley alluvium.

Wells SM-0023 and SM-0040 also have low $^{3}He/^{4}He$ ratios, indicative of a deep crustal component of groundwater. Taken together, these data strongly support a model that involves mixing of relatively young, fresh, shallow groundwater with older artesian groundwater upwelling along fault zones from much greater depths. Mixing of groundwater from multiple sources has clearly contributed to the disparity in groundwater ages derived from the different analytical methods employed in this study.

Summary

The youngest groundwater ages are predominantly found in the high mountain aquifer system, with increases in age down gradient into the Pecos Slope. This supports our finding that the high mountains region is the primary recharge area for the surrounding aquifers. Most groundwater in the southern Sacramento Mountains watershed entered the aquifer approximately 15 to 25 years ago. However, complex flow paths, a thick unsaturated zone, and recycling of groundwater over the course of its down-gradient flow from west to east have resulted in ambiguities in age data among the different groundwater tracers. Mixing of groundwater from multiple ages is strongly indicated by tritium samples, tritium-helium and CFC dating, and helium-3/helium-4 ratios, consistent with mixing of young, fresh groundwater with pre-modern, artesian groundwater upwelling along fault zones.

IV. CONCLUSIONS

In this section, we integrate the results of geologic mapping, water chemistry, stable isotope, and age dating analyses to answer specific questions about the hydrologic system in the southern Sacramento Mountains. We present a regional hydrogeologic conceptual model focused on the high mountain aquifer system and Pecos Slope aquifer. We compare our results and previous studies and then suggest future work to be done.

REGIONAL HYDROGEOLOGIC CONCEPTUAL MODEL

Figure 49 shows our regional hydrogeologic conceptual model along a cross-section. Under average climatic conditions, precipitation (mostly snowmelt) enters the system in the primary recharge area (elevations greater than 8,200 feet), through fractures and conduits on ridges and upper hill slopes and stream beds. Water of different ages mixes in the subsurface due to the heterogeneity of the Yeso Formation and the presence of regional fracture systems. High elevation streams (e.g. Upper Peñasco and Wills Canyon) that are fed by multiple springs allow mixing of water from different perched aquifers. Groundwater flows down gradient from the recharge area through a series of perched carbonate aquifers that are connected to varying degrees by fractures and surface water drainages. These shallow perched carbonate aquifers are located at multiple stratigraphic levels in the Yeso Formation and result in hundreds of springs throughout the high Sacramento Mountains west of Mayhill. Springs at higher elevations feed streams that recharge perched aquifers that discharge at springs at lower elevations.

Groundwater attains an increasingly evaporative isotopic signature as it makes its way through this system due to repeated exposure of water to the atmosphere. Ca and HCO_3 are the dominant ions in the high mountain aquifer system, due to the dissolution of calcite and dolomite in the San Andres and Yeso Formations. Continuous water/mineral interactions cause the water chemistry to evolve and become more SO_4 rich along the regional flow path from west to east. Groundwater hydrographs also suggest the presence of deeper more regional aquifers in the high mountain aquifer system. Most groundwater in the high mountain aquifer system is a mixture of young water (15 to 25 years old) and older water (>50 years old). Groundwater and surface water in the high mountain aquifer system ultimately recharges the Pecos Slope aquifer and the Salt Basin aquifer.

Although snowmelt at high elevations is the contributes more groundwater recharge over long time periods, extreme monsoons, such as those observed in 2006 and 2008 flush large amounts of water stored in the unsaturated zone into the saturated groundwater system, resulting in significant groundwater-level increases.

Unlike the high mountain aquifer system, the Pecos Slope aquifer is one regional aquifer. The stable isotopic composition of groundwater in this aquifer reflects that of groundwater at the eastern edge of the high mountain aquifer system and is fairly uniform throughout the aquifer in our study area. This uniform isotopic composition indicates that little or no recharge from the surface is occurring. However, there is evidence of small amounts of local recharge occurring along the Rio Peñasco and along the eastern boundary of the study area near the principal intake area as described by Fiedler and Nye (1933). Groundwater in the Pecos Slope aquifer has higher SO_4 and Mg concentrations due to the process called dedolomitization. The water chemistry in the Pecos Slope aquifer is different than that of the high mountain aquifer system because it was been in the system longer and has had more time to interact with the rocks. Groundwater in this aquifer takes approximately 1300 years to flow from the western aquifer boundary to the eastern edge of our study area (Morse, 2010). Groundwater in the Pecos Slope aquifer flows into the Roswell Artesian aquifer to the east.

HOW DOES GEOLOGY INFLUENCE GROUNDWATER FLOW?

The Sacramento Mountains form a large, east dipping plateau uplifted along the steep western escarpment by the Alamogordo fault. The plateau is

dissected by deep canyons, some more than 1000 feet deep. This plateau extends into a low relief surface (the Pecos Slope) to the east towards the Roswell Artesian Basin (Fig. 9). The Permian Yeso and San Andres Formations are the most important geologic units in the study area. The Yeso Formation, which is exposed in the high mountain aquifer system, is composed of chaotic layers of limestone, dolomite, shale, siltstone and sandstone that are not continuous for more than a few hundred feet. The overlying San Andres Formation is composed of gray limestone.

Within the study area, the San Andres and Yeso Formations dip gently (2–3°) from the crest of the southern Sacramento Mountains toward the Pecos River. On a regional scale, groundwater generally flows in this same direction as the bedrock dips, from high elevation in the west to low elevation in the east (Fig. 18). However, within the high mountains, where the Yeso Formation is highly fractured, with lateral and vertical heterogeneity, groundwater does not simply flow down dip along bedding planes.

The Yeso Formation is the primary aquifer in the high mountain aquifer system. The heterogeneity of the Yeso Formation has profound effects on how water moves through this system. The spatial variability of rock types of different intrinsic permeabilities and the presence of secondary permeability such as fractures and conduits results in a complex hydrologic system. Karst processes increase the permeability of carbonate rocks, resulting in carbonate layers being the primary water bearing zones. Perched carbonate aquifers, sandwiched between rocks of lower permeabilities exist throughout the area and discharge at hundreds of springs that feed mountains streams. Regional fracture systems also play an important role in the high mountain aquifer system. Fractures allow precipitation to infiltrate quickly through rocks of low intrinsic permeability to recharge aquifers. Recharge through fractured bedrock is especially important in zones of high fracture density, particularly in joint parallel stream reaches that are areas of focused recharge. Groundwater and surface water flow direction also appears to be influenced by regional fracture systems (Walsh, 2008).

Within the Pecos Slope aquifer groundwater occurs in the Yeso and the lower portion of the San Andres Formations. The Yeso Formation is not exposed in this area. A few springs discharge along the Dunken-Tinnie anticlinorium. Karstification of the San Andres limestone manifests in large cavernous fractures and sinkholes and causes the hydraulic gradient to decrease. Unlike the high mountains

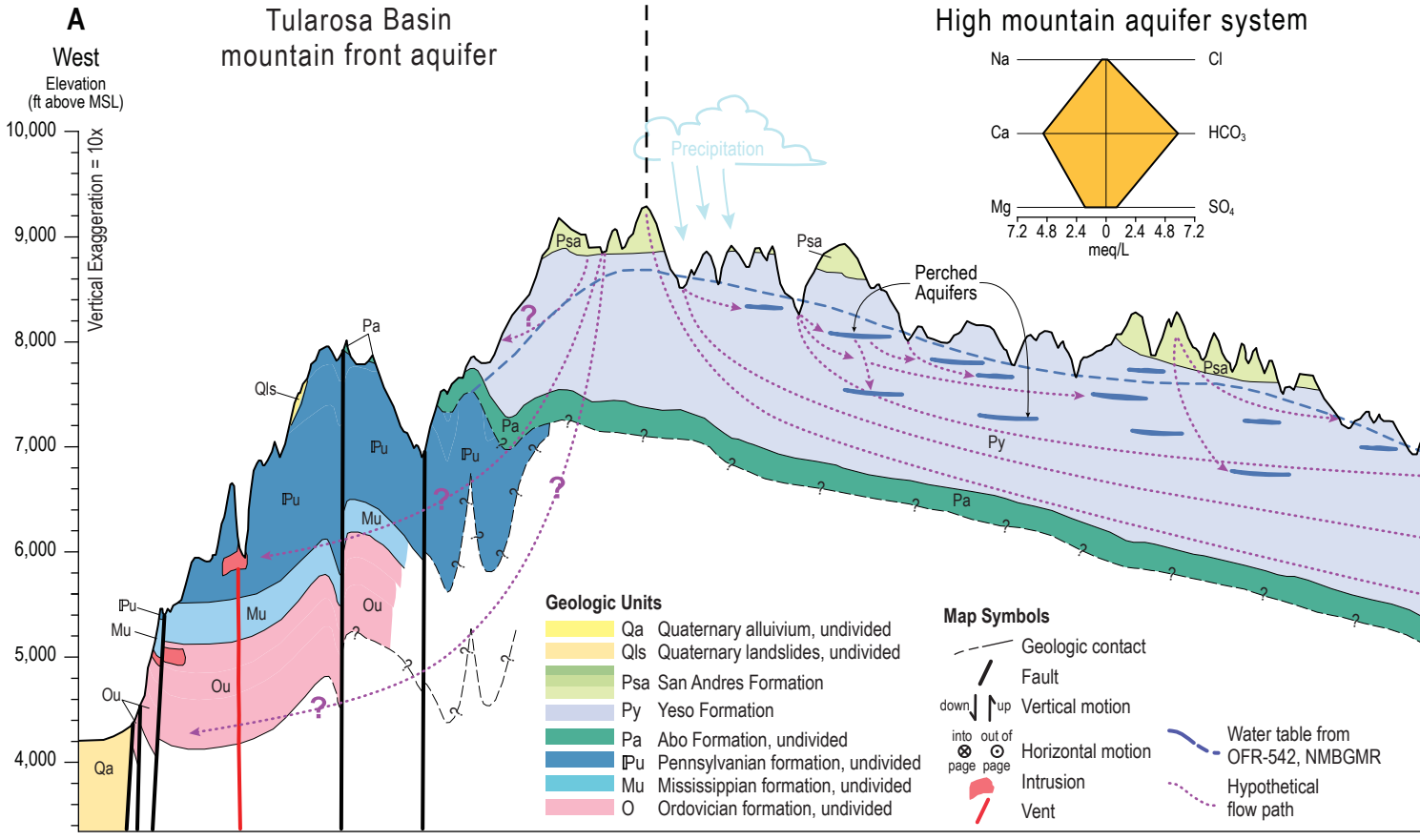

STIFF DIAGRAM

Stiff diagrams are a way of plotting the general chemistry of water. Positively charged ions (sodium (Na), calcium (Ca), and magnesium (Mg)) are plotted to the left of the vertical line, and negatively charged ions (chloride (Cl), bicarbonate (HCO_3), and sulfate (SO_4)) are plotted to the right. Ion concentrations increase as the distance between the plotted point and the center vertical line increases. The shape of the Stiff diagram indicates the relative proportions of the different ions, and the size of the Stiff diagram indicates the absolute concentration of ions in solution. In general, the shape of a Stiff diagram is controlled by the type of rocks with which the water has been in contact. The size of the Stiff diagram is usually controlled by the solubility of the minerals in the rocks and the amount of time the water has been in contact with them.

Figure 49–Regional hydrogeologic conceptual model. From the high mountain aquifer system to the Pecos Slope aquifer, cross section is shown on inset map from A to A'. The San Andres and Yeso Formations generally dip eastward, and the groundwater table roughly mimics this pattern. Recharge to groundwater is from precipitation (primarily snow melt). Hypothetical groundwater flow paths (in purple) within the high mountain aquifer system illustrate focused recharge occurring in canyon bottoms, with some water following deep or shallow flow paths. In the high mountain aquifer system, perched carbonate aquifers are connected via fractures and surface water. Continual evaporation occurs as groundwater resurfaces multiple times. The stable isotopic composition of groundwater increases as it moves east in the high mountains system (δD values -71 to -51‰). The dominant ions in this groundwater are calcium and bicarbonate due to the dissolution of limestone and dolomite. Many springs and wells discharge water which is primarily young water (15–25 years old) mixed with some older groundwater. There is evidence that faulting in the region may cause vertical upwelling of groundwater from deep flow paths, particularly along the Mayhill Fault. Water in the Pecos Slope aquifer mostly resides in the Yeso Formation, but the water table often occurs in the lower San Andres Formation, which becomes more important as an aquifer towards the east. Relatively uniform stable isotope results show that groundwater from the high mountain aquifer system is the primary recharge source to the Pecos Slope aquifer (δD values -65 to -51‰). Water chemistry data shows an increase in sulfate and magnesium due to the dissolution of gypsum and dolomite in a process called dedolomitization. Groundwater may take up to 1300 years to travel from Mayhill to the eastern edge of the study area. Water in the Pecos Slope aquifer ultimately recharges the Roswell Artesian Basin aquifer..

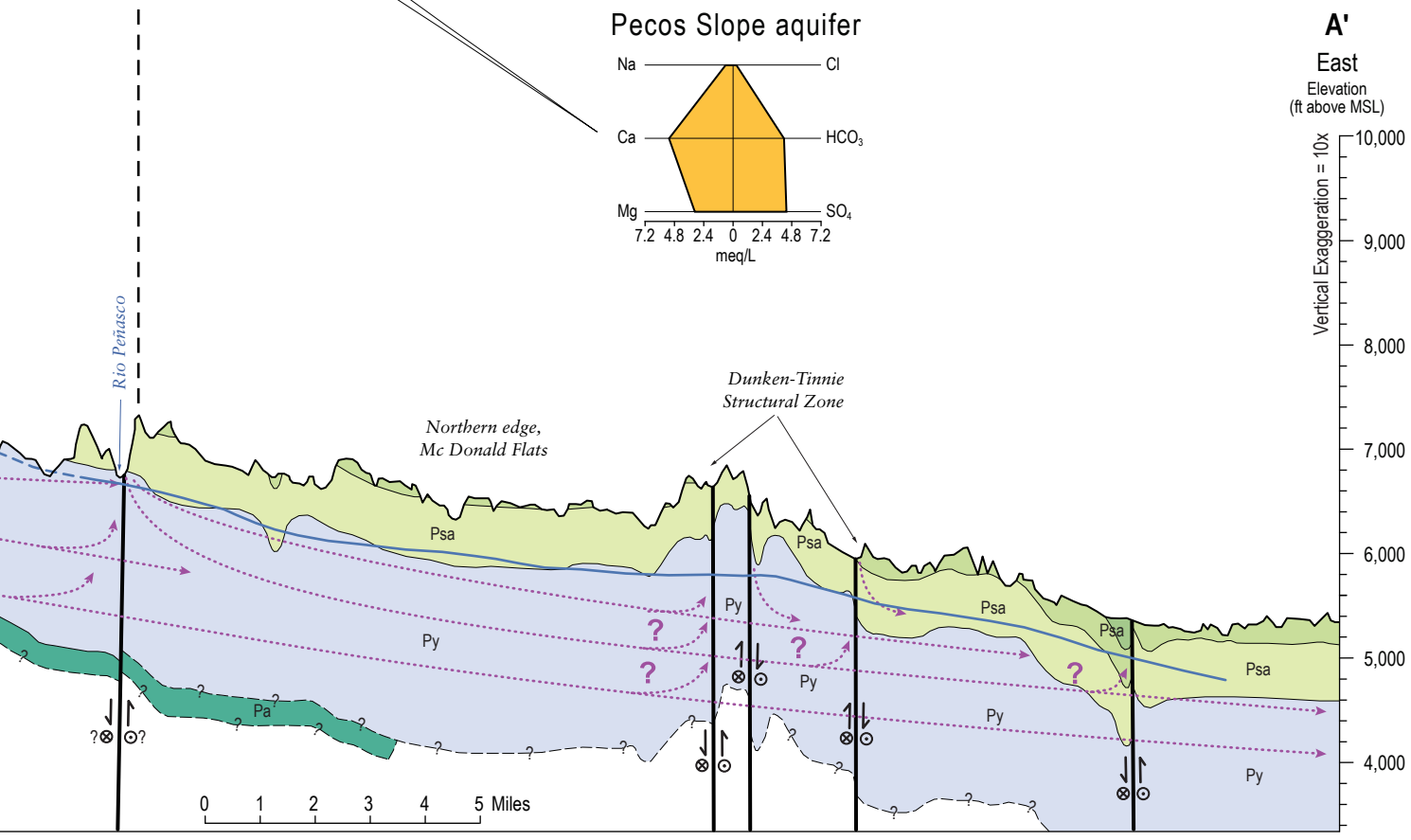

aquifer system, the Pecos Slope aquifer appears to be one regional aquifer that transports groundwater to the south and east.

HOW DOES CLIMATE AFFECT THE GROUNDWATER SUPPLY?

Data collection for this study took place from the fall of 2005 through June of 2009. Over this period, we observed a wide range of climatic events and seasons. The most significant climatic events were the monsoons of 2006 and the remnant of Hurricane Dolly in 2008, both of which were both characterized by extreme precipitation amounts (Fig. 15). When this study began, groundwater-levels were declining and springs were decreasing in flow. The region was in a multi-year drought (NOAA, 2000), which was followed by the extreme rainfall events. With our dataset we were able to observe fluctuations in the groundwater-levels and the stable isotopic compositions of spring and well water with time, which have implications for climatic controls on groundwater recharge.

During times of stable or declining groundwater-levels, recharge (input) still occurs, but it is equal to or less than discharge (output) respectively. A proportion of snowmelt and summer precipitation infiltrates through the unsaturated zone to recharge the groundwater system. Stable isotope results for spring and well water plot along an evaporation line that intersects the local meteoric water line in the range of expected winter precipitation values (Fig. 37), indicating that snowmelt contribution to groundwater recharge exceeds that of summer precipitation. Our data and those of Eastoe (2005) suggest that snowmelt is the primary input to the system. However, the large increases in groundwater-levels observed in 2006 and 2008 (Fig. 21, 22) show that extreme summer monsoons can also contribute significantly to groundwater recharge

The southern Sacramento Mountains are clearly a recharge area, with almost all groundwater being derived from local precipitation. Therefore precipitation patterns and amounts have a direct effect on groundwater-levels in the study area. Observed groundwater-level declines prior to this study were a result of below average precipitation rates in the late 1990s and early 2000s (NOAA, 2000). Extreme monsoons in 2006 and 2008 resulted in a very significant increase in groundwater-levels in most wells in the study area. This link between climate and groundwater-levels is of interest, particularly with the uncertainties associated with global climate change. It is our interpretation that in the past, snowmelt has usually provided most of the recharge to the southern Sacramento Mountains. However, with changes in climate patterns, the monsoon season may play a greater role in recharge to the area.

In a nearby study, stream discharge measurements in the Eagle Creek basin in Lincoln County, west of Ruidoso, show a change in the seasonal timing of peak streamflow (Matherne et al., 2010). From 1970 to 1980, streamflow was dominated by spring snowmelt, whereas from 1989 to 2008, streamflow was dominated by summer monsoon precipitation. Overall, stream discharge was lower during the latter period. Matherne et al. (2010) speculate that such a change in peak precipitation and stream discharge could negatively affect the amount of groundwater recharge, as peak flows during monsoon season are likely of higher magnitude and shorter duration as compared to spring runoff from snowmelt. Similar precipitation and streamflow trends to those in the Eagle Creek basin likely exist in the southern Sacramento Mountains study area (there are no detailed stream gage records in the present study area). However, in contrast to the Eagle Creek basin study, results from the water-level measurements in this study do indicate the occurrence of recharge during intense monsoon events.

WHERE DOES GROUNDWATER RECHARGE OCCUR?

Spatial trends observed for water chemistry, stable isotopes, water ages and groundwater-levels indicate recharge occurs within the area of the high mountain aquifer system, dominantly above 8,200 feet. This high elevation recharge zone is a very important area, as it provides recharge not only for the surrounding high mountain aquifer system, but is also peripherally linked with the Pecos Slope, the Salt Basin, and the Tularosa Basin mountain front aquifers (Fig. 24). We will call this area the primary recharge area.

Most springs and wells above 8,200 feet produce calcium-bicarbonate or calcium-magnesium-bicarbonate type water, as result of the dissolution of limestone and dolomite (Fig. 31). We see geochemical trends along regional flow paths (dominantly from west to east and high-elevation to low-elevation) within the high mountain aquifer system. The ongoing process of dedolomitization causes groundwater to become more enriched in SO_4 and Mg as it flows down gradient (Fig. 32). This geochemical trend that represents cumulative water mineral interactions along a flow path indicates a common recharge area located at high elevations.

Similarly, stable isotope data also exhibit a spatial trend that indicates a continual systematic change along the regional flow path. Isotopic compositions of water produced in wells and springs at high elevations (>8,200 feet) plot close to the LMWL. Groundwater becomes more isotopically enriched due to evaporation as it flows down gradient (Fig. 40). This trend supports a model of groundwater recharge at high elevations, within the high mountain aquifer system. This trend is only observed in the high mountain aquifer system. As groundwater leaves the high mountain aquifer system, and enters the Pecos Slope aquifer, stable isotope results show little change (Fig. 39) indicating that little to no additional recharge occurs. Water from the recharge zone leaves rather quickly, moving through the high mountain aquifer system and into surrounding aquifers.

Age data from CFC concentrations suggest that most groundwater entered the recharge zone about 15–25 years ago. Within the recharge zone, groundwater residence time is highly variable, as mixing occurs between resident water and recent recharge. Once groundwater leaves the recharge zone, the residence time begins to increase with the oldest groundwater occurring within the Pecos Slope aquifer. It should be noted that Morse (2010) observed some evidence of some young water contributing to this system near the eastern boundary of the study area.

Most recharge occurs within the primary recharge area under average climatic conditions. For recharge events observed during the summers of 2006 and 2008, water entered the groundwater system throughout the high mountain aquifer system and possibly along the Pecos slope also.

HOW DOES PRECIPITATION GET INTO THE GROUNDWATER SYSTEM?

Under average climatic conditions, most recharge occurs above about 8,200 feet elevation (primary recharge area) mainly by snowmelt. However, extreme monsoons, such as those observed in 2006 and 2008 can also significantly recharge the groundwater system. Mechanisms of recharge can be examined at many scales. We have identified two recharge mechanisms: 1) the primary recharge mechanism that appears to maintain the hydrologic system at or near steady state (inflow = outflow) and 2) the secondary recharge mechanism that is a response to extreme precipitation events and can result in very large groundwater-level increases is a relatively short amount of time.

The primary recharge mechanism occurs at high elevations in the primary recharge area. A key indicator of the primary recharge mechanism is the evaporative signature exhibited by stable isotope data for spring and well samples. Spring and well samples collected in and around our study area in 2003 by Eastoe (2005) exhibited isotopic compositions that plotted along a single evaporation line (Fig. 37). Several of our spring and well samples also display isotopic compositions that plot along this same evaporation line (Figs. 40, 41). This evaporation line indicates that the hydrologic system in the primary recharge area is a well-mixed system, which suggests that recharge flow paths are interconnected. The point at which the evaporation line intersects with the LMWL, which represents a mixture of summer rain and snowmelt that infiltrates past the root zone, plots among isotope values expected for winter precipitation. Therefore, snowmelt normally contributes more to groundwater recharge than summer rains. Stable isotope values for water from springs and wells within the primary recharge area have a slight evaporative signature (Fig. 43), indicating that some water enters the system as focused recharge in high mountain streams. Rainfall and snowmelt in the primary recharge zone enters the groundwater system via fractures and conduits in the San Andres Formation on ridges and upper hill slopes and by focused recharge in high mountain streams. Aquifer/aquifer interactions and groundwater/surface water interactions in the recharge area result in a well-mixed system (Figs. 40, 47). Groundwater of different ages are mixed by leaking from one perched aquifer to another, merging of two or more perched aquifers, and mixing in streams that are fed by multiple springs that drain different aquifers.

Spatial trends in water chemistry (Fig. 32) and the stable isotopic composition of springs (Fig. 40) indicates that groundwater flows down gradient from the primary recharge area through an interconnected system of perched aquifers and stream systems. Spring discharge feeds mountain streams that infiltrates through stream beds to recharge other shallow aquifers. This water then discharges at springs at lower elevations that feed mountains streams. As water goes through this recycling process, repeated exposure to the atmosphere causes the isotopic composition of water from springs and wells to evolve along the evaporation line. Water samples collected from wells and springs at lower elevations plot farther along the evaporation line, indicating a higher degree of evaporation (Fig. 40).

Groundwater-level increases associated with monsoons in 2006 and 2008 (Figs. 21, 22) are representative of the secondary recharge mechanism. The key indicator of this recharge mechanism is groundwater with isotopic values that plot along the local meteoric water line (Fig. 41). Unlike the primary

recharge mechanism, recharge that occurs by the secondary mechanism likely takes place over the entire high mountain aquifer system and possibly along the Pecos Slope rather than just at high elevations. Precipitation on ridge tops and hill slopes infiltrates quickly through the thin soils into epikarst, fractures and pores in underlying bedrock without undergoing evaporation. Therefore the isotopic composition of this water represents that of local precipitation, which is controlled by elevation (Figs. 36, 43). Unlike the primary recharge mechanism, for the secondary mechanism, recharge flow paths are not interconnected, resulting in a non-mixed system. Much of this water is stored in the unsaturated zone until it is flushed into saturated groundwater system. The 2006 and 2008 Recharge events caused the stable isotopic compositions of water in wells and springs to shift towards the LMWL (Figs. 41, 42) as a result of this water being flushed into saturated system.

This recharge mechanism has been observed by other researchers. In a karst hydrologic system in south-central Indiana, Lee and Krothe (2001) estimated that flushing of unsaturated zone water into the underlying saturated system accounted for 55.4% of the spring discharge response to a precipitation event. In that karst system, with wetter climatic conditions of Indiana, epikarst water (stored in the unsaturated zone) was easily flushed into the saturated hydrologic system as a response to individual precipitation events. In the Sacramento Mountains, a single precipitation event does not appear to significantly flush water residing in fractures and epikarst into the saturated groundwater system. There is an apparent threshold of monsoon precipitation that must be exceeded for this type of recharge event to happen. Monsoons in 2006 and 2008 were among the wettest on record (Fig. 15). Monsoon rainfall in 2007 was more average and did not cause large groundwater-level increases or a shift in the isotopic compositions of groundwater.

It appears that the primary recharge mechanism provides a more constant supply of groundwater recharge over long time periods. Groundwater-levels respond to changes in primary recharge rates gradually. If recharge rates in the primary recharge area increase over several years, groundwater-levels will gradually increase, and if recharge rates gradually decrease with time, groundwater-levels will gradually fall. In contrast, the secondary recharge mechanism provides groundwater recharge in large pulses over a much greater area as a result of extreme monsoons. A single secondary recharge event can result in very large groundwater-level increases (Figs. 21, 22).

HOW MUCH PRECIPITATION RECHARGES THE GROUNDWATER SYSTEM?

Estimating recharge to a regional aquifer system is a difficult task. We used two methods to estimate recharge both as a relative proportion of surface infiltration (precipitation that infiltrates into the subsurface) and as actual volumes over an estimated recharge area. In this section, we briefly describe the results and recharge estimates from these two methods. For a more detailed description of how these recharge estimates were calculated see Appendix 9.

For the first recharge estimate, we used the water table fluctuation method. The water table fluctuation method estimates recharge within a small mountain drainage area, using individual precipitation events and their effects on groundwater-level fluctuations. Well SM-0049, located near the crest of the southern Sacramento Mountains, was evaluated using precipitation events that occurred in 2006. A relative recharge rate of 5–10% of precipitation was calculated based on the water table fluctuation method of hydrograph analysis. This recharge rate is a reasonable estimate for the small spatial and temporal scale that was considered. It is highly probable that much of this recharge water leaves the system as evapotranspiration (ET) as it moves through the high mountain aquifer system before reaching an adjacent aquifer such as the Pecos Slope or Salt Basin aquifer. Therefore, a local recharge rate, such as the one estimated by the water table fluctuation method probably correlates to a much smaller rate on the regional scale.

For the second recharge estimate, we used the chloride mass balance method (CMB), wherein chloride concentrations are used to measure the relative volume reduction of water within the aquifer due to ET. The CMB method yields a good first approximation of the long-term average recharge on a regional scale. Most groundwater that recharges regional aquifers adjacent to the high mountain aquifer system originates at high elevations and, at some point, flows through the shallow groundwater system. As water flows through the shallow groundwater and surface water systems, it is available to be taken up by vegetation and lost by ET. For well samples, using the CMB method, relative recharge estimates ranged from 4 to 42% with an average of 22%. In the southwestern US, an estimated relative recharge rate of 22% is a fairly high estimate. However, with the high average annual precipitation rate in the mountains (~26 inches/year), thin soils, and highly permeable fractured bedrock, this high recharge estimate seems reasonable.

Assuming the main recharge area lies within the area encompassed by the 8,200 feet surface elevation contour, the recharge zone within the study area encompasses approximately 131,000 acres. Average annual surface infiltration in this area was estimated as a percentage of the average annual precipitation rate of 26 inches in Cloudcroft. Canaris et al. (2011) estimated that canopy interception in the high Sacramento Mountains can be as high as 40%, suggesting that a significant portion of annual precipitation never makes it to the surface, evaporating from the tree canopy. Using a canopy interception loss of 30%, annual surface infiltration was estimated to be approximately 18 inches. Using the CMB method results, we estimate recharge from the high mountain region going into the Pecos Slope aquifer to be 43,230 acre-feet/year.

HOW FAST DOES GROUNDWATER FLOW?

Groundwater flow velocities are highly variable, but relatively fast in the high mountain aquifer system. Most water samples from the high mountains region are relatively young and contain a significant amount of tritium (Fig. 45). CFC data indicates that most groundwater in the high mountains was recharged approximately 15–25 years ago. The extreme heterogeneity of the Yeso Formation and the presence of regional fracture systems results in a variety of flow paths characterized by different flow velocities. These features within the high mountains allow groundwater of differing ages to mix. Variability of flow rates is best exemplified by the discrepancies in the age dating techniques, especially ages from CFC and $^{3}H/^{3}He$ (Table 6). This mixing also occurs as upwelling along fault zones and is reflected in age dating results.

Tritium concentrations in Hay Canyon (Appendix 10) suggest that groundwater in the high mountains may flow as rapidly as 6 feet per day. This flow velocity estimate is high relative to most hydrologic systems, and suggests that the high mountain aquifer system may include a karstic component. However, with the high hydraulic gradients associated with the mountain topography and the low effective porosity observed for fractured hydrologic systems, the high flow velocity estimate is reasonable.

As a part of this study, Morse (2010) used groundwater carbon-14 age estimates to calculate the groundwater flow velocity in the San Andres Formation along an apparent flow path between McDonald Flats and Hope. Morse (2010) determined a groundwater age of approximately 1300 years at the end of the flow path (about 56 miles long) yielding a groundwater flow velocity of 89 feet per year (0.23 feet per day) for the Pecos Slope aquifer.

IMPLICATIONS AND FUTURE WORK

The results of this study have significantly increased our knowledge about the hydrologic system in the southern Sacramento Mountains, which provides surface water and groundwater not only for communities within the mountains, but also to surrounding areas and agriculture in the Roswell Artesian Basin, Salt Basin, and Tularosa Basin. Prior to the 1970s, the Yeso Formation was not considered an important regional aquifer due to the low permeability of the siltstones and sandstones. According to the conceptual model developed by Fiedler and Nye (1933), most recharge to the Roswell Artesian Aquifer occurs within a narrow belt called the Principal Intake Area (PIA) on the Pecos Slope a few miles west of Roswell (Fig. 3). Along the PIA, streams such as the Rio Hondo, Rio Felix, and Rio Peñasco lose their water into the San Andres Formation. As part of our study, Morse (2010) found evidence of young water being added to the groundwater system at the eastern edge of the study area, supporting Fiedler and Nye's assertion that recharge does occur in the PIA. However, our data suggests that very little recharge enters the Pecos Slope aquifer from the surface west of the PIA to Mayhill, except along the Rio Peñasco. Along the Rio Peñasco there is a slight increase in tritium values, suggesting that some surface water infiltrates and recharges the proximal, shallow groundwater system (Fig. 45). Our study conclusively shows that the Yeso Formation is the primary geologic unit that transmits water from the high mountains to adjacent aquifer systems as water flows from the crest of the Sacramento Mountains to the east, toward Hope and the Pecos Slope. Recharge to the Pecos Slope within the study area is estimated to be 43,230 acre-feet/year.

Our results are consistent with the findings of Dr. Gerardo Gross and his students at New Mexico Tech, where the high mountains of the Sacramento Mountains play a very important role recharging surrounding regional aquifers (see Previous Work). Gross and his students suggested that the Yeso Formation contributes a substantial amount of recharge to the Roswell Artesian aquifer by underflow into the San Andres Formation along the western margin of the Roswell Artesian Basin. Because surface recharge from these losing streams could not account for total basin recharge, Gross and his students argued that a deep recharge component is more important than previous workers had assumed.

This study identifies the importance of snowmelt in recharging the regional aquifer system. However, we also emphasize that extreme summer precipitation events can contribute significant recharge during above-average monsoon seasons such as those that occurred in 2006 and 2008. This observation has important implications on how this hydrologic system may respond to climate change. A decrease in snowfall and snow pack may result in a change in the primary mechanisms that control the temporal and spatial variability of groundwater recharge in the high mountains. Large summer storm events may become the most important source of groundwater recharge. Indeed, they may already be so, as research in the Eagle Creek Basin west of Ruidoso has documented a shift in maximum stream discharge from spring runoff to the monsoon season (Matherne et al. 2010). Future research on the effects of global climate change on the North American monsoon and hurricane systems will help to predict how climatic controls on groundwater recharge may change in the near future. An increase in the importance of summer precipitation as a source of recharge to the regional aquifer may present new challenges in the management of groundwater and surface water resources.

Detailed information about the regional hydrologic framework and the different recharge mechanisms gained from this study will help water managers and users to evaluate different strategies and methods for managing future groundwater and surface water resources. For example, methods of artificially recharging the regional aquifer where surface runoff is injected into the groundwater system may be advantageous. The short-term and long-term water-level responses to summer recharge events observed in wells in this study may be useful in identifying suitable locations for the storage of artificial recharge water in the subsurface.

There is also great interest in how thinning trees will affect local and regional recharge. We are currently working on a watershed-scale study in the Sacramento Mountains to evaluate the effects of tree thinning on the local hydrologic system. As part of this study, we are trying to determine the different sources of water for uptake and evapotranspiration by trees. We are also using results from this regional hydrogeologic study to identify regional and local aquifer systems within the watershed study area, and local inputs and outputs to and from the local hydrologic system.

It is clear that knowledge gained by large-scale, interdisciplinary hydrogeologic investigations, such as the Sacramento Mountains hydrogeology study, is invaluable for sustainable future management of groundwater and surface water resources.

PROJECT PERSONNEL AND ACKNOWLEDGEMENTS

AQUIFER MAPPING PROGRAM MANAGER

Peggy S. Johnson, M.S., Senior hydrogeologist and Aquifer Mapping Program Manager, NMBGMR, peggy@gis.nmt.edu
Tasks: Project development and management, technical oversight, technical report.

PROJECT PERSONNEL

Lewis Land, Ph.D., Cave and karst hydrogeologist, NMBGMR, lland@gis.nmt.edu
Tasks: Karst hydrology, water chemistry sampling, hydrogeochemistry and environmental tracers, data interpretation, technical report.

B. Talon Newton, M.S., Project hydrogeologist, NMBGMR, talon@gis.nmt.edu
Tasks: Task manager watershed studies, data collection, stable isotopes, hydrogeochemistry, data interpretation, technical report.

Geoffrey C. Rawling, Ph.D., Field geologist, NMBGMR, geoff@gis.nmt.edu
Tasks: Task manager geologic mapping, hydrologic data collection, map and data compilation and interpretation, technical report, public outreach

J. Michael Timmons, Ph.D., Manager Geologic Mapping Program, NMBGMR, mtimmons@gis.nmt.edu
Tasks: Project development and management, data compilation and interpretation, geologic mapping, technical report.

Stacy Timmons, M.S., Senior geologic research associate and assistant manager for Aquifer Mapping Program, NMBGMR, stacyt@gis.nmt.edu
Tasks: Site inventory and network data maintenance, water-level measurements, water quality sampling, data compilation and interpretation, technical report, public outreach.

SUPPORT PERSONNEL

Brigitte Felix, GIS Specialist and Production coordinator, NMBGMR, bfk@gis.nmt.edu
Tasks: ARC GIS, cartography, drafting, report design, layout and production.

Bonnie Frey, M.S., Chemistry Lab Manager, Geochemist, NMBGMR, bfrey@nmt.edu
Tasks: Geochemical sample analysis, hydrologic data collection.

Trevor Kludt, Ph.D., Hydrogeologic lab associate, NMBGMR, tkludt@nmt.edu
Tasks: Field instrumentation and monitoring, data collection, map and data compilation, data analysis, ARC GIS, cartography.

GEOLOGIC MAPPERS

Bruce Allen, Ph.D., Field geologist, NMBGMR, allenb@gis.nmt.edu
Tasks: Geologic mapping and data compilation.

Shari Kelley, Ph.D., Field geologist, NMBGMR, sakelley@gis.nmt.edu
Tasks: Geologic mapping and data compilation.

Dan Koning, M.S., Field geologist, NMBGMR, dkoning@nmt.edu
Tasks: Geologic mapping and data compilation.

STUDENTS

David Burkhard, New Mexico Tech B.S. student,
Tasks: Field and laboratory assistance.

Jeremiah Morse, New Mexico Tech M.S. student
Tasks: hydrology sampling and studies related to M.S. degree.

OTHER

Lewis Gillard, GIS technician, formerly with NMBGMR,
Tasks: ARC GIS; cartography.

Frederick Partey, Ph.D., Geochemist, formerly with NMBGMR,
Tasks: Geochemical sample analysis, water chemistry data interpretation, technical report.

Patrick Walsh, M.S., Subsurface fluids geologist, formerly with NMBGMR
Tasks: Geologic mapping and lineament analysis, groundwater hydrology, surface water/groundwater interaction, technical report.

Shannon Williams, M.S., Lab associate, formerly with NMBGMR
Tasks: Assistance with hydrologic data collection.

CONTRACTORS

Ben Hallet, M.S., University of Idaho
Giovanni Romero, M.S., NM State University
Sean Long, M.S., Idaho State University
Amy Luther, M.S., University of New Mexico
Colin Shaw, Ph.D., University of New Mexico
Jedidiah Frechette, M.S., University of NM
Kate Zeigler, Ph.D., University of New Mexico
Steve Skotnicki, Ph.D., Arizona State University
Katherine Giles, Ph.D., NM State University
Randy Goossen, B.S., Harvey Mudd College

ACKNOWLEDGMENTS

This project would not have been possible without the kind cooperation of the many residents and land owners of the Sacramento Mountains who have granted access to their property, wells, and springs. Anna Szynkiewicz has assisted with analytical work, data analysis and interpretation. Lab analyses and assistance in interpretation were performed at the Stable Isotope Laboratory of New Mexico Tech, the New Mexico Bureau of Geology and Mineral Resources Chemistry Laboratory, the University of Utah Dissolved Gas Service Center, the University of Miami Tritium Laboratory, Indiana University and Beta Analytic, Inc. Necessary and helpful scientific review by Peggy Johnson, Fred Phillips, John Hawley, John Shomaker, and others is also very appreciated.

RELATED PROJECT PRODUCTS

POSTERS, PRESENTATIONS, MANUSCRIPTS, AND THESES

Canaris, N., Kludt, T. J., and Newton, B. T., 2011, *Canopy interception loss for a mixed coniferous forest in southern New Mexico prior to tree-thinning treatment,* in New Mexico Geological Society, Proceedings Volume, 2011 Annual Spring Meeting, Socorro, New Mexico.

Garduño, H., Fernald, A., Shukla, M., Newton, B. T., Vanleeuwen, D., 2010, *Plot-scale soil water flux and runoff in a missed conifer forest in the Sacramento Mountains, NM.* in New Mexico Geological Society, Proceedings Volume, 2010 Annual Spring Meeting, Socorro, New Mexico.

Land, L. Rawling, G. and Timmons, S., 2010, *Regional water table map of the southern Sacramento Mountains watershed, New Mexico,* in New Mexico Geological Society, Proceedings Volume, 2010 Annual Spring Meeting, Socorro, New Mexico.

Land, L., Timmons, S., Rawling, G., and Felix, B., 2012, *Water table map of the southern Sacramento Mountains, New Mexico,* New Mexico Bureau of Geology and Mineral Resources, Open-file Report 542, scale 1:150,000.

Land, L. A., and Timmons, S. S., 2012, *Regional investigation of groundwater residence time using multiple tracers: southern Sacramento Mountains, New Mexico,* Geological Society of America Abstracts with Programs, Vol. 44, No. 6, p. 22.

Land, L.A., Rawling, G. C., and Timmons, S. S., 2012, *Regional water table map of the southern Sacramento Mountains, New Mexico,* Geological Society of America Abstracts with Programs, Vol. 44, No. 6, p. 13.

Morse, J., 2010, *The hydrogeology of the Sacramento Mountains using environmental tracers,* Masters Thesis [unpublished], New Mexico Institute of Mining and Technology, Socorro, 120 p.

Newton, B. T., 2012, *Stable isotopic compositions of waters in the Sacramento Mountains, New Mexico: Implications for groundwater recharge mechanisms,* Geological Society of America Abstracts with Programs, Vol. 44, No. 6, p. 22.

Newton, B. T., Timmons, S. S., Rawling, G. C., Kludt, T., Eastoe, C. J., 2008, *The use of Stable Isotopes to Assess Climatic Controls on Ground water Recharge in the Southern Sacramento Mountains, New Mexico*. Eos Trans. AGU, 89(53), Fall Meeting, Abstract A23-0303.

Newton, B. T., Fernald, A., Garduño, H., Kludt, T., 2010, *The Sacramento Mountains watershed study: Pre-treatment analyses and considerations,* in New Mexico Geological Society, Proceedings Volume, 2010 Annual Spring Meeting, Socorro, New Mexico.

Newton, B. T., Rawling, G. C., Timmons, S. S., and Kludt, T., 2010, *The stable isotopic compositions of natural waters in the southern Sacramento Mountains, New Mexico: Implications for climatic and hydrogeologic controls on ground water recharge,* in New Mexico Geological Society, Proceedings Volume, 2010 Annual Spring Meeting, Socorro, New Mexico.

Rawling, G., Timmons, S., and Johnson, P., 2007, *Multiple Aquifer Types in the Southern Sacramento Mountains, New Mexico, as Revealed by Water Level Monitoring in Wells,* Geological Society of America Abstracts with Program, October 2007.

Rawling, G. C., 2012, *Geology of the southern Sacramento Mountains, Otero and Chaves Counties, New Mexico,* Geological Society of America Abstracts with Programs, Vol. 44, No. 6, p. 12.

Rawling, G. C., 2012, *Recharge Estimates and Hydrologic Properties of the Yeso Formation in the Southern Sacramento Mountains derived from Hydrograph Analysis,* Geological Society of America Abstracts with Programs v.44, no. 6, p. 22.

Szynkiewicz, A., Newton, B. T., Timmons, S. S., Borrok, D. M., 2012, *The sources and budget for dissolved sulfate in a fractured carbonate aquifer, southern Sacramento Mountains, New Mexico, USA,* Applied Geochemistry, Available online 3 May 2012, ISSN 0883-2927

Szynkiewicz, A., Newton, B. T., Timmons, S. S., and Borrok, D.M., 2012, *The sources and budget for dissolved sulfate in a carbonate aquifer in the southern Sacramento Mountains, New Mexico,* Geological Society of America Abstracts with Programs, Vol. 44, No. 6, p. 22.

Timmons, S., Rawling, G., Johnson, P., Land, L., and Morse, J., 2007, W*ater Level Responses and Preliminary Spring Chemistry Results: Progress Report on the Hydrogeologic Study in the Southern Sacramento Mountains, NM,* New Mexico Geological Society Abstracts with Program, April 2007.

Timmons, S., Rawling, G., Land, L., and Johnson, P., 2007, *Preliminary Water Chemistry Results From a Hydrogeologic Study in the Southern Sacramento Mountains, New Mexico,* Geological Society of America Abstracts with Program, October 2007.

Timmons, S. S., Newton, B. T., and Partey, F. K., 2010, *Water chemistry trends from wells and springs in the southern Sacramento Mountains, New Mexico,* in New Mexico Geological Society, Proceedings Volume, 2010 Annual Spring Meeting, Socorro, New Mexico.

Timmons, S. S., Johnson, P. S., Newton, B. T., Rawling, G. R., Land, L. A., Timmons, J. M., Kludt, T. K., 2012, *The Aquifer Mapping Program approach in the southern Sacramento Mountains, New Mexico,* Geological Society of America Abstracts with Programs, Vol. 44, No. 6, p. 21.

Walsh, P., 2007, *Fracture effects on surface and ground water flow in the Sacramento Mountains, southeast New Mexico,* in New Mexico Geological Society, Proceedings Volume, 2007 Annual Spring Meeting, Socorro, New Mexico.

Walsh, P., 2008, *A new method for analyzing the effects of joints and stratigraphy on spring locations: a case study from the Sacramento Mountains, south central New Mexico, USA*. Hydrogeology Journal, Volume 16, p. 1458-1467.

Zeigler, K., Newton, B. T., and Timmons, S. S., 2010, *Effects of Lateral and Vertical Heterogeneity in the Yeso Formation on the Regional Hydrogeology in the Sacramento Mountains, NM.* in New Mexico Geological Society, Proceedings Volume, 2010 Annual Spring Meeting, Socorro, New Mexico.

GEOLOGIC MAPS

Hallett, B., 2006, *Preliminary geologic map of the Bluff Springs quadrangle, Otero County, New Mexico:* New Mexico Bureau of Geology and Mineral Resources, Open-file Geologic Map OF-GM 137, scale 1:24,000.

Hallett, B., 2006, *Preliminary geologic map of the Cloudcroft quadrangle, Otero County, New Mexico:* New Mexico Bureau of Geology and Mineral Resources, Open-file Geologic Map OF-GM 135, scale 1:24,000.

Hallett, B., 2006, *Preliminary geologic map of the Rogers Ruins quadrangle, Otero County, New Mexico:* New Mexico Bureau of Geology and Mineral Resources, Open-file Geologic Map OF-GM 139, scale 1:24,000.

Hallett, B., 2007, *Preliminary geologic map of the Harvey Ranch quadrangle, Otero County, New Mexico:* New Mexico Bureau of Geology and Mineral Resources, Open-file Geologic Map OF-GM 154, scale 1:24,000.

Hallett, B., 2007, *Preliminary geologic map of the Mayhill quadrangle, Otero County, New Mexico:* New Mexico Bureau of Geology and Mineral Resources, Open-file Geologic Map OF-GM 155, scale 1:24,000.

Rawling, G. C., 2007, *Preliminary geologic map of the Sacramento quadrangle, Otero County, New Mexico:* New Mexico Bureau of Geology and Mineral Resources, Open-file Geologic Map OF-GM 156, scale 1:24,000.

Rawling, G. C., 2007, *Preliminary geologic map of the Surveyors Canyon quadrangle, Otero County, New Mexico:* New Mexico Bureau of Geology and Mineral Resources, Open-file Geologic Map OF-GM 161, scale 1:24,000.

Rawling, G. C., 2007, *Preliminary geologic map of the Woodson Canyon quadrangle, Otero County, New Mexico:* New Mexico Bureau of Geology and Mineral Resources, Open-file Geologic Map OF-GM 157, scale 1:24,000.

Rawling, G. C., 2008, *Preliminary geologic map of the Loco Canyon quadrangle, Chaves County, New Mexico:* New Mexico Bureau of Geology and Mineral Resources, Open-file Geologic Map OF-GM 174, scale 1:24,000.

Rawling, G., 2012, *Generalized geologic map of the southern Sacramento Mountains, Otero and Chaves Counties, New Mexico:* New Mexico Bureau of Geology and Mineral Resources, Open-file report 537, scale 1:100,000.

Rawling, G. C. and Luther, A., 2007, *Preliminary geologic map of the Avis quadrangle, Otero County, New Mexico:* New Mexico Bureau of Geology and Mineral Resources, Open-file Geologic Map OF-GM 159, scale 1:24,000.

Rawling, G. C. and Luther, A., 2007, *Preliminary geologic map of the Bear Spring quadrangle, Otero County, New Mexico:* New Mexico Bureau of Geology and Mineral Resources, Open-file Geologic Map OF-GM 158, scale 1:24,000.

Rawling, G.C., and Shaw, C., 2007, *Preliminary geologic map of the Piñon quadrangle, Otero County, New Mexico:* New Mexico Bureau of Geology and Mineral Resources, Open-file Geologic Map OF-GM 162, scale 1:24,000.

Skotnicki, S., 2008, *Preliminary geologic map of the Dunken quadrangle, Chaves County, New Mexico:* New Mexico Bureau of Geology and Mineral Resources, Open-file Geologic Map OF-GM 178, scale 1:24,000.

Skotnicki, S., 2008, *Preliminary geologic map of the Robertson Canyon quadrangle, Otero and Chaves Counties, New Mexico:* New Mexico Bureau of Geology and Mineral Resources, Open-file Geologic Map OF-GM 177, scale 1:24,000.

Timmons, J. M., 2008, *Preliminary geologic map of the Flying H NW quadrangle, Chaves and Lincoln Counties, New Mexico:* New Mexico Bureau of Geology and Mineral Resources, Open-file Geologic Map OF-GM 173, scale 1:24,000.

Zeigler, K. E., 2008, *Preliminary geologic map of the Elk quadrangle, Otero and Chaves Counties, New Mexico:* New Mexico Bureau of Geology and Mineral Resources, Open-file Geologic Map OF-GM 175, scale 1:24,000.

Zeigler, K. E., 2008, *Preliminary geologic map of the Thimble Canyon quadrangle, Chaves County, New Mexico:* New Mexico Bureau of Geology and Mineral Resources, Open-file Geologic Map OF-GM 176, scale 1:24,000.

Zeigler, K. E., 2009, *Preliminary geologic map of the Chimney Lake quadrangle, Chaves and Otero Counties, New Mexico:* New Mexico Bureau of Geology and Mineral Resources, Open-file Geologic Map OF-GM 190, scale 1:24,000.

Zeigler, K. E., 2009, *Preliminary geologic map of the Cornucopia Canyon quadrangle, Chaves and Otero Counties, New Mexico:* New Mexico Bureau of Geology and Mineral Resources, Open-file Geologic Map OF-GM 192, scale 1:24,000.

Zeigler, K. E., 2009, *Preliminary geologic map of the Lewis Peak quadrangle, Chaves County, New Mexico:* New Mexico Bureau of Geology and Mineral Resources, Open-file Geologic Map OF-GM 191, scale 1:24,000.

Zeigler, K. E., 2009, *Preliminary geologic map of the Piñon Ranch quadrangle, Chaves and Otero Counties, New Mexico:* New Mexico Bureau of Geology and Mineral Resources, Open-file Geologic Map OF-GM 193, scale 1:24,000.

REFERENCES

Abercrombie, D., 2003, *Waters of the Sacramento Mountains forest*, in Johnson, P. S., Land, L., Price, L. G., and Titus, F., eds., *Water Resources of the Lower Pecos Region, New Mexico: Science, Policy, and a Look to the Future:* New Mexico Bureau of Geology and Mineral Resources, 2003 New Mexico Decision Makers Guidebook, p. 88-92.

Adams, D. C. and Keller, G. R., 1994, *Crustal structure and basin geometry in south-central New Mexico, in Keller, G. R. and Cather, S. M., eds., Basins of the Rio Grande Rift: Structure, stratigraphy, and tectonic setting:* Geological Society of America Special Paper 291, p. 241-255.

Ahrens, C. Donald, 2003, *An introduction to Weather, Climate, and the Environment,* Meteorology Today, 7th Edition, Thompson Learning, Inc.

Amundson, R., Stern, L., Baisden, T., Wang, Y., 1998, *The isotopic composition of soil and soil-respired CO2,* Geoderma, Volume 82, p. 83-114.

Back, W., Hanshaw, B. B., Plummer, L. N., Rahn, P. H., Rightmire, C. T., Rubin, M., 1983, *Process and rate of dedolomitization: mass transfer and 14C dating in a regional carbonate aquifer,* Geological Society of America Bulletin, Vol. 94, p.1415-1429.

Bailly-Comte, V., Martin, J. B., Jourde, H., Screaton, E. J., Pistre, S., and Langston, A., 2010, *Water exchange and pressure transfer between conduits and matrix and their influence on hydrodynamics of two karst aquifers with sinking streams.* Journal of Hydrology, v. 386, p. 5566.

Barker, J. M., Kues, B. S., Austin, G. S., Lucas, S. G. [eds.], 1991, *Geology of the Sierra Blanca, Sacramento, and Capitan Ranges, New Mexico,* NMGS Fall Field Conference Guidebook, 361 p.

Bates, R. L., 1961, *Drainage development, southern Sacramento Mountains,* The Ohio Journal of Science, Volume 61, p. 113-124.

Bean, R. T., 1949, *Geology of the Roswell Artesian Basin, New Mexico, and its relation to the Hondo Reservoir:* New Mexico State Engineer Office, Technical Report 9, 31 p.

Bell, F. C., 1979, *Precipitation, in Goodall, D.W., and Perry, R.A., (eds.), Arid Land Ecosystems: Structure, Functioning, and Management,* Volume 1: Cambridge University Press, Cambridge, p. 373-392.

Bethke, C. M. and Johnson, T. M., 2002a, *Paradox of groundwater age,* Geology, Volume 30, p. 107-110.

Bethke, C. M. and Johnson, T. M., 2002b, *Ground water age,* Ground Water, Volume 40, p. 337-339.

Black, B. A., 1973, *Geology of the northern and eastern parts of the Otero platform, Otero and Chaves counties, New Mexico,* [Ph.D. dissertation], University of New Mexico, 158 p.

Black, B. A., 1975, *Geology and oil and gas potential of the northeast Otero platform area, New Mexico,* New Mexico Geological Society Guidebook 26, p. 323-332.

Black, B. A., 1976, *Tectonics of the northern and eastern parts of the Otero platform, Otero and Chaves Counties, New Mexico,* in Woodward, L. A., and Northrop, S. A., eds., *Tectonics and mineral resources in southwestern North America:* New Mexico Geological Society Special Publication 6, p. 39-45.

Bonacci, O., 1993, *Karst springs hydrographs as indicators of karst aquifers.* Hydrological Sciences, Journal des Sciences Hydrologiques, v. 38, no. 1, p. 51-62.

Broadhead, R. F., 2002, *Petroleum geology of the McGregor Range, Otero County, New Mexico:* New Mexico Geological Society, Guidebook 53, p. 331-338.

Busenberg, E. and Plummer, L. N., 2006, CFC-2005-2a: *USGS spreadsheet program for preliminary evaluation of CFC data, in Use of chlorofluorocarbons in hydrology:* A guidebook: International Atomic Energy Agency, Vienna.

Canaris, N., Kludt, T., and Newton, B. T., 2011, *Canopy interception loss for a mixed coniferous forest in southern New Mexico prior to tree-thinning treatment,* in New Mexico Geological Society, Proceedings Volume, 2011 Annual Spring Meeting, Socorro, New Mexico.

Cather, S. M., 1991, *Stratigraphy and provenance of upper Cretaceous and Paleogene strata of the western Sierra Blanca Basin, New Mexico,* in Barker, J. M., Kues, B. S., Austin, G. S., and Lucas, S. G. (eds.), *Geology of the Sierra Blanca, Sacramento, and Capitan Ranges, New Mexico:* New Mexico Geological Society, Guidebook 42, p. 265-275.

Childers, A. and Gross, G. W., 1985, *The Yeso aquifer of the middle Pecos basin, analysis and interpretation:* New Mexico Tech, Geophysical Research Center, Report H-16, 162 p.

Clark, I. and Fritz, P., 1997, *Environmental Isotopes in Hydrogeology,* Lewis Publishers, New York.

Cook, P. G., Plummer, L. N., Solomon, D. K., Buesenberg, E., and Han, L. F., 2006, *Effects that can modify apparent CFC age, in Use of chlorofluorocarbons in hydrology:* A guidebook: International Atomic Energy Agency, Vienna, p. 31-58.

Craig, H., 1961, *Isotopic Variations in Meteoric Waters,* Science, Vol. 133, p. 3702-3703.

Crossey, L. J., Fischer, T. P., Patchett, P. J., Karlstrom, K. E., Hilton, D. R., Newell, D. L., Huntoon, P., Reynolds, A.C., and de Leeuw, G. A. M., 2006, *Dissected hydrologic system at the Grand Canyon: Interaction between deeply derived fluids and plateau aquifer waters in modern springs and travertine,* Geology, Volume 34, p. 25-28.

Davis, P., Wilcox, R., and Gross, G. W., 1979, *Spring characteristics of the western Roswell Artesian Basin:* New Mexico Water Resources Research Institute Report 116, 93 p.

Davis, S. N., Whittemore, D. O., Fabryka-Martin, J., 1998, *Uses of Chloride/Bromide Ratios in Studies of Potable Water,* Ground Water, Vol. 36, No. 2, p. 338-350.

Duffy, C. J., Gelhar, L. W., and Gross, G. W., 1978, *Recharge and groundwater conditions in the western region of the Roswell Basin:* New Mexico Water Resources Research Institute Report 100, 111 p.

Earman, S., 2004, *Groundwater recharge and movement through mountain-basin systems of the Southwest: a case study in the Chiricahua Mountains-San Bernardino Valley system, Arizona and Sonora,* Ph. D dissertation [unpublished], New Mexico Institute of Mining and Technology, Socorro, NM.

Eastoe, C. J., 2005, *Stable and Radiogenic Isotope Evidence Relating to Regional Groundwater Flow Systems Originating in the High Sacramento Mountains, New Mexico.* Eos Trans. AGU 86(52), Fall Meet. Suppl., Abstract H33G-04.

Fiedler, A. G. and Nye, S. S., 1933, *Geology and ground-water resources of the Roswell Artesian Basin:* U.S. Geological Survey, Water-Supply Paper 639, 372 p.

Ford, D. C. and Williams, P. W., 1989, *Karst Geomorphology and Hydrology,* UNWIN HYMAN, London. 601 p.

Ford, D. and Williams, P., 2007, *Karst Hydrogeology and Geomorphology.* John Wiley & Sons, Chichester, West Sussex, England. 562 pp.

Frechette, J. L., 2008, *Three L Canyon soil geomorphic units,* Unpublished consultant report to the NMBGMR, 10 p.

Freeze, R. A., and Cherry, J. A., 1979, *Groundwater,* Prentice Hall, Inc. Upper Saddle River, NJ.

Frye, J. C., Leonard, A. B. and Glass, H. D., 1982, *Western extent of Ogallala Formation in New Mexico:* New Mexico Bureau of Mines and Mineral Resources Circular 175, 41 p.

Garduño, H., Fernald, A., Shukla, M., Newton, B. T., Vanleeuwen, D., 2010, *Plot-scale soil water flux and runoff in a mixed conifer forest in the Sacramento Mountains, NM.* in New Mexico Geological Society, Proceedings Volume, 2010 Annual Spring Meeting, Socorro, New Mexico.

Gibson, J. J., Birks, S. J., and Edwards, T. W. D., 2008, *Global prediction of A and ^{2}H-^{18}O evaporation slopes for lakes and soil water accounting for seasonality.* Global Biochemical Cycles. V. 22.

Gochis, D. J., and Higgins, W. R., 2007, *The Path to Improving Predictions of the North American Monsoon:* U.S. Clivar, v. 5, no. 1.

Gonfiantini, R., Roche, M. A., Olivry, J. C., Fontes, J. C., and Zuppi, G. M., 2001, *The altitude effect on the isotopic composition of tropical rains,* Chemical Geology, v. 181, p. 147-167.

Gross, G. W., 1982, *Recharge in semiarid mountain environments,* New Mexico Water Resources Research Institute Report 153, 36 p.

Gross, G. W., 1985, *The Yeso aquifer of the middle Pecos basin, part II: Hydrology of the Rio Felix drainage:* Final report submitted to New Mexico Interstate Stream Commission, 73 p.

Gross, G. W. and Hoy, R. N., 1980, *A geochemical and hydrological investigation of ground water recharge in the Roswell Basin of New Mexico: Summary of results and updated listing of tritium determinations:* New Mexico Water Resources Research Institute Report 122, 141 p.

Gross, G. W., Hoy, R. N., and Duffy, C. J., 1976, *Application of environmental tritium in the measurement of recharge and aquifer parameters in a semi-arid limestone terrain:* New Mexico Water Resources Research Institute Report 080, 212 p.

Gross, G. W., Davis, P., and Rehfeldt, K. R., 1979, *Paul Spring: An investigation of recharge in the Roswell (NM) Artesian Basin,* New Mexico Water Resources Research Institute Report 113, 135 p.

Gross, G. W., Hoy, R. N., Duffy, C. J., and Rehfeldt, K. R., 1982, *Isotope studies of recharge in the Roswell Basin,* in Perry, Jr., E. C. and Montgomery, C. W. (eds.), Isotope Studies of Hydrologic Processes: DeKalb, Northern Illinois University Press, p. 25-33.

Han, L. F., Pang, Z. and Groening, M., 2001, *Study of groundwater mixing using CFC data. Science in China 44: 21-28*

Happell, James D., Stephen Opsahl, Zafer Top, and Jeffery P. Chanton, 2006, *Apparent CFC and $^{3}H/^{3}He$ age differences in water from Floridan Aquifer springs,* Journal of Hydrology, Volume 319, p. 410-426.

Harbour, R. L. 1970, *The Hondo Sandstone Member of the San Andres Limestone of south-central New Mexico,* U.S. Geological Survey Professional Paper 700C, p. 175–182.

Havenor, K. C., 1968, *Structure, stratigraphy, and hydrogeology of the northern Roswell Artesian Basin:* New Mexico Bureau of Mines and Mineral Resources Circular 93, 30 p.

Hawley, J. W., 1993a, *Overview of geomorphic history of the Carlsbad area:* New Mexico Geological Society Guidebook, 44th Field Conference, p. 2-3.

Hawley, J. W., 1993b, *The Ogallala and Gatuña Formations in the southeastern New Mexico region:* New Mexico Geological Society Guidebook, 44th Field Conference, p. 261-269.

Hounslow, A.W., 1995, *Water quality data analysis and interpretation,* Lewis Publishers, Boca Raton.

Hood, J. W., 1960, *Availability of groundwater in the vicinity of Cloudcroft, Otero County, New Mexico,* U.S. Army Corp of Engineers Open-File Report, 27 p.

Hoy, R. N. and Gross, G. W., 1982, *A baseline study of oxygen 18 and deuterium in the Roswell, New Mexico, ground water basin,* New Mexico Water Resources Research Institute Report 144, 94 p.

Hydro-Geochem, 1982, *Numerical simulation of Pajarita well field, Mescalero Apache Indian Reservation,* [unpublished report].

International Atomic Energy Agency, 2006, *Use of chlorofluorcarbons in Hydrology:* A Guidebook. International Atomic Energy Agency, Vienna

Jennings, J., 1986, *The hydrogeology of the Sacramento Mountains between Cloudcroft and Alamogordo, Otero County, New Mexico:* New Mexico Tech, Geophysical Research Center, Report H-17, 123 p.

Kalin, R. M., 2000, *Radiocarbon dating of groundwater systems,* in Cook, P. G. and Herczeg, A. L., eds., *Environmental tracers in subsurface hydrology,* Kluwer Academic Publishers, Boston, p. 111-144.

Kazemi, G. A., Lehr, J. H. and Perrochet, P., 2006, *Groundwater Age,* John Wiley and Sons, Hoboken

Kelley, V. C., 1971, *Geology of the Pecos country, southeastern New Mexico,* New Mexico Bureau of Geology and Mineral Resources, Memoir 24, 78

Kelley, V. C., 1980, *Gatuña Formation (Late Cenozoic), Pecos Valley, New Mexico and Trans-Pecos Texas:* New Mexico Geological Society Guidebook, Trans-Pecos Region, 31st Field Conference, p. 213-217.

King, W. E., and Harder, V. M., 1985, *Oil and gas potential of the Tularosa Basin-Otero platform-Salt Basin graben area, New Mexico and Texas:* New Mexico Bureau of Mines and Mineral Resources Circular 198, 36 p.

Land, L. and Huff, G. F., 2010, *Multi-tracer investigation of groundwater residence time in a karstic aquifer:* Bitter Lakes National Wildlife Refuge, New Mexico, USA. Hydrogeology Journal 18, p. 455-472.

Land, L., Lueth, V. W., Raatz, W., Boston, P., Love, D. L. [eds.], 2006, *Caves and Karst of Southeastern New Mexico,* NMGS Fall field Conference Guidebook, 344 p.

Land, L. and Newton, B. T., 2008, *Seasonal and long-term variations in hydraulic head in a karstic aquifer: Roswell Artesian Basin, New Mexico:* Journal of the American Water Resources Association, v. 44, p. 175-191.

Lawrence, J. R., Gedzelman, S. D., Gamache, J., and Black, M., 2002, *Stable Isotope Ratios: Hurricane Olivia:* Journal of Atmospheric Chemistry, v.41, p. 67-82.

Liebmann, B., Blade, I., Bond, N. A., Gochis, D., Allured, D., and Bates, G. T., 2008, *Characteristics of North American Summertime Rainfall with Emphasis on the Monsoon:* Journal of Climate v. 21, p.1277-1294

Lee, W. S. and Krothe, N. C., 2001, *A four-component moxing model for water in a kast terrain in south-central Indiana, USA. Using solute concentration and stable isotopes as tracers.* Chemical Geology, v.179, p. 129-143.

Long, A., Sawyer, J. and Putnam, L., 2008, *Environmental tracers as indicators of karst conduits in groundwater in South Dakota, USA,* Hydrogeology Journal, v. 16, p. 263-280.

Love, D. W., Hawley, J. W., Kues, B. S., Austin, G. S., Lucas, S. G. [eds.], 1993, *Carlsbad Region (New Mexico and West Texas),* NMGS Fall Field Conference Guidebook, 357 p.

Lueth, V., Giles, K. A., Lucas, S. G., Kues, B. S., Myers, R. G., Ulmer-Scholle, D. [eds.], 2002, *Geology of White Sands.* NMGS Fall Field Conference Guidebook, 362 p.

Malm, Norman R., 2003, *Climate Guide Las Cruces, 1892-2000,* New Mexico Agricultural Experimental Station Research Report 749.

Matherne, A. M., Myers, N. C., and McCoy, K. J., 2010. *Hydrology of Eagle Creek Basin and effects of groundwater pumping on streamflow, 1969–2009,* U.S. Geological Survey Scientific Investigations Report 2010-5205, 73 p.

Mayer, J. M. and Sharp, J. M., Jr., 1998, *Fracture control of regional ground-water flow in a carbonate aquifer in a semi-arid region:* GSA Bulletin, v. 110, p. 269-283.

Mazor, E. and Nativ, R., 1992, *Hydraulic calculation of groundwater flow velocity and age: Examination of the basic premises.* Journal of Hydrology 138: 211-222

McLean, J. S., 1970, *Saline ground-water resources of the Tularosa Basin, New Mexico:* U.S. Dept. of the Interior, Office of Saline Water Research and Development Progress Report 561, 128 p.

McLean, J. S., 1975, *Saline ground water in the Tularosa Basin, New Mexico,* in Seager, W. R., Clemons, R. E., and Callender, J. F., eds., Las Cruces Country: New Mexico Geological Society, Guidebook 26, p. 237-238.

Meinzer, O. E. and Hare, R. E., 1915, *Geology and water resources of the Tularosa Basin, New Mexico:* U.S. Geological Survey Water-Supply Paper 343, 317 p.

Moore, S. L., Foord, E. E., and Meyer, G. A., 1988a, *Geologic and aeromagnetic map of a part of the Mescalero Apache Indian Reservation, Otero County, New Mexico:* U. S. Geological Survey Miscellaneous Investigations Series Map I-1775, scale 1:50,000.

Moore, S. L., Foord, E. E., Meyer, G. A., and Smith, G. W., 1988b, *Geological Map of the northwestern part of the Mescalero Apache Indian Reservation, Otero County, New Mexico:* U. S. Geological Survey Miscellaneous Investigations Series Map I-1895, scale 1:24,000.

Moore, S. L., Thompson, T. B., and Foord, E. E., 1991, *Structure and igneous rocks of the Ruidoso region, New Mexico,* in Barker, J. M., Kues, B. S., Austin, G. S., and Lucas, S. G. (eds.), *Geology of the Sierra Blanca, Sacramento, and Capitan Ranges, New Mexico:* New Mexico Geological Society, Guidebook 42, p. 265-275.

Morse, J., 2010, *The hydrogeology of the Sacramento Mountains using environmental tracers,* M. S. Thesis [unpublished], New Mexico Institute of Mining and Technology, Socorro, 120 p.

Motts, W. S. and Cushman, R. L., 1964, *An appraisal of the possibilities of artificial recharge to ground-water supplies in part of the Roswell Basin, New Mexico:* U.S. Geological Survey Water-Supply Paper 1785, 86 p.

Mourant, W. A., 1963, *Water resources and geology of the Rio Hondo drainage basin:* New Mexico State Engineer Office, Technical Report 28, 85 p.

Muehlberger, W. R., Belcher, R. C., and Goetz, L. K., 1978, *Quaternary faulting in Trans-Pecos Texas.* Geology, vol. 6, p. 337-340.

National Weather Service Climate Prediction Center, 2003, "*Reports to the Nation: The North American Monsoon*", http://www.cpc.noaa.gov/products/outreach/Report-to-the-Nation- Monsoon_aug04.pdf

National Weather Service Southern Region Headquarters, 2006, *Special Feature: The North American Monsoon.* http://www.srh.noaa.gov/abq/climate/Monthlyreports/July/nams.htm.

National Weather Service Forecast Office, n.d. a, *The North American Monsoon:* http://www.wrh.noaa.gov/twc/monsoon/monsoon_info.php (May 2010).

National Weather Service Forecast Office, n.d. b, *Monsoon Inter-annual Variability:* http://www.wrh.noaa.gov/twc/monsoon/monsoon_info.php (May 2010).

Newton, B. T., Timmons, S. S., Rawling, G. C., Kludt, T., Eastoe, C. J., 2008, *The use of Stable Isotopes to Assess Climatic Controls on Ground water Recharge in the Southern Sacramento Mountains, New Mexico.* Eos Trans. AGU, 89(53), Fall Meeting, Abstract A23-0303.

Newton, B. T., Fernald, A., Garduño, H., Kludt, T., 2010, *The Sacramento Mountains watershed study: Pre-treatment analyses and considerations,* in New Mexico Geological Society, Proceedings Volume, 2010 Annual Spring Meeting, Socorro, New Mexico.

Newell, D. L., Crossey, L. J., Karlstrom, K. E., and Fischer, T. P., 2005, *Continental-scale links between the mantle and groundwater systems of the western United States: Evidence from travertine springs and regional He isotope data.* GSA Today 15: 4-10

NOAA National Climatic Data Center, 2000. *State of the Climate: Drought for May 2000,* published online June 2000, retrieved from http://www.ncdc.noaa.gov/sotc/drought/2000/5.

Parkhurst, D. L., Appelo, C. A. J., 1999, *User's guide to PHREEQC (Version 2)-A computer program for speciation, batch-reaction, one-dimensional transport, and inverse geochemical calculations,* U.S. Geological Survey Water-Resources Investigations Report 99-4259, 312 p.

Pasch, R. J. and Kimberlain, T. B., 2009, *Tropical Cyclone Report, Hurricane Dolly (AL042008), 20-25 July 2008,* National Hurricane Center.

Phillips, F. M. and Castro, M. C., 2003, *Groundwater dating and residence time measurements,* in Holland, H. D. and Turekian, K. K. (eds.), *Treatise on Geochemistry vol. 5: Surface and Groundwater, Weathering and Soils* (ed. J. I. Drever), Oxford University Press, Oxford.

Plummer, L. N. and Busenberg, E., 2000, *Chlorofluorcarbons.* in Cook, P. and Herczeg, A. L. (eds.), *Environmental Tracers in Subsurface Hydrology,* Kluwer Academic, Dordrecht, p. 441-478.

Plummer, L. N., Busby, J. F., Lee, R. W., Hanshaw, B. B., 1990, *Geochemical modeling of the Madison Aquifer in parts of Montana, Wyoming, and South Dakota,* Water Resources Research, Volume 26, p.1981-2014.

Plummer, L. N., Busenberg, E., and Han, L., 2006, *CFCs in binary mixtures of young and old groundwater, in Use of Chlorofluorocarbons in Hydrology:* A Guidebook, International Atomic Energy Agency, Vienna, p. 59-72.

Powers, D. W. and Holt, R. M., 1993, *The Upper Cenozoic Gatuña Formation of southeastern New Mexico:* New Mexico Geological Society, Guidebook 44, p. 271-282.

Powers, J. G., and Shevenell, L., 2000, *Transmissivity estimates from well hydrographs in karst and fractured aquifers.* Ground Water, v. 38, p. 361-369.

Pray, Lloyd D., 1961, *Geology of the Sacramento Mountains escarpment, Otero County, New Mexico,* New Mexico Bureau of Geology and Mineral Resources, Bulletin 35, 144 p.

Rabinowitz, D. and Gross, G. W., 1972, *Environmental tritium as a hydrometeorologic tool in the Roswell Basin, New Mexico:* New Mexico Water Resources Research Institute Report 016, 268 p.

Rabinowitz, D., Gross, G. W, and Holmes, C., 1977, *Environmental tritium as a hydrometeorological tool in the Roswell Basin, New Mexico, I, II, III:* Journal of Hydrology, Volume 32, p. 3-46.

Rantz, S. E., and others, 1982, *Measurement and computation of streamflow,* U.S. Geological Survey, Water Supply Paper 2175, Volumes 1 and 2, 631 p.

Rasmussen, T. C. and Crawford, L. A., 1997, *Identifying and removing barometric pressure effects in confined and unconfined aquifers,* Groundwater, Volume 35, p. 502-512.

Rawling, G. C., 2009, *Geology of the Ruidoso area, Lincoln and Otero counties, New Mexico,* New Mexico Bureau of Geology and Mineral Resources Open-File Report 507, 2 sheets, scale 1:24000.

Rehfeldt, K. R. and Gross, G. W., 1981, *The carbonate aquifer of the central Roswell Basin: Recharge estimation by numerical modeling:* New Mexico Water Resources Research Institute Report 142, 136 p.

Reiter, M. and Jordan, D. L., 1996, *Hydrogeothermal studies across the Pecos River Valley, southeastern New Mexico:* Geological Society of America Bulletin, v. 108, p. 747-756.

Renick, B. C., 1926, *Geology and ground-water resources of the drainage basin of the Rio Peñasco above Hope, New Mexico:* New Mexico State Engineer 7th Biennial Report, p. 123-127.

Riesterer, J., Drakos, P., Lazarus, J., and Chudnoff, M., 2006, *Hydrogeology of Hale Spring and evaluation of declining spring discharge, Ruidoso Downs, New Mexico,* in Land, L., Lueth, V., Raatz, B., Boston, P., and Love, D. (eds.), *Caves and Karst of Southeastern New Mexico:* New Mexico Geological Society, Guidebook 57, p. 287-295.

Richter, B. C. and C. W. Kreitler, 1986. *Geochemistry of salt water beneath the rolling plains, North-Central Texas,* Ground Water, v. 24, p. 735-742.

Ritchie, A., 2011, *Hydrogeologic Framework and Development of a Three-Dimensional Finite Difference Groundwater Flow Model of the Salt Basin, New Mexico and Texas,* M. S. Thesis [unpublished], Socorro, New Mexico Institute of Mining and Technology, 886 p.

Ritchie, E. and Szenasi, D., 2006, *The Impact of Tropical Cyclone Remnants on the Rainfall of the North American Southwest Region,* Paper presented at the 27th Conference on Hurricanes and Tropical Meterology, Monterey, CA.

Ritchie, E., Wood, K., White, S., and Gutzler, D., 2007, *The Impact of Tropical Cyclone Remnants on the Rainfall of the North American Southwest Region*, Paper presented at the 28th Conference on Hurricanes and Tropical Meterology, Orlando, FL.

Rozanski, K., Araguas, L., and Gonfiantini, R., 1993, *Isotopic Patterns in Modern Global Precipitation,* in Swart, P. K., Lohmann, K. C., McKenzie, J., Savin, S. (eds.), *Climate Change in Continental Isotopic Records:* American Geophyxical Union, Geophysical Monograph 78, p.1-36.

Seager, W. R., Hawley, J. W., Kottlowski, F. E., and Kelley, S. A., 1987, *Geology of east half of Las Cruces and Northeast El Paso 1° x 2° sheets, New Mexico,* New Mexico Bureau of Geology and Mineral Resources Geologic Map 57, 4 sheets, scale 1:125000.

Sharp, J. M., Jr., Mayer, J. R., and McCutcheon, E., 1993, *Hydrogeologic trends,* in the Del City area, Hudspeth Co., Texas, in Love, D. W., Hawley, J. W., Kues, B. S., Adams, J. W., Austin, G. S., and Barker, J. M., eds., *Carlsbad Region, New Mexico and West Texas,* New Mexico Geological Society, Guidebook 44, p. 327-330.

Sigstedt, S. C., 2010, *Environmental Tracers in Groundwater of the Salt Basin, New Mexico, and Implications for Water Resources,* M.S. Thesis [unpublished], New Mexico Institute of Mining and Technology, 202 p.

Simcox, A. C. and Gross, G. W., 1985, *The Yeso aquifer of the middle Pecos Basin:* Hydrology Research Program, New Mexico Institute of Mining and Technology, Report H-15, 152 p.

Szynkiewicz, Anna, Newton, B. T., Timmons, S. S., Borrok, D. M., 2012, *The sources and budget for dissolved sulfate in a fractured carbonate aquifer, southern Sacramento Mountains, New Mexico, USA,* Applied Geochemistry, Available online 3 May 2012, ISSN 0883-2927

Sloan, C. E. and Garber, M. S., 1971, *Ground-water hydrology of the Mescalero Apache Indian Reservation, south-central New Mexico:* U.S. Geological Survey, Hydrologic Investigation Atlas HA-349, 1 sheet.

Solomon, D. K. and Sudicky, E. A., 1991, *Tritium and helium-3 isotope ratios for direct estimation of spatial variations in groundwater recharge.* Water Resources Research 27: 2309-2319

Solomon, D. Kip, 2000, *^{4}He in groundwater,* in Cook, Peter, and Herczeg, Andrew L., (eds.), Environmental tracers in subsurface hydrology, p. 425-439.

Solomon, D. Kip, and Peter G. Cook, 2000, *^{3}H and ^{3}He,* in Cook, Peter, and Herczeg, Andrew L., (eds.), Environmental tracers in subsurface hydrology, p. 397-424.

Solomon, D. K., Cook, P. G. and Plummer, L. N., 2006, *Models of groundwater ages and residence times, In Use of chlorofluorocarbons in hydrology:* A guidebook, International Atomic Energy Agency, Vienna, p. 73-88.

Stensrud, D. J., Gall, R. L., Mullen, S. L., and Howard, K. W., 1995, *Model Climatology of the Mexican Monsoon:* Journal of Climate v. 8, p.1775-1794.

Street, J. B., and Peery, R., 2007, *Well report: Village of Cloudcroft, Apache replacement well PN-409-S-6, Cloudcroft, New Mexico,* John Shomaker and Associates, INC. Report prepared for US Bureau of Reclamation and the Village of Cloudcroft, 40 p.

Stute, M. and Schlosser, P., 2000, *Atmospheric noble gases,* in Cook, P. and Herczeg, A. L. (eds.), Environmental Tracers in Subsurface Hydrology, Kluwer Academic, Dordrecht, p. 349-377.

Walsh, P., 2008, *A new method for analyzing the effects of joints and stratigraphy on spring locations: a case study from the Sacramento Mountains, south central New Mexico, USA.* Hydrogeology Journal, Volume 16, p. 1458-1467.

Wasiolek, M., 1991, *The hydrogeology of the Permian Yeso Formation within the upper Rio Hondo Basin and the eastern Mescalero Apache Indian Reservation, Lincoln and Otero Counties, New Mexico,* in Barker, J. M., Kues, B. S., Austin, G. S., and Lucas, S. G. (eds.), *Geology of the Sierra Blanca, Sacramento, and Capitan Ranges, New Mexico:* New Mexico Geological Society, Guidebook 42, p. 343-351.

Wasiolek, M. and Gross, G. W., 1983, *Hydrogeology of the upper Rio Peñasco drainage basin between James and Cox Canyons, Otero County, New Mexico:* New Mexico Tech, Geophysical Research Center, Report H-13, 122 p.

Welder, G. E., 1975, *Hydrologic investigation of drill sites on the Mescalero Apache Indian Reservation,* U.S. Geological Survey, Open-File Report (preliminary, no number), 22 p.

White, W. B., 1969, *Conceptual Models for Carbonate Aquifers.* Ground Water, Volume 7, No. 3, p. 180-186.

Woodward-Clyde Consultants, 1978, *Groundwater resource investigation, Mescalero Apache Indian Reservation* [unpublished report].

Zeigler, K., Newton, B. T., and Timmons, S. S., 2010, *Effects of Lateral and Vertical Heterogeneity in the Yeso Formation on the Regional Hydrogeology in the Sacramento Mountains, NM,* in New Mexico Geological Society, Proceedings Volume, 2010 Annual Spring Meeting, Socorro, New Mexico.

New Mexico Bureau of Geology and Mineral Resources

A Division of New Mexico Institute of Mining and Technology

Socorro, NM 87801
(575) 835-5490
Fax (575) 835-6333
www.geoinfo.nmt.edu